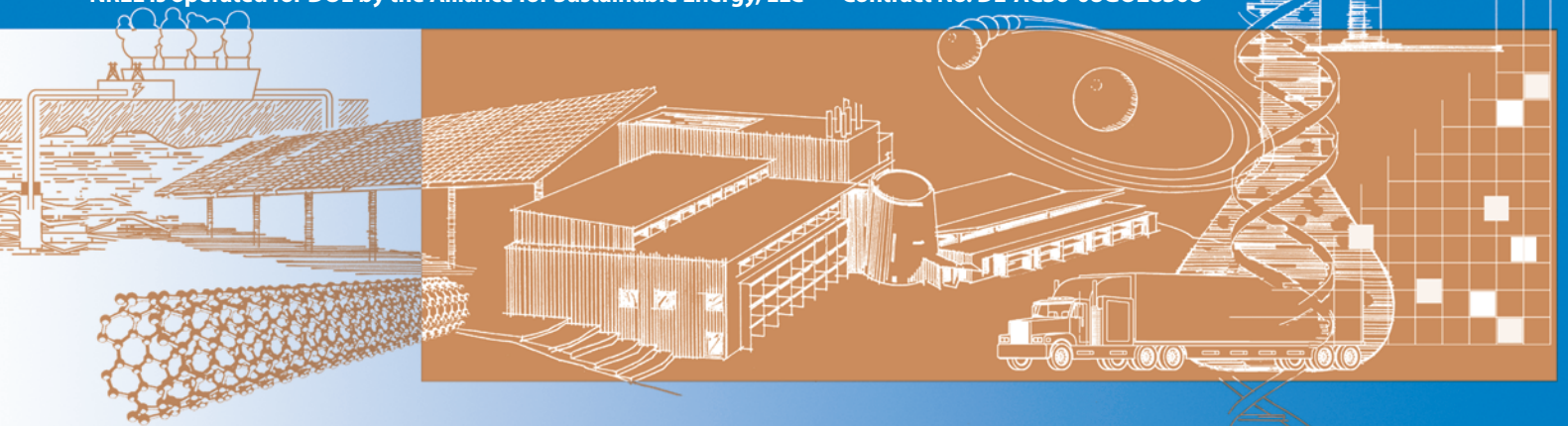# CONCENTRATING SOLAR POWER

Best Practices Handbook for the Collection and Use of Solar Resource Data

Tom Stoffel, Dave Renné, Daryl Myers, Steve Wilcox, Manajit Sengupta, Ray George, Craig Turchi

Technical Report
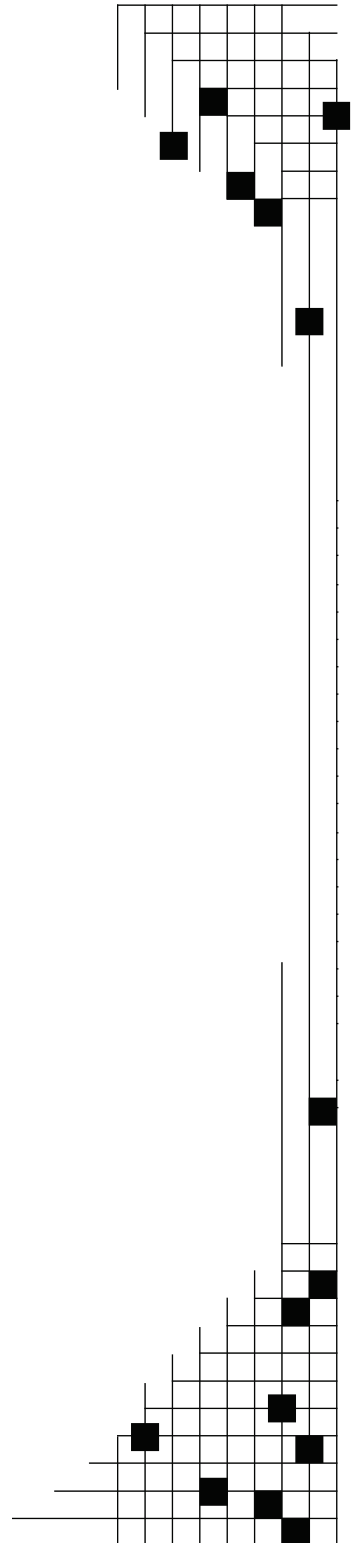**NREL/TP-550-47465**
September 2010

CONCENTRATING SOLAR POWER

Best Practices Handbook for the Collection and Use of Solar Resource Data

Tom Stoffel, Dave Renné, Daryl Myers, Steve Wilcox, Manajit Sengupta, Ray George, Craig Turchi

Acknowledgments

Foreword

This *Handbook* was developed in response to a growing need by the Concentrating Solar Power community for a single document addressing the key aspects of solar resource characterization.

The material was assembled by scientists and engineers who have many decades of combined experience in atmospheric science, radiometry, meteorological data processing, and renewable energy technology development. In essence, this *Handbook* represents the culmination of more than 30 years of research and development investment by the U.S. Department of Energy and the National Renewable Energy Laboratory to advance our understanding of the nation's renewable energy reserves.

You are encouraged to provide feedback to the authors for future revisions and expansion of the *Handbook* scope and content.

Preface

As the world looks for low-carbon sources of energy, solar power stands out as the single most abundant energy resource on Earth. Harnessing this energy stands forth as the challenge for this century. Photovoltaics (PV) and concentrating solar power (CSP) are two primary forms of electricity generation using sunlight. These two solar power generation approaches use different technologies, collect different fractions of the solar resource, and have different siting and production capabilities. Although PV systems are most often deployed as distributed generation sources, CSP systems favor large, centrally located systems. Accordingly, large CSP systems require a substantial investment, sometimes exceeding $1 billion in construction costs. Before such a project is undertaken, the best possible information about the quality and reliability of the fuel source must be made available. That is, project developers need to have reliable data about the solar resource available at specific locations, including historic trends with seasonal, daily, hourly, and (preferably) subhourly variability to predict the daily and annual performance of a proposed CSP plant. Without these data, no financial analysis is possible.

In September 2008, the U.S. Department of Energy (DOE) hosted a meeting of prominent CSP developers and stakeholders. One purpose was to identify areas where the DOE's CSP Program should focus its effort to help the industry develop and deploy projects. At the top of the priority list was the need to provide high-quality solar resource data and recommend to industry the best way to use these data for site selection and estimating plant performance. The direct result is the National Renewable Energy Laboratory's (NREL) *Concentrating Solar Power Best Practices Handbook for the Collection and Use of Solar Resource Data*. The content is based on the experiences of scientists and engineers from industry, academia, and DOE for identifying the sources, quality, and methods for applying solar and meteorological data to CSP projects.

This handbook presents detailed information about solar resource data and the resulting data products needed for each stage of the project, from initial site selection to systems operations. It is not meant to be read from cover to cover, but to be used as a reference during each project stage. The figure below lists these stages and shows which chapters contain information about the corresponding available data and resulting products.

Credit: David Renné and Connie Komomua, NREL
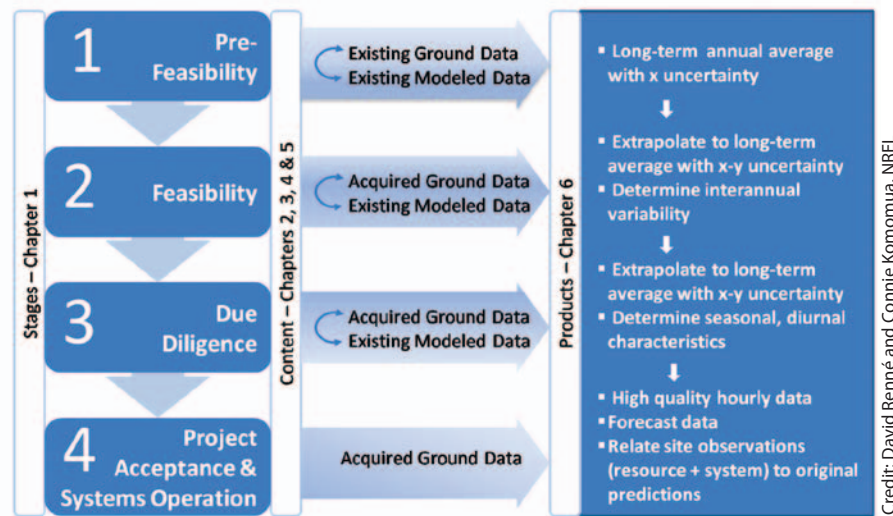
Project developers, engineering procurement construction firms, utility companies, energy suppliers, financial investors, and others involved in CSP plant planning and development will find this handbook a valuable resource for the collection and interpretation of solar resource data.

Acronyms

AC	alternating current
AM	air mass
AOD	aerosol optical depth
AU	astronomical unit
BSRN	Baseline Surface Radiation Network
C	circumsolar brightness 0.3 degrees to 3.2 degrees from the center of the solar disk
CSP	concentrating solar power
COV	coefficient of variation
DEM	digital elevation model
DHI	diffuse horizontal irradiance
DIF	diffuse horizontal irradiance
DISC	direct solar insolation code
DNI	direct normal irradiance
DOE	U.S. Department of Energy
ESRA	European Solar Radiation Atlas
ETR	extraterrestrial radiation
FOV	field of view
GHI	global horizontal irradiance
GIS	geographic information system
GOES	Geostationary Operational Environmental Satellite
GUM	Guide to Measurement Uncertainty
ISCCP	International Satellite Cloud Climatology Project
ISIS	Integrated Surface Irradiance Study
ISO	International Standards Organization
JRC	Joint Research Council
K	Kelvin
kWh/m²/day	kilowatt hours per square meter per day
MBE	mean bias error
MCP	measure-correlate-predict
MESoR	Management and Exploitation of Solar Resource
METEONORM	commercial data product of Meteotest, Bern, Switzerland
METSTAT	meteorological-statistical transfer model
MSG	METEOSTAT Second Generation
NCAR	National Center for Atmospheric Research
NCDC	National Climatic Data Center
NCEP	National Center for Environmental Prediction
NIP	The Eppley Laboratory, Inc. Model Normal Incidence Pyrheliometer

NM	nanometer
NOAA	National Oceanic and Atmospheric Administration
NREL	National Renewable Energy Laboratory
NSRDB	National Solar Radiation Database
NWS	National Weather Service
POA	plane of array
POWER	Prediction of Worldwide Energy Resources
PV	photovoltaics
PVGIS	photovoltaic geographical information system
QA	quality assurance
R&D	research and development
RRDC	Renewable Resource Data Center
Rs	responsivity
RSR	rotating shadowband radiometer
S	solar brightness 0.0 degrees to 0.3 degrees from the center of the solar disk
SI	International System of Units
SOLEMI	Solar Energy Mining
SOLMET	Solar and Meteorological hourly dataset
SRB	Surface Radiation Budget
SRRL	Solar Radiation Research Laboratory
SSE	surface meteorology and solar energy
SUNY	State University of New York
SURFRAD	Surface Radiation Network
SWERA	solar wind energy resource assessment
SZA	solar zenith angle
TOA	top of atmosphere
TSI	total solar irradiance (formerly solar constant)
TMM	Typical Meteorological Month
TMY	Typical Meteorological Year
TMY2	Typical Meteorological Year (Version 2)
TMY3	Typical Meteorological Year (Version 3)
UPS	uninterruptible power supply
USI	upwelling shortwave irradiance
WCRP	World Climate Research Programme
W/m²	watts per square meter
WMO	World Meteorological Organization
WWC	World Radiation Center
WRR	World Radiometric Reference

Contents

Figures

Tables

Chapter 1. Why Solar Resource Data Are Important to Concentrating Solar Power

Sunlight is the fuel for all concentrating solar power (CSP) generation technologies. Like any generation source, knowledge of the quality and future reliability of the fuel is essential to accurate analysis of system performance and financial viability of a project. With CSP systems, the variability of the supply of sunlight probably represents the single greatest uncertainty in a plant's predicted performance. Solar resource data and modeling factor into three elements of a CSP project's life:

- Site selection

- Predicted annual plant output

- Temporal performance and operating strategy.

The first two items are interrelated. Site selection includes numerous factors, but a top priority is a good solar resource. For site selection, a representative annual solar resource is required to make comparisons with alternative sites and estimate plant output. Because site selection is always based on historical solar resource data and changes in weather patterns from year to year, more years of data are better for determining a representative annual dataset. Defining a typical meteorological year (TMY) dataset is not a trivial exercise and is described in Chapter 5. TMY data are used to compare the solar resource at alternative sites and to define the probable annual performance of a proposed CSP plant. Data from individual years are useful to assess the annual variability that can be expected for the proposed location.

Note: Because they rely on reflecting collectors, all CSP technologies use direct normal irradiance (DNI). In this context, discussion of the solar resource for CSP plants implies the analysis of DNI.

Development of TMY data for large regions requires the use of models that rely on satellite imagery. In regional terms, the identification of prime solar resource areas is fairly simple. The southwestern United States, for example, has broad areas of excellent solar resource. However, narrowing down the data to a specific few square kilometers of land requires consideration of local impacts; although satellite data are very useful in mapping large regions, individual sites should be vetted with ground monitoring stations. Local measurements can be compared with same-day satellite data to test for bias in the satellite model. Any correction in the satellite model can then be applied to the historical datasets.

Once a plant is built, resource data are immediately required to complete acceptance testing. The owner and financiers will insist on verifying that the plant output meets its design specifications for a specific solar input. Often the acceptance tests will be for a short duration, perhaps a few days, but the owners will want to extrapolate the results to estimate annual performance. Annual performance estimates can be improved by comparing locally measured ground data to the satellite-derived data for the same time interval. Correcting any bias in the satellite data will allow the modeler to more accurately apply multiple years of satellite data to generate an improved TMY dataset for the site.

Accurate resource data will remain essential to the plant's efficient operation throughout its service life. Comparison of plant output as a function of solar radiation resource is one global indicator of plant performance. A drop in overall efficiency implies a degradation of one or more plant components and indicates that maintenance is required. Lastly, the realm of resource forecasting is becoming more important for plant dispatch as higher penetration of solar power is planned for the electric grid. An accurate forecast can increase plant profits by optimizing energy dispatch into the time periods of greatest value. Although not explicitly covered in this handbook, forecasting requires the same principles described here for historical resource assessment—proper use of satellite- and ground-based data sources and models.

Chapter 2. Overview of Solar Radiation Resource Concepts

Introduction

Describing the relevant concepts and applying a consistent terminology are important to the usefulness of any handbook. This chapter uses a standard palette of terms to provide an overview of the key characteristics of solar radiation, the fuel source for CSP technologies.

Beginning with the sun as the source, we present an overview of the effects of the Earth's orbit and atmosphere on the types and amounts of solar radiation available for energy conversion. An introduction to the concepts of measuring and modeling solar radiation is intended to prepare the reader for the more in-depth treatment in Chapters 3 and 4. The overview concludes with an important discussion of the estimated uncertainties associated with solar resource data based on measurements and modeling methods used to produce the data.

Properties of Extraterrestrial Solar Radiation

Any object with a temperature above absolute zero emits radiation. With an effective temperature of approximately 6000 K, the sun emits radiation over a wide range of wavelengths, commonly labeled from high-energy shorter wavelengths to lower energy longer wavelengths as gamma ray, x-ray, ultraviolet, visible, infrared, and radio waves. These are called *spectral regions* (Figure 2-1). Most (97%) of solar radiation is in the wavelength range of 290 nm to 3000 nm. Future references to broadband solar radiation refer to this spectral range.
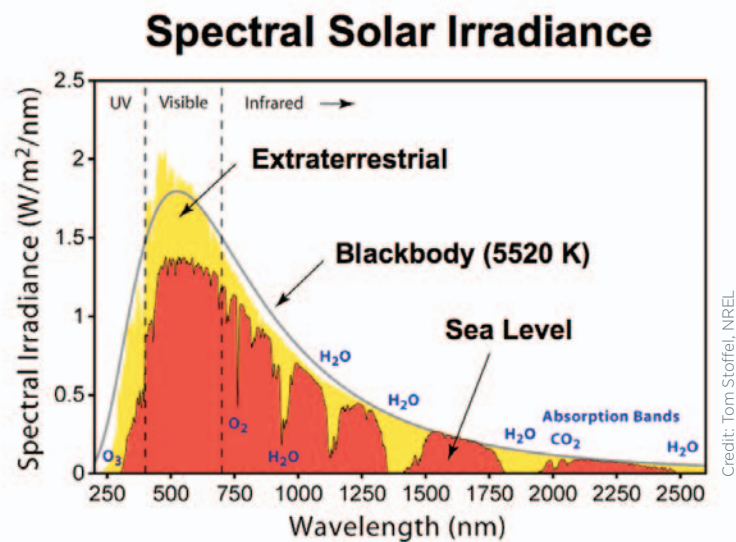
Figure 2-1. The atmosphere affects the amount and distribution of solar radiation reaching the ground

Before continuing our discussion of solar radiation, it is important to understand a few basic radiometric terms. Radiant energy, flux, power, and other concepts used in this handbook are summarized in Table 2-1.

Table 2-1. Radiometric Terminology and Units

Quantity	Symbol	SI Unit	Abbreviation	Description
Radiant energy	Q	Joule	J	Energy
Radiant flux	φ	Watt	W	Radiant energy per unit time (radiant power)
Radiant intensity	I	Watt per steradian	W/sr^{-1}	Power per unit solar angle
Radiant emittance	M	Watt per square meter	W/m^{-2}	Power emitted from a surface
Radiance	L	Watt per steradian per square meter	$W/sr^{-1}/m^{-2}$	Power per unit solid angle per unit of projected source area
Irradiance	E, I	Watt per square meter	W/m^{-2}	Power incident on a surface
Spectral irradiance	E_λ	Watt per square meter per nanometer	$W/m^{-2} nm^{-1}$	Power incident on a surface per wavelength

The total radiant power from the sun is remarkably constant. In fact, the solar output (radiant emittance) has commonly been called the *solar constant,* but the currently accepted term is *total solar irradiance* (TSI) to account for the actual variability with time. There are cycles in the number of sunspots (cooler, dark areas on the sun) and general solar activity of approximately 11 years. Figure 2-2 shows a composite of space-based measurements of the TSI, normalized to 1 astronomical unit (AU), since 1975, encompassing the last three, 11-year sunspot cycles (see De Toma et al. 2004).
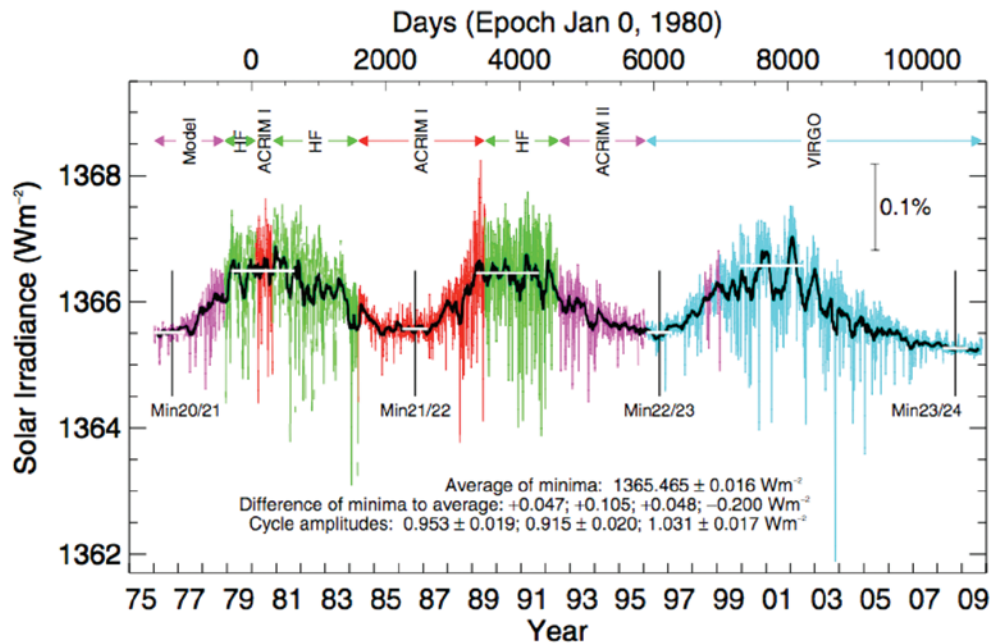
Figure 2-2. Three solar cycles show the variations of TSI in composite measurements from satellite-based radiometers (color coded) and model results produced by the World Radiation Center
(www.pmodwrc.ch/pmod.php?topic=tsi/composite/SolarConstant)
(Used by permission of Physikalish-Meteorologisches Observatorium Davos World Radiation Cente**r)**

The measured variation in TSI resulting from the sunspot cycle is ± 0.2%, only twice the precision (repeatability, not total absolute accuracy, which is about ± 0.5%) of the most accurate radiometers measuring the irradiance in space. There is, however, some large variability in a few spectral regions, especially the ultraviolet (wavelength less than 400 nm), caused by solar activity.

The amount of radiation exchanged between two objects is affected by their separation distance. The Earth's elliptical orbit (eccentricity 0.0167) brings us closest to the sun in January and farthest from the sun in July. This annual variation results in variation of the Earth's solar irradiance of ± 3%. The average Earth-sun distance is 149,598,106 km (92,955,953 miles), or 1 AU. Figure 2-3 shows the Earth's orbit in relation to the northern hemisphere seasons, caused by the average 23.5-degree tilt of the Earth's rotational axis with respect to the plane of the orbit. The solar irradiance available at the top of atmosphere (TOA) is called the *extraterrestrial solar radiation* (ETR). ETR (see Equation 2-1) is the power per unit area, or flux density in Watts per square meter (W/m^2), radiated from the sun and available at the TOA. ETR varies with the Earth-sun distance (r) and annual mean distance (r_0):

$$\text{ETR} \quad = \quad \text{TSI} \cdot (r_0/r)^2 \tag{2-1}$$
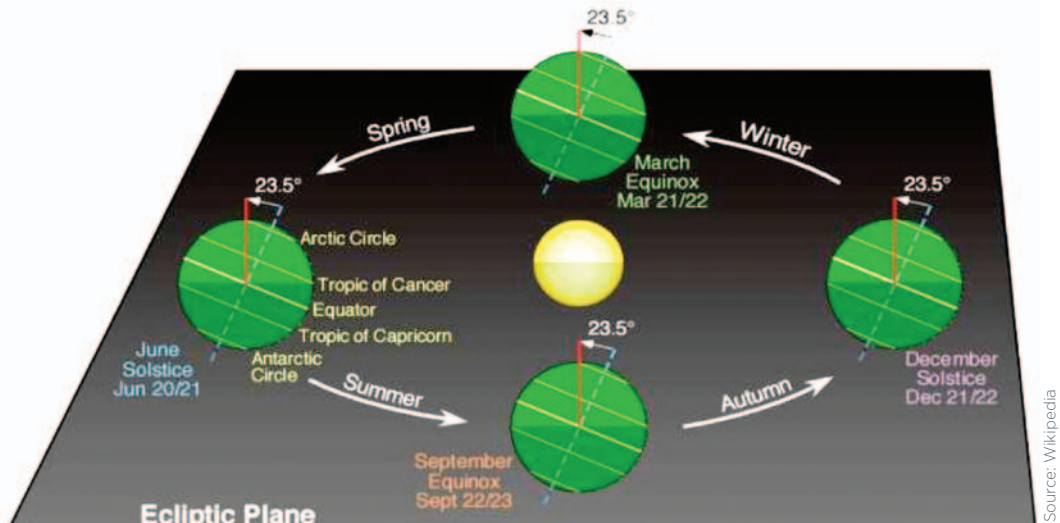
Figure 2-3. Schematic of the Earth's orbit

Source: Wikipedia

As measured by multiple satellites over the past 30 years, the TSI is 1,366 ± 7 W/m^2 at 1 AU. According to astronomical computations, such as NREL's solar position software, the variation in the Earth-sun distance causes the ETR to vary from about 1,415 W/m^2 around January 3 to about 1,321 W/m^2 around July 4.

From the Earth, the sun appears as a very bright disk with an angular diameter of about 0.5 degrees. This means that a point on the Earth intercepts a cone of light from the hemisphere of the sun facing the Earth with an angle of 0.5 degrees at the apex, and a divergence angle from the center of the disk of 0.25 degrees (half the apex angle). Because the divergence angle is very small, the rays of light from the sun are considered parallel for most applications, and are called the *solar beam* or *direct normal irradiance* (DNI).

Solar Radiation and the Earth's Atmosphere

The Earth's atmosphere is a continuously variable filter for the solar ETR as it reaches the surface. Figure 2-1 illustrates the "typical" absorption of solar radiation by ozone, oxygen, water vapor, and carbon dioxide. The amount of atmosphere the solar photons must traverse, also called the *atmospheric path length or air mass* (AM), depends on the relative solar position of the observer (Figure 2-4). By convention, air mass one (AM1) is defined at the amount of

atmospheric path length observed when the sun is directly overhead from a location at sea level. AM is geometrically related to the solar zenith angle (SZA) as AM = secant of SZA, or 1/Cos(SZA). Because SZA is the complement of the solar elevation angle, AM is also equal to 1/Sin (solar elevation angle). Air mass two (AM2) occurs when the SZA is 60 degrees and has twice the path length of AM1. Weather systems, specifically clouds and storm systems, are the major elements that modify the extraterrestrial solar radiation on its way to the surface or to a solar collector. The cloudless atmosphere also contains gaseous molecules, dust, aerosols, particulates, etc., which reduces the ETR as it moves through the atmosphere. This reduction is due to absorption (capturing the radiation) and scattering (essentially a complex sort of reflection).
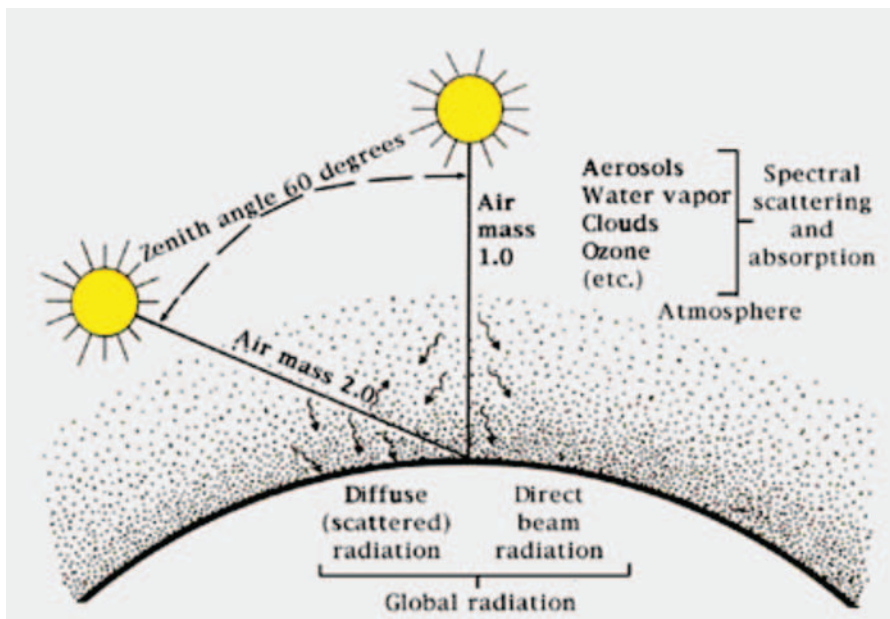
Figure 2-4. Scattering of the direct-beam photons from the sun by the atmosphere produces diffuse radiation that varies with AM
(from Marion et al. 1992)

Absorption removes radiation from the DNI, converting that radiation to heat and raising the temperature of the absorber. The longer the path length through the atmosphere, the more radiation is absorbed. Scattering redistributes the radiation in the hemisphere of the sky dome above the observer, including reflecting part of the radiation back into space. The probability of scattering—and hence of geometric and spatial redistribution of the solar radiation—increases as the path (AM) from the TOA to the ground increases.

Part of the radiation that reaches the Earth's surface will be reflected back into the atmosphere. The actual geometry and flux density of the reflected and scattered radiation depend on the reflectivity and physical properties of the ground and constituents in the atmosphere.

Research into the properties of atmospheric constituents, ways to estimate them, and their influence on the magnitude of solar radiation in the atmosphere at various levels and at the ground continues, and is of great importance to those who measure and model solar radiation fluxes (see Chapters 3 and 4).

Relative Motions of the Earth and Sun

The amount of solar radiation available at the TOA is a function of the TSI and the Earth-sun distance at the time of interest. The slightly elliptical orbit of the Earth around the sun was briefly described above and shown in Figure 2-3. The Earth rotates around an axis through the geographical north and south poles, inclined at an average angle of about 23.5 degrees to the plane of the Earth's orbit. The resulting yearly variation in the solar input results in the climate and weather at each location. The axial tilt of the Earth's rotation also results in daily variations in the solar geometry over the course of a year.

In the northern hemisphere, at latitudes above the Tropic of Cancer near midday, the sun is low on the horizon during the winter and high in the sky during the summer. Summer days are longer as the sun rises north of east and sets north of west. Winter days are shorter as the sun rises south of east and sets south of west. Similar transitions take place in the southern hemisphere. All these changes result in changing geometry of the solar position in the sky with respect to a specific location (see Figure 2-5 generated for Denver, Colorado, by the program available from the University of Oregon at http://solardat.uoregon.edu/SunChartProgram.php). These variations are significant and are accounted for in analysis and modeling of solar radiation components using solar position calculations such as NREL's solar position or Solar Position Algorithm (see www.nrel.gov/rredc/models_tools.html).
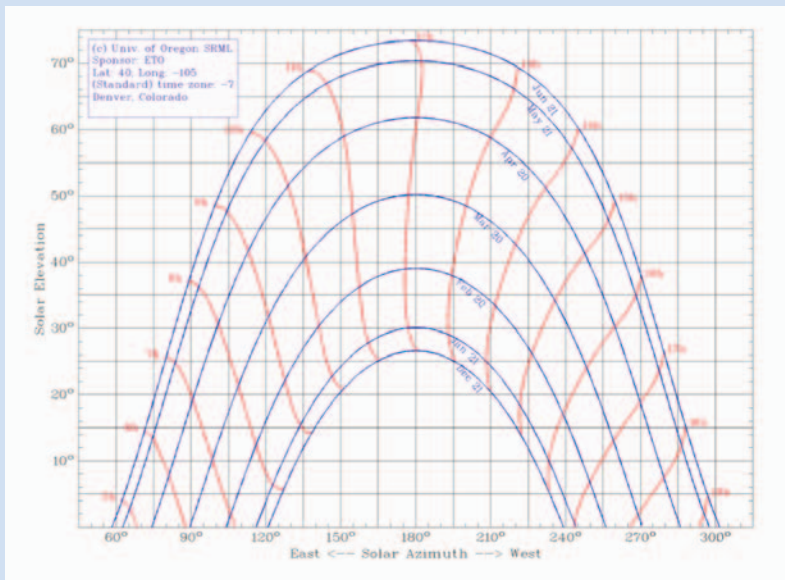
Credit: Tom Stoffel, NREL

Figure 2-5. Apparent sun path variations during a year for a northern hemisphere location

Solar Resources: The Solar Components

Radiation can be transmitted, absorbed, or scattered by an intervening medium in varying amounts depending on the wavelength (see Figure 2-1). Complex interactions of the Earth's atmosphere with solar radiation result in three fundamental broadband components of interest to solar energy conversion technologies:

• Direct normal irradiance (DNI) – Solar (beam) radiation available from the solar disk (of particular interest to CSP)

• Diffuse horizontal irradiance (DHI) – Scattered solar radiation from the sky dome (not including DNI)

• Global horizontal irradiance (GHI) – Geometric sum of the DNI and DHI (total hemispheric irradiance).

These basic solar components are reacted to the SZA by the expression,

$$GHI = DNI \times Cos\,(SZA) + DHI \qquad (2\text{-}2)$$

These components are shown in Figure 2-6.

Credit: Al Hicks, NREL
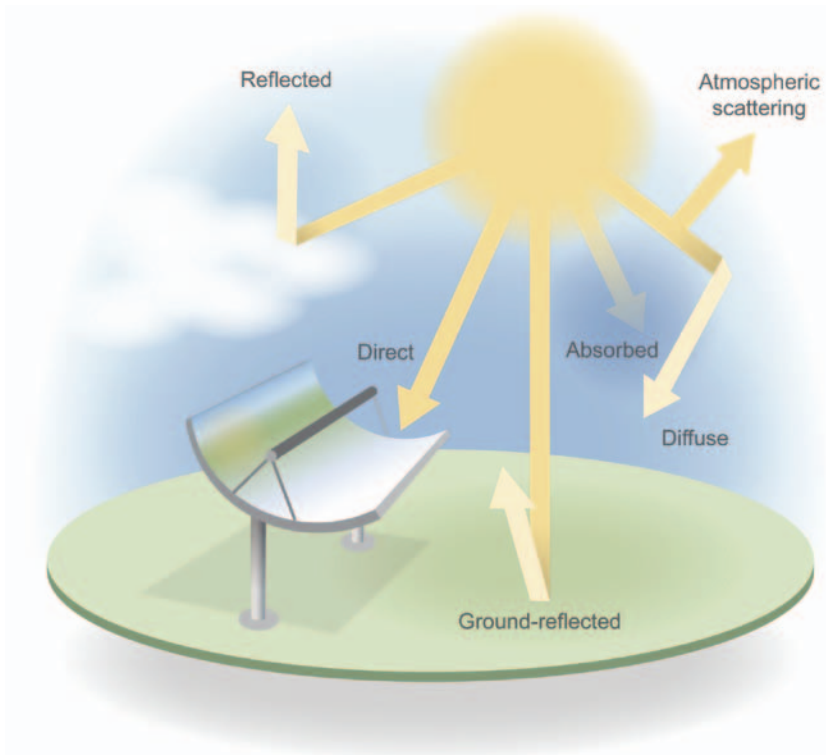
Figure 2-6. Solar radiation components resulting from interactions with the atmosphere

Direct Normal Irradiance

The World Meteorological Organization (WMO) defines DNI as the amount of radiation from the sun and a narrow annulus of sky as measured with a pyrheliometer designed with about a 5-degree field of view (FOV) full angle. In the absence of scattering by the atmosphere, the sun would appear to have a diameter subtending a 0.5-degree FOV. Therefore, DNI includes the forward-scattered radiation near the solar disk (also called circumsolar radiation). The effects of this scattering are as variable as the composition of the atmosphere at the time of observation. A sample of cloudless sky measurements from a circumsolar telescope illustrating this effect is shown in Figure 2-7 (see Grether et al. 1975). The five momentary measurements of relative DNI brightness from Barstow, California, and Atlanta, Georgia, are plotted as a function of angle from the center of the solar disk. The FOVs for two commonly used pyrheliometers are indicated for convenience (*cavity radiometer* refers to the electrically self-calibrating instrument used to maintain the measurement standard; *NIP pyrheliometer* refers to the field instruments used to monitor DNI [see Chapter 3]). The ratio C/S is computed from the energy available from the circumsolar brightness (C = 0.3 degrees to 3.2 degrees from the center of the solar disk) and the solar disk (S = 0.0 degrees to 0.3 degrees from the center of the solar disk). These ratios can range from a few percent to several tens of percent of the total (C + S). More information about circumsolar radiation is available from http://rredc.nrel.gov/solar/old_data/circumsolar/ and Major (1994). With the resurgence of interest in concentrating solar technology, there is a renewed interest and research in the amount of circumsolar radiation, or sunshapes, as affected by the variable properties of the atmosphere.

Part of the DNI can be reflected by the Earth's surface and local clouds. The magnitude and direction of this reflected radiation depend on the optical properties of the surface. Some of this radiation can also be reflected upward, and is subject to scattering and reflection by the atmosphere, resulting in a small additional contribution to the diffuse horizontal, or sky irradiance, discussed in the next section.
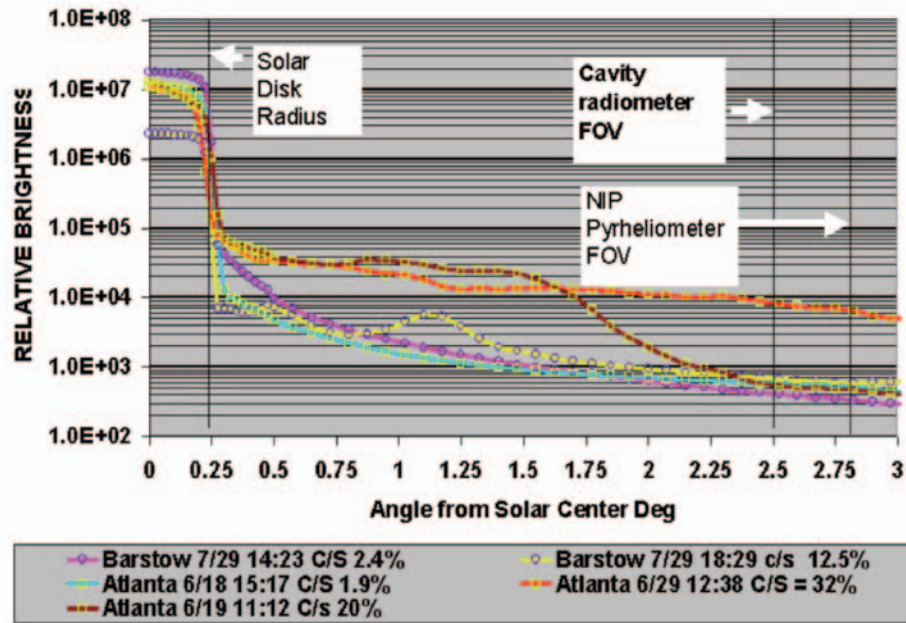
Credit: Daryl Myers, NREL

Figure 2-7. Sample measurements from a circumsolar telescope at Barstow, California, and Atlanta, Georgia (circa 1977)

Diffuse Horizontal Irradiance

A cloudless atmosphere absorbs and scatters radiation as the DNI penetrates to the ground. Parts of the DNI radiation are absorbed (removed) and reflected (scattered) in many other directions away from the path of this beam radiation. It is the scattered radiation we see as the sky radiation in the hemisphere above the ground. Lord Rayleigh (1871), Mie (1908), and Young (1981) developed theories for the mechanism of scattering in the atmosphere. These theories explain why the sky radiation appears blue (short wavelength, or blue light, is scattered more efficiently by atmospheric gases) and the solar disk tends to appear yellow and red at sunrise and sunset (the blue wavelengths are scattered a great deal out of our line of sight, but the longer red wavelengths from the solar disk come through unscattered). The sky radiation in the hemisphere above the local horizontal is called the DHI. A more technical definition of DHI is that it represents all radiation from the sky dome except the DNI (considered to be the quasi-parallel ray radiation from the solar disk). This includes radiation reflected or scattered by clouds (if present) and ground-reflected radiation is re-reflected downward by the atmosphere or clouds. Sky-reflected radiation is difficult to model because the photon interactions with the atmosphere are complex, clouds have varying compositions, and the ground has complex optical properties.

Global Horizontal Irradiance

The total hemispherical solar radiation on a horizontal surface is the sum of the flux density resulting the DNI at the given SZA, and the additional DHI:

$$\text{GHI} = \text{DNI} \cdot \text{Cos (SZA)} + \text{DHI} \tag{2-3}$$

SZA is the solar zenith angle computed from the date and time of measurement at a specific location.

This fundamental equation is the basis of most solar radiation measurement system designs, data quality assessments, and atmospheric radiative transfer models addressing the needs for solar resource data.

Solar Radiation Resources for Solar Energy Conversion

Determining the solar radiation components—GHI, DNI, or DHI, or some combination—that are applicable to a conversion system is the first step in evaluating design criteria and performance. Systems with concentrating optics rely on DNI availability. Low concentration systems may be able to use DHI radiation by light trapping techniques. Flat-plate collectors, fixed or variable in their mounting, can use all radiation components. GHI is most often the only available measured, or modeled, solar radiation data. In this case, conversion models are used to derive estimates of the appropriate quantities (Perez et al. 1987). The solar radiation scientific research community, peer-reviewed publications, and published reports are presently used to evaluate, validate, and assess the quality of these conversion algorithms. Models for estimating solar radiation are constantly appearing and being evaluated (Badescu 2008). A few classic examples are discussed in the next sections.

Model inputs are limited to site location, hour of interest, and GHI for the hour. We describe a quasi-physical model, based on the following premises:

- A physical model is used to calculate clear sky limits for the direct normal atmospheric transmittance.

- An exponential function of AM, similar in form to physical equations used to calculate energy transmission or propagation losses, is used to calculate deviations from clear sky transmittance values, based on atmospheric composition.

- The equations for computing Kn and other direct normal coefficients are continuously variable relative to Kt and AM and reproduce real-world variations in the relationship between DNI and GHI over monthly intervals.

The model is not a rigorous physical algorithm because the coefficients for computing clear sky transmittance values were derived from empirical regression analyses of measured DNI and GHI data from Atlanta, Georgia. Hourly average and thermopile radiometer data were used to derive the model. Applicability to higher time resolution (subhourly) data and solid-state (photodiode) radiometers that are subject to spectral effects, which do not sense the entire solar spectrum, is an open research question (see Maxwell 1987).

Estimating Direct Horizontal Irradiance From Global Horizontal Irradiance or Direct Normal Irradiance

Under clear and partly cloudy conditions, DHI is often a relatively small part (< 30%) of the GHI. Under overcast conditions, the GHI and DHI should be identical. When DHI measurements are not available, estimates of the diffuse may be needed in conjunction with GHI data to estimate DNI (as in the DISC model). DHI is also useful for daylighting applications. Many models based on empirical correlations between GHI and DHI data have been developed. Liu and Jordan (1960) developed a model for estimating monthly average hourly diffuse. Erbs et al. (1982), Orgill and Hollands (1977), Iqbal (1983), Spencer (1982), and many others have developed algorithms for estimating hourly DHI. These algorithms generally use correlations of global and diffuse clearness indices, Kt and Kd:

Estimating Direct Normal Irradiance From Global Horizontal Irradiance

One of the few models for estimating DNI from GHI is the Maxwell DISC (Direct Solar Insolation Code) and the Perez variation on this approach, DIRINT (Perez et al. 1990). This model is based on empirical relations between clearness indices Kt and Kn (Liu and Jordan 1960):

Kt	=	Clearness index or global horizontal transmittance of the atmosphere
	=	$GHI/TSI \cdot (r_0/r)^2 \cdot Cos\ (SZA)$
Kn	=	Direct normal transmittance of the atmosphere
	=	$DNI/TSI \cdot (r_0/r)^2$
where		
TSI	=	Total solar irradiance (mean TSI, ~ 1366.7 $Wm^{-2} \pm 7\ Wm^{-2}$)
r_0	=	mean Earth-sun distance (149,598 km)
r	=	Earth-sun distance at the time of interest
SZA	=	Solar zenith angle at the time of interest.

Kt   =   Clearness index or global horizontal transmittance of the atmosphere
           $GHI/[TSI \cdot (r_0/r)^2 \cdot Cos(SZA)]$

Kd   =   Diffuse transmittance of the atmosphere
           $DHI/[TSI \cdot (r_0/r)^2 \cdot Cos(SZA)]$

Modeled Datasets

As mentioned above, long-term measured datasets are rare, have variable periods of record, and inconsistent ease of access. Measurement networks or stations providing high-accuracy, up-to-the-minute measured data are rare. A wide variety of agricultural research station solar radiation data of highly variable quality are available. These types of data require careful evaluation and comparison with other sources of data, perhaps estimated or modeled data, to establish appropriateness of use. There are many sets of modeled solar radiation, typically GHI, sometimes with DNI, and DHI. A few examples are the National Solar Radiation Database (NSRDB), the Swiss Meteotest METEONORM dataset, the *European Solar Radiation Atlas, the* NASA *SSE,* and the European Community *Solar Data (SoDa)* datasets (see Chapter 5 for more details about these and other sources of data).

A popular modeled dataset is the TMY for a specific location. TMY datasets were originally designed for simplified building heating and cooling load calculations. The TMY consists of 8,760 hourly data records for one year. A TMY is the concatenation of 12 Typical Meteorological Months (TMMs) of data selected from a long-term period based on an optimized (weighted parameters) match of frequency distribution characteristics for the target month relative to the longer term. The TMM selection algorithm takes into account the distributions of solar radiation and several meteorological parameters. Thus, the resulting mean of a TMY parameter will be near (but not equal to) the mean of the parameter in the long-term dataset represented by the TMY. By design, a TMY does not include extremes of the dataset. The representative months may come from different years but are spliced together to give the continuous one-year time series. These datasets are used mainly to evaluate relative performance of different conversion system designs with respect to a standard dataset, and may not be appropriate for optimizing performance. Many software applications, however, use the TMY data to predict the typical performance of a solar conversion system.

Individual detailed descriptions of the properties of specific datasets will be discussed in Chapter 5.

Uncertainty Measurements and Models

Measurements of solar radiation are among the most uncertain in any measurement discipline. Empirical models developed from measured solar radiation data, and validation of any model with measured data, always include the measurement uncertainties in addition to the inherent model accuracy.

Solar radiation models based on physics are impossible to validate to an overall accuracy better than the uncertainty of the measured data. Measurement uncertainty analysis has been formalized by several organizations, including the International Bureau of Weights and Measurements (French acronym BIPM) and published by the International Standards Organization (ISO) as the *Guide to the Expression of Uncertainty in Measurements* (BIPM 1995).

Measurement Uncertainty

Uncertainty in measurements begins with the uncertainty in calibration references, calibration processes, and sensor design characteristics. As summarized in Figure 2.8, the resulting uncertainty in calibration factors must then be combined with the influence of additional sources of uncertainty in the field measurement instrumentation, installation methods, data acquisition, and operations and maintenance (O&M) processes. (More detailed information is provided in Chapter 4.)

Credit: Daryl Myers, NREL
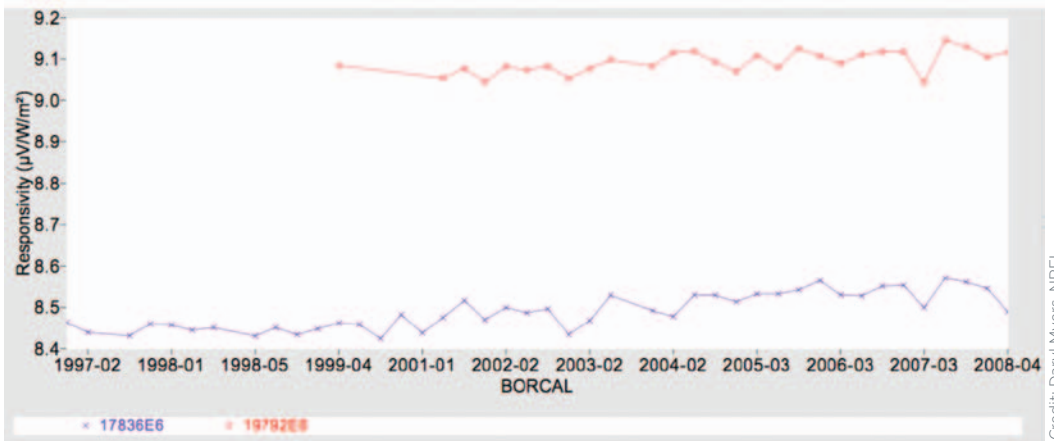
Figure 2-8. Calibration histories for two pyrheliometer control instruments spanning 12 years (arrows are ± 1% error bars)

Calibration Reference and Direct Normal Irradiance Uncertainty

The internationally accepted System Internationale (SI) traceable reference for the measurement of terrestrial solar radiation is the World Radiometric Reference (WRR). This internationally recognized measurement reference is a detector-based standard maintained by a group of electrically self-calibrating absolute cavity pyrheliometers at the World Radiation Center (WRC) maintained by the Physical Meteorological Observatory, Davos (PMOD), in Switzerland (see Chapter 3). The present accepted inherent uncertainty in the WRR is ± 0.30%. Reference cavity pyrheliometers used as national and institutional standards are calibrated against the WRR at international pyrheliometer comparisons conducted by the WRC once every five years. Transfer of calibration from WRR to national standards results in an expanded uncertainty[1] for these measurement standards of ± 0.45%. The annual transfer of calibration from national reference absolute cavity radiometers to pyrheliometers for field measurements results in absolute uncertainty (in the calibration factors) of ± 1.0%, mainly because of the environmental influences on the performance of field pyrheliometers. The calibration stability of commercially available pyrheliometers is generally < 1% change in responsivity (Rs) per year (see Figure 2-8). Results of a field pyrheliometer calibration for clear sky comparisons with an absolute cavity are shown in Figure 2-9. When finally deployed in the field, factors such as accuracy of solar tracking, data logger accuracy, cleanliness of the windows, frequency of recalibration, etc., may contribute more sources of uncertainty resulting in typical uncertainties of ± 2.0% to ± 2.5% (or greater) in DNI measurements from a very carefully conducted, high-quality measurement system (see Chapter 3 for more details).

---

[1] See page 29 for measurement uncertainty terminology.
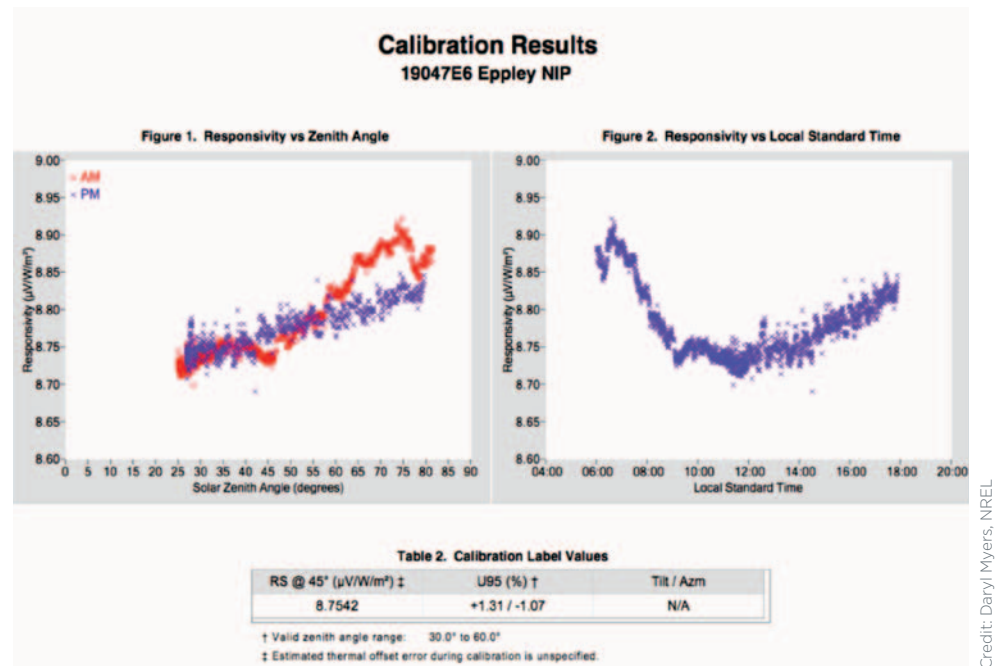
Figure 2-9. Pyrheliometer calibration results summarizing Rs versus SZA (left) and versus local standard time (right)

Uncertainty in Pyranometer Calibrations and Global Horizontal Irradiation Measurements

The WRR is also the reference for calibration of pyranometers used to measure GHI and DHI. Physically, it is assumed the hemispherical detectors in a pyranometer respond only to the vertical component of the DNIVertical based on the SZA at the time of measurement:

$DNI_{Vertical}$ = $DNI \cdot Cos(SZA)$.

The pyranometer detector is assumed to have no response to the horizontal component of

$DNI_{Horizontal}$

$DNI_{Horizontal}$ = $DNI \cdot Sin(SZA)$.

Using the relationship described in section 2.5.3 for GHI, DNI, DHI, and SZA:

GHI = $DNI \cdot Cos(SZA) + DHI$

we can compute the DNI as:

DNI = $(GHI – DHI)/Cos(SZA)$.

The GHI and DHI are measured by unshaded and shaded pyranometers, respectively (see Chapter 3). Thus, we can use the above relationship to calibrate a single pyranometer.

By alternately shading and unshading the detector surface of a pyranometer on a clear day, the difference in output signal between shaded (V_{shade}) and unshaded ($V_{unshade}$) conditions can be compared with the reference DNI measurement to compute the Rs of the pyranometer under test:

Rs (Volts/W/m^2) = $[(V_{unshade} – V_{shade})/Cos(SZA)]/DNI$.

This is called the *shade/unshade* calibration technique, and is described in more detail by Reda et al. (2003).

Alternatively, the radiometer can be calibrated by using a reference pyrheliometer to measure DNI and a continuously shaded pyranometer (calibrated using the above shade/unshade

technique) to compute a reference GHI. The Rs of pyranometer(s) under calibration can be computed from their unshaded signal ($V_{unshade}$):

$$Rs\ (Volts/W/m^2)\ \ =\ \ \ V_{unshade}/(DNI \cdot cos\ (SZA) + DHI).$$

Computing the Rs in this way is called the *component summation calibration technique.*

The shade/unshade and component summation techniques, when conducted over a range of SZA, demonstrate pyranometers, which by design have differing non-Lambertian, or nonideal response as a function of the SZA (or incidence angle) of the DNI. The differences in Rs as a function of SAZ are like fingerprints or signatures for each individual (not just type) of pyranometer detector. Figure 2-10 shows that variations of pyranometer Rs can be symmetrical with respect to solar noon, or highly skewed, depending on the mechanical alignment of the pyranometer detector, the detector surface structure, and the detector absorber material properties.
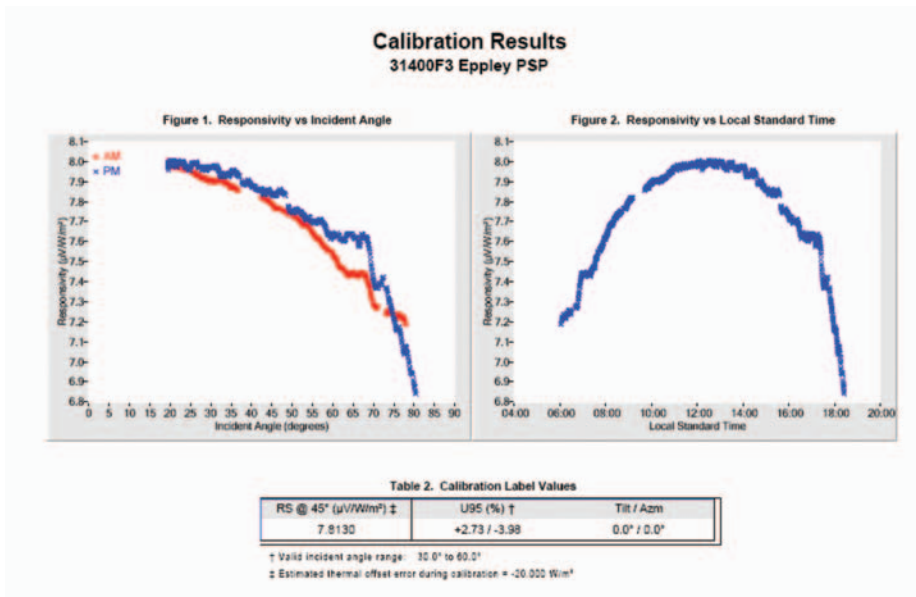
Figure 2-10. Pyranometer calibration results summarizing Rs versus SZA (left) and local standard time (right)

Typical calibration uncertainty for any sensor with respect to a WRR reference cavity radiometer is about 0.5% at any one very narrow range (± 2 degrees to ± 5 degrees) of zenith angle. Over a wide range of zenith angles (0 degrees to 85 degrees), the Rs can vary by 10 to 20 times that over a narrow range, or from ± 3% to ± 10% or even more. These effects then need to be combined with the field measurement influences, just as with the DNI measurement uncertainty estimate (e.g., include pyranometer installation, data logger accuracy, and cleanliness).

These larger high zenith angle-related uncertainties occur over parts of the day (morning and afternoon) when the available solar resource is much smaller than typical midday resources, when the zenith angles are smaller. Because the maximum elevation (minimum zenith) angles vary through the seasons, the uncertainty in hemispherical radiation data will vary as well.

Even in the good measurement regime of midday, hemispherical field measurement uncertainty is typically two to three times that of direct-beam measurements, or ± 4% to ± 5%, over a year, mainly because of these seasonal uncertainty variations. Better instrumentation design and careful applications of correction factors as a function of zenith angles are ways to improve (reduce) the uncertainty in GHI measurements. The alternative is to use high-quality DNI and DHI measurements using a tracking shading disk/ball to compute GHI. The

measurement uncertainties for GHI then approach that of the DNI (± 2%) for clear sky measurements.

Figure 2-11 shows the calibration traceability for pyrheliometers used to measure DNI and pyranometers used to measure GHI or DHI and indicates how measurement uncertainties accumulate from calibration to field deployment. Broad arrow boxes show accumulated uncertainty at each phase of the process. The resulting field deployment uncertainties for pyrheliometers used for measuring DNI is ± 2.0%. Measurement uncertainties for pyranometers used to measure GHI in the field range from ± 3.0% for SZA between 30 degrees and 60 degrees and up to ± 7% to ± 10% for SZA greater than 60 degrees.

An overview for estimating the measurement uncertainty of DNI is available in Chapter 3.
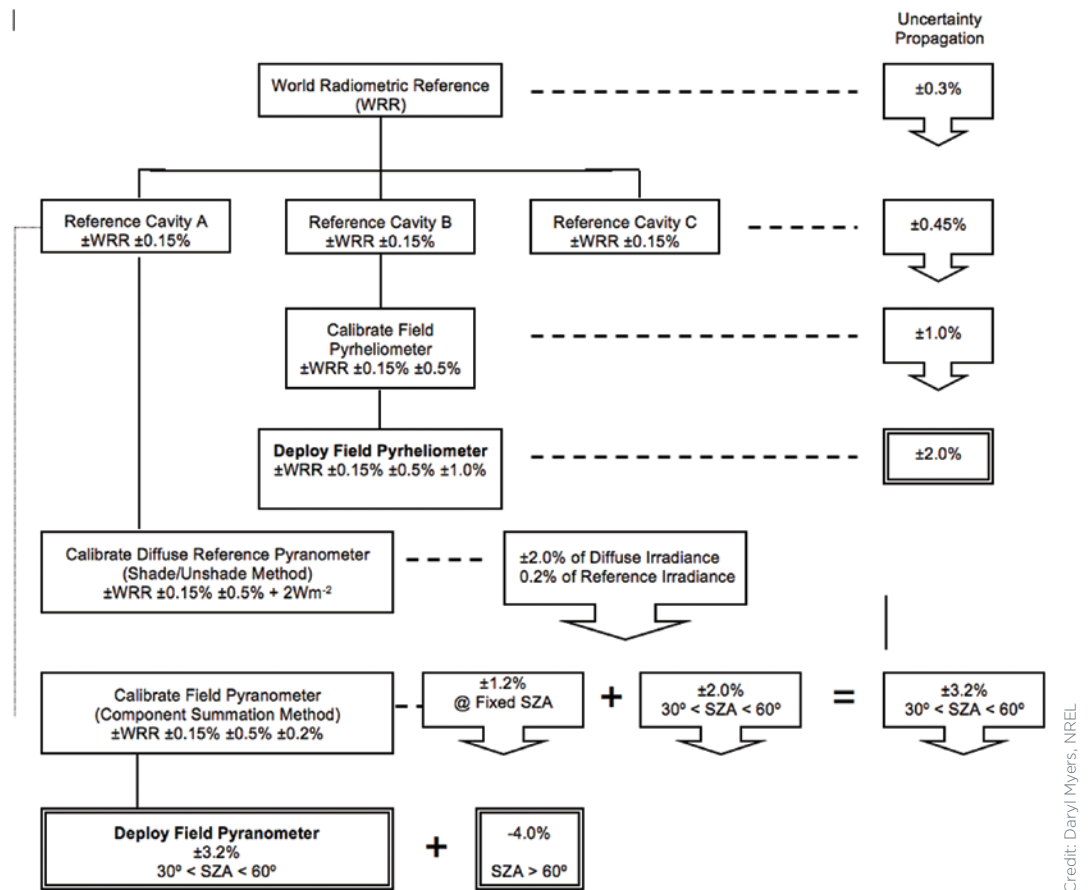
Figure 2-11. Calibration traceability and accumulation of measurement uncertainty for pyrheliometers and pyranometers

Model Estimate Uncertainties

Empirical models derived from measured data correlations with independent parameters inherently carry measurement uncertainty embedded in the ultimate model accuracy. Models based on 2% or 5% or 10% accurate measurements can be no more accurate than the data used to generate the model. Typically, scatter about model regression lines increases the random component of uncertainty further. Models based on first principles of physics and radiation transfer cannot be validated or verified to a level of accuracy greater than that of the measurements. Beware of claims of high accuracy in models or measurements without a thoroughly documented uncertainty analysis (Gueymard and Myers 2009).

Spatial and Temporal Variability of Solar Resources

We described earlier the variation of the ETR as a function of the 11-year sunspot cycle (less than ± −0.2%), and the annual variation of the Earth-sun distance (± −3%). These are minor variations compared with the influences of the atmosphere, weather, climate, and geography on the variation of solar resources at the Earth's surface. Variations in solar radiation from month to month, especially in the latitudes outside the tropics, follow an annual pattern, generally during the summer, with lower values during the winter. The year-to-year variation in these patterns is called the *interannual variability*. The coefficient of variation (COV), or ratio of the standard deviation to the mean of a set of given averages, can be used to quantify this variability. Studies of GHI and DNI distributions in the United States show the range of GHI interannual variability is typically 8%–10%. This is generally about half, or less, of the variability of DNI, which can be 15% or more at the 66% confidence interval (Wilcox and Gueymard 2010).

A typical measure of variability is the COV, defined as the standard deviation of a dataset (e.g., annual averages for several years) divided by the average of the dataset. Studies show the COV for annual averages of DNI can approach 10%, depending on climate stability (NSRDB Daily Statistics Files indicate COV for Daggett, California, is 6.2%). Interannual COV for annual averages GHI is typically 5%. The COV is based on a single standard deviation, and is typically about one-third the range of data in a sample.

Differences between radiation resources in the same months in different years are generally larger during the winter and smaller during the summer in the continental United States. Variations in weather and natural events such as forest fires, volcanic eruptions, dust clouds from drought regions, and agricultural activity all can contribute to interannual variations. Figure 2-12 compares the mean and maximum and minimum monthly average daily total GHI from the 1961–1990 NSRDB (modeled from meteorological data) with eight individual years of estimates based on satellite data (1998–2005) for Daggett, California. Variations much greater or somewhat smaller than this can be seen for locations with more or less variable weather patterns.
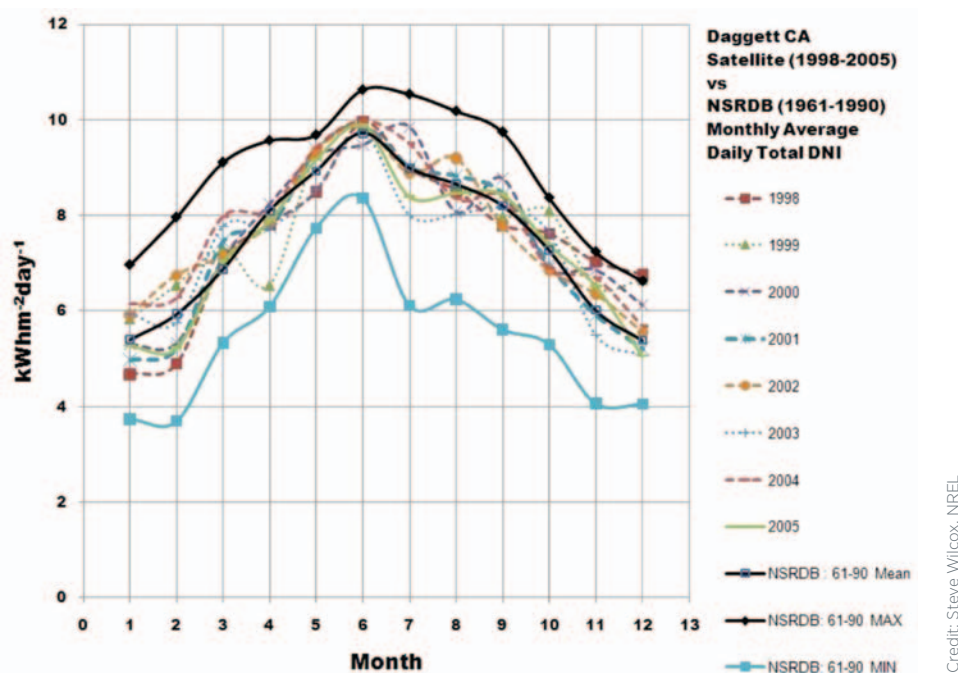
Figure 2-12. Example of direct-beam monthly average daily total (kWh/m²/day) interannual variability from 1961 through 2005 for Daggett, California
(Data from NSRB)

Spatial variations in solar resources often come into question, especially if nearby or neighboring measured data are available for a site without measured data. Mountainous terrain or highly variable urban, agricultural, or other microclimate influences may contribute to high spatial variability of the solar resource. Analysis of measured and modeled data correlations with distances between stations has generally shown that correlations decrease with increasing station spacing and higher time resolution (e.g., 15 minute versus hourly) data integration periods. One study of 17 sites in Wisconsin showed that correlations for hourly data fall from 0.995 to 0.97 as spacing increases from 5 km to 60 km. For 15-minute data, the correlations fall from 0.98 to less than 0.75 at more than 100 km (see Chapter 6).

Prevailing winds and cloud motion patterns can also affect both spatial and temporal variability over distances from a few to hundreds of kilometers. A study of a dense solar measurement network in Oklahoma showed correlations between stations degrade from 95% or better for nearby stations to less than 45% for stations greater than 300 km away, depending on the geographical relationship (east, west, northwest, etc.) between the stations. Barnett et al. (1998) provided a correlelogram for these analyses. Attempts to interpolate between stations to estimate solar resources should be used with caution. Attention to the data sample period, geography, terrain, weather patterns, and spacing is important and requires careful analyses.

Chapter 3. Measuring Solar Radiation

Accurate measurements of DNI are essential to CSP project design and implementation. Because DNI data are relatively complex, and therefore expensive compared with other meteorological measurements, they are available for only a limited number of locations. Increasingly, developers are in need of DNI data for site resource analysis, system design, and plant operation. DNI measurements are also used to develop and test models for estimating DNI and other solar irradiance components based on available surface meteorological observations or satellite remote sensing techniques. DNI measurements will also play an important role in developing solar resource forecasting techniques.

This chapter focuses on the instrument selection, installation, design, and O&M of measurement systems suitable for collecting DNI resource measurements.

Instrumentation Selection Options

Before considering instrumentation options and the associated costs, the user must first evaluate the data accuracy or uncertainty levels that will satisfy the ultimate analyses based on the DNI measurements. This ensures the best value can be achieved after the available various measurement and instrumentation options are considered (see the Appendix for a list of radiometer manufacturers and distributors).

By first establishing the project needs for DNI accuracy, the user can base instrument selection and the levels of effort for operating and maintaining the measurement system on an overall cost-performance determination. Specifically, "first-class" instrumentation should not be purchased if the project resources cannot support the maintenance required to ensure measurement quality consistent with the radiometer design specifications and manufacturer recommendations.

Redundant instrumentation is another important consideration to ensure confidence in data quality. Multiple radiometers within the project location and/or providing for the measurement of all three solar irradiance components (GHI, DHI, and DNI), regardless of the primary measurement need, can greatly enhance opportunities for post-measurement data quality assessment (see page 39).

Instrument Types

Instruments designed to measure any form of radiation are called radiometers. In this section, we will summarize the types of radiometers most commonly used to measure solar radiation resources for application to CSP technology needs.

Pyrheliometers and Pyranometers

Pyrheliometers and pyranometers are two types of radiometers used to measure solar irradiance. Their ability to receive solar radiation from two distinct portions of the sky distinguishes their designs. As described in Chapter 2, pyrheliometers are used to measure DNI and pyranometers are used to measure GHI, DHI, or plane-of-array (POA) irradiances. Table 3-1 summarizes some key attributes of these two radiometers.

Table 3-1. Solar Radiation Instrumentation

Radiometer Type	Measurement	FOV (full angle)	Installation
Pyrheliometer	DNI	5.7 degrees to 6.0 degrees	Mounted on automatic solar tracker for alignment with the solar disk
Pyranometer	GHI	2 π steradians	Mounted on stable horizontal surface free of local obstructions*
Pyranometer	DHI	2 π steradians	Mounted on automatic solar tracker fitted with shading mechanism or on a manually adjusted shadowband platform for blocking DNI from detector surface*
Pyranometer	POA	2 π steradians	Mounted in the POA of the flat plate solar collector*

* Optionally installed with powered ventilator to reduce contamination of optical surfaces.

Pyrheliometers and pyranometers commonly use either a thermoelectric or photoelectric detector for converting solar flux (W/m^2) into a proportional electrical signal (μVdc). Thermoelectric detectors have an optically black coating that allows for a broad and uniform spectral response to all solar radiation wavelengths between about 300 nm and 3,000 nm (Figure 3-1). Due to the relatively large thermal mass of this detector design, the time-response characteristics are typically 1–5 s.[2] That is, the output signal lags the changes in solar flux. Photoelectric detectors, however, generally respond to only the visible and near infrared spectral regions from about 400 nm to 1,100 nm (Figure 3-2). These detectors have very fast time-response characteristics—on the order of microseconds. For either detector, as installed in commercially available instruments, the electrical signal generated by exposure to solar irradiance levels of about 1,000 W/m^2, is on the order of 10 mVdc (assuming no amplification of the output signal). This rather low-level signal requires proper electrical grounding and shielding considerations during installation (see Chapter 5).

NREL/PIX 03962

Figure 3-1. Thermopile assembly used in The Eppley Laboratory, Inc. Model PSP

_____

[2] Physically, the constant represents the time it takes the system's step response to reach (1−1/e) or about 36.8% of the total stimulus change.
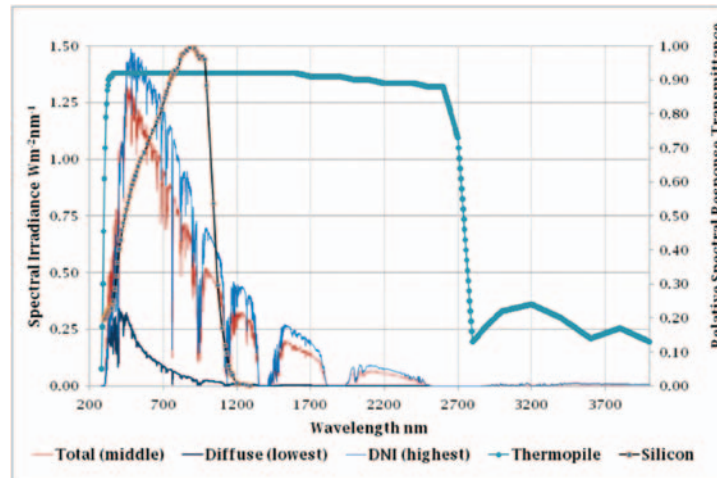
Figure 3-2. Typical photodiode detector (left) and spectral response of LI-COR pyranometer (right). Used by permission of LI-COR Biosciences, Inc.

Because of their narrow FOV (typically 5.7 degrees or 6.0 degrees full-angle), pyrheliometers are mounted in automatic solar trackers to maintain the instrument's alignment with the solar disk and fully illuminate the detector from sunrise to sunset (Figures 3-3 and 3-4). Alignment of the pyrheliometer with the solar disk is determined by a simple diopter, or sighting device in which a small spot of light (the solar image) falls on a mark in the center of a target located near the rear of the instrument (Figure 3-5). By convention and to allow for small variations in tracker alignment, view-limiting apertures inside a pyrheliometer allow for the detection of radiation in a narrow annulus of sky around the sun (WMO 2008). This circumsolar radiation component is due to the forward scattering of radiation near the solar disk caused by atmospheric aerosols and other constituents that can scatter solar radiation. Depending on the FOV and tracker alignment, pyrheliometer measurements include varying amounts of circumsolar irradiance contributions to the DNI.
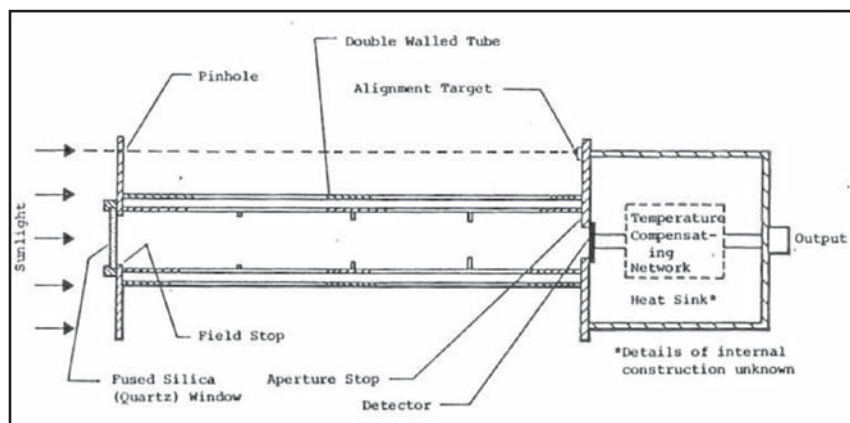
Figure 3-3. The Eppley Laboratory, Inc. Model NIP (normal incidence pyrheliometer) schematic (Bahm and Nakos 1979)

Credit: Tom Stoffel, NREL

Figure 3-4. Pyrheliometers mounted on automatic solar tracker
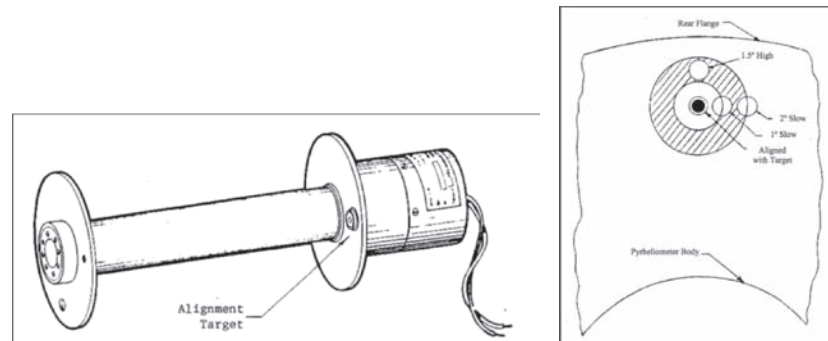
Figure 3-5. Pyrheliometer alignment diopter configuration
(Micek 1981) (Used by permission of Leonard Micek.)

The most accurate measurements of DNI are accomplished using an electrically self-calibrating absolute cavity radiometer (see Figure 3-6). Described in Chapter 2, this type of pyrheliometer is the basis for the WRR, the internationally recognized detector-based measurement standard for DNI as shown in Figure 3-7 (Fröhlich 1991). By design, absolute cavity radiometers have no window and are therefore generally limited to fully attended operation under clear sky conditions to protect the integrity of the receiver cavity (Figure 3-8). Removable windows and temperature-controlled "all-weather" designs are available for automated continuous operation of these pyrheliometers. However, the installation of the protective window nullifies the "absolute" nature of the DNI measurement. The window introduces additional measurement uncertainties associated with the optical transmittance properties of the window (made from either quartz or calcium fluoride) and the changes to the internal heat exchange due to the now sealed system.

Credit: Tom Stoffel, NREL

Figure 3-6. Multiple electrically self-calibrating absolute cavity radiometers mounted on solar trackers with control and data acquisition electronics

NREL/PIX 08087

Figure 3-7. The World Standard Group of six absolute cavity radiometers is used to define the WRR or DNI measurement standard

Figure 5.15
Schematic of a typical absolute cavity pyrheliometer.

Credit: NREL
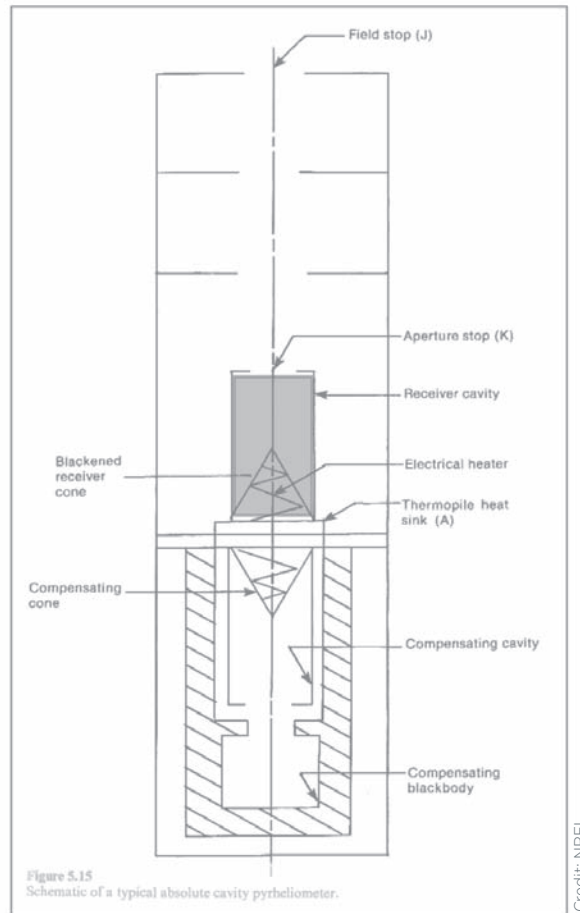
Figure 3-8. Schematic of The Eppley Laboratory, Inc. Model AHF absolute cavity pyrheliometer
(after Reda 1996)

A pyranometer has a thermoelectric or photoelectric detector with a hemispherical or "fish-eye" FOV (360 degrees or 2π steradians) (see Figure 3-9). This type of radiometer is generally mounted on a horizontal platform for measuring GHI. In this orientation, the pyranometer has a complete view of the sky dome. Ideally, the mounting location for this instrument is free of natural or artificial obstructions on the horizon. The pyranometer detector is mounted under a protective precision-ground quartz (or other material) dome or a diffuser. Both designs protect the detector from the weather and provide optical properties consistent with receiving hemispheric solar radiation. To reduce the potential for contaminating the pyranometer optics caused by dust, dew, frost, snow, ice, insects, or other material, pyranometers can be fitted with ventilators that constantly blow air—sometimes heated—from under the instrument and over the dome (Figure 3-10). These ventilation devices can, particularly when heated, require a significant amount of electrical power, adding to the required capacity for on-site power generation in remote areas. Ventilators also affect the thermal offset characteristics of pyranometers with single-black detectors (Vignola et al. 2009). Consistent with their low-cost design based on a photodiode detector, these pyranometer designs employ a diffuser above the detector (Figure 3-11). Acrylic diffusers can be more dust tolerant than optical glass domes (Maxwell et al. 1999).
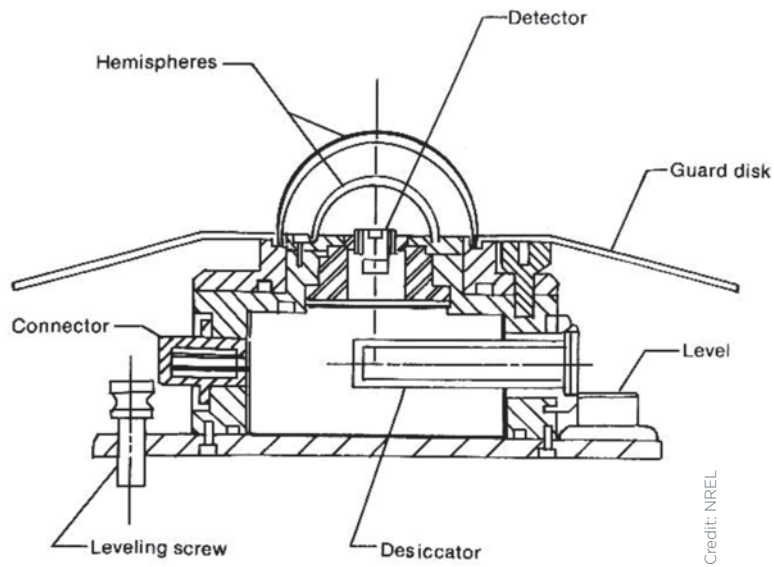
Credit: NREL

Figure 3-9. Schematic of The Eppley Laboratory, Inc., Model PSP (precision spectral pyranometer)

Credit: Tom Stoffel, NREL

Figure 3-10. Kipp & Zonen Model CM22 pyranometers installed in CV2 ventilators

Credit: Tom Stoffel, NREL

Figure 3-11. LI-COR Model 200SA pyranometer with photodiode detector and acrylic diffuser fore optic
(from www.licor.com)

Pyrheliometer and Pyranometer Classifications

The ISO and the WMO have established classifications and specifications for the measurement of solar irradiance (ISO 1990; WMO 2008). We encourage the reader to review these documents in more detail as part of the project planning for solar resource measurements before acquiring pyrheliometers or pyranometers.

Estimated measurement uncertainty is the basis for these pyrheliometer and pyranometer classifications. The WMO (2008) recognizes the difficulties associated with measuring solar irradiance:

> It may be said generally that good quality measurements are difficult to achieve in practice, and for routine operations they can be achieved only with modern equipment and redundant measurements. Some systems still in use fall short of best practice, the lesser performance having been acceptable for many applications. However, data of the highest quality are increasingly in demand.

The WMO characteristics of operational pyrheliometers and pyranometers are presented in Tables 3-2 and 3-3. The ISO specification lists for these radiometers are presented in Tables 3-4 and 3-5. Our purpose for providing these classifications is to address questions about differences in data quality and to give the reader a better understanding of the data quality afforded by particular instrument classes.

Table 3-2. WMO Characteristics of Operational Pyrheliometers for Measuring DNI

Characteristic	High Quality	Good Quality
Response time (95% response).	< 15 s	< 30 s
Zero offset – response to 5 K/h change in ambient temperature.	2 W/m^2	4 W/m^2
Resolution – smallest detectable change in W/m^2.	.051	1
Stability – change per year, percentage of full scale.	.01	.05
Temperature response – percentage maximum error due to any change of ambient temperature within an interval of 50 K.	1	2
Nonlinearity – percentage deviation from the responsivity at 500 W/m2 due to any change of irradiance within the range 100 to 1100 W/m^2.	.02	.05
Spectral sensitivity – percentage deviation of the product of spectral absorptance and spectral transmittance from the corresponding mean within the range of 300 to 3000 nm.	.05	1.0
Tilt response – percentage deviation from the responsivity at 0 degrees tilt (horizontal) due to change in tilt from 0 degrees to 90 degrees at 1000 W/m^2.	.02	.05
Achievable uncertainty (95% confidence level): **1-min totals** Percent kJ/m2 Wh/m2 **1-h totals** Percent kJ/m^2 Wh/m^2	 0.9 0.56 0.16 0.7 21 5.83	 1.8 1 0.28 1.5 54 15.0

Table 3-3. WMO Characteristics of Operational Pyranometers for Measuring GHI or DHI

Characteristic	High Quality	Good Quality	Moderate Quality
Response time – 95% response	< 15 s	< 30 s	< 60 s

Zero offset
    Response to 200 W/m^2 net thermal radiation (ventilated)
    Response to 5 K/h change in ambient temperature
	7 W/m^2
	2 W/m^2
		7 W/m^2
		2 W/m^2
			7 W/m^2
			2 W/m^2

Resolution – smallest detectable change	1 W/m^2	5 W/m^2	10 W/m^2
Stability – change per year, percentage of full scale	.08	1.5	3.0
Directional response for beam radiation – the range of errors caused by assuming that the normal incidence Rs is valid for all directions when measuring, from any direction, a beam radiation whose normal incidence irradiance is 1000 W/m^2	10 W/m^2	20 W/m^2	30 W/m^2
Temperature response – percentage maximum error due to any change of ambient temperature within an interval of 50 K	2	4	8
Nonlinearity – percentage deviation from the Rs at 500 W/m^2 caused by any change of irradiance within the range of 100 to 1000 W/m^2	.05	1	3
Spectral sensitivity – percentage deviation of the product of spectral absorptance and spectral transmittance from the corresponding mean within the range 300 to 3 000 nm	2	5	10
Tilt response – percentage deviation from the Rs at 0 degrees tilt (horizontal) caused by change in tilt from 0 degrees to 90 degrees at 1000 W/m^2	0.5	2	5

Achievable uncertainty – 95% confidence level
    Hourly totals
    Daily totals
	3%
	2%
		8%
		5%
			20%
			10%

Even among the instrument classifications and specifications, there can be some measurement uncertainty variations. The user should research various instrument models to gain familiarity with the design and measurement characteristics in view of a particular application (Myers and Wilcox 2009; Wilcox and Myers 2008).

Table 3-4. ISO Specifications Summary for Pyrheliometers Used To Measure DNI

Pyrheliometer Specification List			
Specification	**Class of Pyrheliometer**		
	Secondary Standard	**First Class**	**Second Class**
Response time – 95% response	< 15 s	< 20 s	< 30 s
Zero offset – Response to 5 K h^{-1} change in ambient temperature	± 2 Wm^{-2}	± 4 Wm^{-2}	±8 Wm^{-2}
Resolution – smallest detectable change in Wm^{-2}	± 0.5 Wm^{-2}	± 1 Wm^{-2}	± 5 Wm^{-2}
Stability – percentage of full scale, change/year	± 0.5%	± 1%	± 2%
Nonlinearity – percentage deviation from the responsivity at 500 W/m^2 due to change in irradiance within 100 Wm^{-2} to 1000 Wm^{-2}	± 0.2%	± 0.5%	± 2%
Spectral selectivity – percentage deviation of the product of the spectral absorptance and the spectral transmittance from the corresponding mean within 0.3 µm and 3.0 µm	± 0.5%	± 1%	± 5%
Temperature response – total percentage deviation due to change in ambient temperature within an interval of 50 K	± 1%	± 2%	± 10%
Tilt response – percentage deviation from the responsitivity at 0 degrees tilt (horizontal) due to change in tilt from 0 degrees to 90 degrees at 1000 W/m^{-2} irradiance	± 0.2%	± 0.5%	± 2%
Traceability – maintained by periodic comparison	With a primary standard pyrheliometer	With a secondary standard pyrheliometer	With a first class pyrheliometer or better

Table 3-5. ISO Specifications Summary for Pyranometers Used To Measure of GHI and DHI

Pyrheliometer Specification List			
Specification	**Class of Pyrheliometer***		
	Secondary Standard	**First Class**	**Second Class**
Response time – 95% response	< 15 s	< 30 s	< 60 s
Zero offset 　Response to 200 Wm^{-2} net thermal radiation (ventilated) 　Response to 5 K h^{-1} change in ambient temperature	+ 7 Wm^{-2} ± 2 Wm^{-2}	+ 15 Wm^{-2} ± 4 Wm^{-2}	+ 30 Wm^{-2} ± 8 Wm^{-2}
Resolution – smallest detectable change	± 1 Wm^{-2}	± 5 Wm^{-2}	± 10 Wm^{-2}
Stability – percentage change in responsivity per year	± 0.8%	± 1.6%	± 2%
Nonlinearity – percentage deviation from the responsivity at 500 W/m^{-2} due to change in irradiance within 100 Wm^{-2} to 1000 Wm^{-2}	± 0.2%	± 0.5%	± 2%
Directional response for beam radiation (the range of errors caused by assuming that the normal incidence responsivity is valid for all directions when measuring, from any direction, a beam radiation whose normal incidence irradiance is 1000 Wm^{-2}	± 10 Wm^{-2}	± 20 Wm^{-2}	± 30 Wm^{-2}
Spectral selectivity – percentage deviation of the product of the spectral absorptance and the spectral transmittance from the corresponding mean within 0.3 μm and 3.0 μm	± 2%	± 5%	± 10%
Temperature response – total percentage deviation due to change in ambient temperature within an interval of 50 K	2%	4%	8%
Tilt response – percentage deviation from the responsitivity at 0 degrees tilt (horizontal) due to change in tilt from 0 degrees to 90 degrees at 1000 W/m^{-2} irradiance	± 0.5%	± 2%	± 5%

* The highest category for pyranometers is the secondary standard, because the most accurate determination of GHI has been suggested to be the sum of the DNI as measured by an absolute cavity radiometer and the DHI as measured by a secondary standard pyranometer shaded from the DNI by a disk.

Rotating Shadowband Radiometers

Rotating shadowband radiometers (RSRs) use a pyranometer that is periodically shaded by a motorized shadowband that moves across the detector's FOV (Figure 3-12). By design, the instrument measures GHI when unshaded and DHI when shaded. Using the following equation relating GHI, DHI, and DNI, the DNI is calculated from GHI, DHI, and the solar position at the time of band rotation (Figure 3-13). Although this instrument is motorized and requires energy for electronics necessary to operate the system, the electrical power requirements of some commercially available units is low enough to be powered by a small photovoltaic (PV) panel and storage battery. Such a design is well suited for remote installations where conventional power is not available. Most models incorporate some type of postprocessing where the measurements are corrected for known errors, such as effects of shade band

geometry and pyranometer response characteristics for temperature and solar spectral distributions. Sometimes the corrections are site-specific, requiring empirical testing to establish their magnitude. Users should inquire of the manufacturer about whether such postprocessing is part of the instrument package and is readily available.

$$DNI = \frac{(GHI - DHI)}{Cos\,(SZA)}$$

Figure 3-12. Two commercially available RSRs: Irradiance, Inc. Model RSR (left) and Yankee Environmental Systems, Inc. Model SDR-1 (two units shown on right)
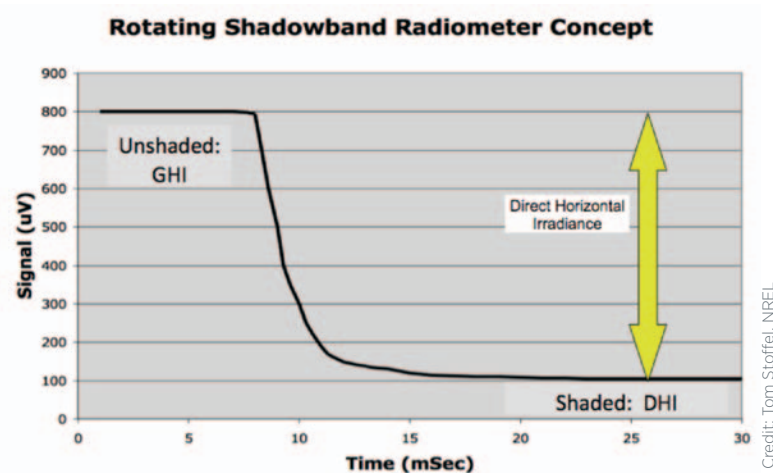
Figure 3-13. Time-series data concept for RSR measurements illustrating the difference between the two measured quantities (GHI and DHI) is proportional to the vertical component (direct horizontal or DH) of the DNI (DNI = DH/Cos (SZA)

Measurement Uncertainty

Every measurement only approximates the quantity being measured, and is incomplete without a quantitative statement of uncertainty. Each element of a measurement system contributes to the final uncertainty of the data. Accurate measurements of solar irradiance depend on the radiometer design, hardware installation scheme, data acquisition method, measurement system O&M, calibration method and frequency, and possible real-time or a posteriori corrections to the data. A successful measurement uncertainty analysis produces no properly measured data that exceed the expected range of uncertainty.

This overview of measurement uncertainty is based on Myers et al. (2002), Reda et al. (2007), Stoffel et al. (2000), and Wilcox and Myers (2008).

Terminology

Historically, uncertainty analysis treated sources of uncertainty in terms of "random" and "bias" error types. Random sources were related to the standard deviation or variance of measured datasets. Biases were estimates of deviations from a "true value" primarily based on engineering judgments of the measurement system performance. Total uncertainty (UT) was computed as the square root of the sum of the squares for these two error types:

$$\text{UT} \quad = \quad [\Sigma\,(\text{Bias})^2 + \Sigma(2\cdot\text{Random})^2]^{1/2}$$

where the factor of 2 in the random term was necessary to "inflate" the random component to provide approximately a 95% confidence interval for the computed value of UT, assuming the data were normally distributed (i.e., random).

The WMO (2008) is currently the accepted guide for measurement uncertainty (BIPM et al. 1995). GUM defines Type A uncertainty values as derived from statistical methods, and Type B sources as evaluated by "other means," such as scientific judgment, experience, specifications, comparisons, and calibration data. GUM defines the concept of a *standard uncertainty* (U_{std}) for each uncertainty type, which is an estimate of an *equivalent* standard deviation (of a specified distribution) of the error source. The *combined uncertainty* (U_C) is computed from the Type A and Type B standard uncertainties summed under quadrature. The GUM replaces the historical factor of 2 with a *coverage factor*, k (which depends on the known or assumed statistical distribution of uncertainties) and computes the *expanded uncertainty* (U_E) as:

$$U_E \quad = \quad [\Sigma\,(\text{Type B})^2 + \Sigma\,(k \cdot \text{Type A})^2]^{1/2}$$

For small samples (n < 20) from a normal distribution, k may be selected from the Student's t-distribution. The coverage factor (k) is usually in the range of 2 to 3 for confidence intervals of 95% and 99%, respectively (Taylor and Kuyatt 1987). For a 95% confidence interval, UE is twice the value of U_C.

When a result, R, is functionally dependent on several variables x_i, where i = 1 to n, the propagation of error is used:

$$U_R \quad = \quad [\Sigma i\,(\partial X_i\, R \cdot e\, X_i)^2]^{1/2}$$

where

U_R	=	Uncertainty in the resultant
e_{Xi}	=	estimated uncertainty in variable x_i
$\partial_{Xi}\, R$	=	the partial derivative of the response R with respect to x_i (sensitivity function for variable x_i).

The GUM procedure can be summarized in four steps:

1. Determine the process measurement equation.

2. List or estimate the standard uncertainty for each variable in the measurement equation and for each component (curve fitting uncertainty, environmental conditions uncertainty, etc.) that might introduce uncertainty to the measurement process.

3. Calculate the combined standard uncertainty using the root-sum-of-squares method of all standard uncertainties in step 2.

4. Calculate the expanded uncertainty by multiplying the combined standard uncertainty by the coverage factor, typically by applying Student's "t" analysis to determine the appropriate coverage factor (typically 2 for 95% and 3 for 98% confidence, respectively, for large datasets).

Estimating Direct Normal Irradiance Measurement Uncertainty

There are two measurement processes applicable to DNI measurement uncertainty analysis:

- Pyrheliometer calibration
- Field measurements.

Estimating the Uncertainty of Pyrheliometer Calibrations

The pyrheliometer responsivity (Rs_i) is computed as the microvolts (µV) per W/m^2 at each measurement comparison (i) typically made at 1-s to 60-s intervals with a reference or transfer standard radiometer (typically an electrically self-calibrating absolute cavity radiometer traceable to the WRR) and the output signal from the pyrheliometer under calibration:

$$Rs_i \quad = \quad V_i/REF_i$$

where

V_i =   Pyrheliometer output voltage (µV)

REF_i =   Reference DNI (W/m^2)

Applying the GUM procedure to the pyrheliometer calibration, Table 3-6 summarizes the uncertainties for 95% confidence interval for the individual pyrheliometer responsivity results.

Table 3-6. Estimated Pyrheliometer Calibration Uncertainties in Rsi

Type A Error Source	U_{std}(%)	Type B Error Source	U_{std}(%)
WRR transfer	0.200	WRR uncertainty (U_E, k=2)	0.3
Absolute cavity responses to environmental conditions	0.013	Absolute cavity bias responses to environmental conditions	0.013
Data logger precision	0.0025	Data logger bias (9µV/10mV)	0.09
Pyrheliometer detector temperature response	0.25	Pyrheliometer detector temperature response	0.25
Pyrheliometer detector linearity	0.100	Event to event temperature bias (10ºC)	0.125
Solar tracker alignment variations	0.125	Solar tracker alignment bias	0.125
Pyrheliometer window spectral transmittance	0.500	Pyrheliometer window spectral transmittance	0.5
Electromagnetic interference and Electromagnetic field	0.005	Electromagnetic interference and electromagnetic field	0.005
TOTAL Type A*	0.615	TOTAL Type B*	0.665

*Summed under quadrature.

The *combined* uncertainty, U_C, can be determined from the above standard uncertainties for Type A and Type B errors:

$$U_C \quad = \quad [(0.615)^2 + (0.665)^2]^{1/2} = 0.906\%$$

The *expanded* uncertainty (UE) with a 95% confidence interval can therefore be computed based on the effective degrees of freedom (greater than 100 for pyrheliometer calibrations that can be based on more than 1000 measurements over the course of a day) and a coverage factor, k, of 2.0:

$$U_E \quad = \quad 2 \cdot U_C = 1.8\%$$

Therefore, the expanded uncertainty of the *calibration* for each Rs_i is ± 1.8%.

With this in mind, the reader can review the radiometer calibration certificate issued for each instrument and contact the manufacturer for additional information about the calibration process. NREL assigns a single value for Rsi, Rs, corresponding to SZA = 45 degrees and values of Rs for each 2-degree interval in the range of SZA encountered during the outdoor calibrations (additional information is available from www.nrel.gov/solar_radiation).

Estimating the Uncertainty of Direct Normal Irradiance Field Measurements

Accounting for this calibration uncertainty and other sources of measurement errors (condition of radiometer optics and the relevant issues similar to those considered for the calibration measurement uncertainty estimates), the expanded measurement uncertainty for subhourly DNI measurements is ± 2.5% for a well-maintained measurement station equipped with a thermopile-based pyrheliometer and ± 5% for a photodiode-based RSR (Wilcox and Myers 2008). Table 3-7 identifies the error sources used for our uncertainty analysis of DNI measurements from two types of radiometers.

Table 3-7. Estimated Direct-Normal Subhourly Measurement Uncertainties (Percent)

Type A Error Source	U_{std}(%) TP#	U_{std}(%) Si^	Type B Error Source	U_{std}(%)	U_{std}(%) Si^
"Fossilized" calibration error	0.615	0.615	"Fossilized" calibration error	0.665	0.665
Data logger precision (± 50 µV/10 mV)*	0.5	0.5	Data logger bias (1.7 µV/10 mV)*	0.02	0.02
Si detector cosine response	0	0.5	Si detector cosine response	0	1.5
Pyrheliometer detector temperature response (D20°C)	0.25	0.05	Detector temperature response	0.25	0.05
Pyrheliometer detector linearity	0.100	0.10	Day-to-day temperature bias (10°C)	0.125	0.10
Solar alignment variations (tracker or shade band) and pyranometer level for Si	0.2	0.10	Solar alignment variations (tracker or shade band) and pyranometer level for Si	0.200	0.20
Pyrheliometer window spectral transmittance	0.1	1.0	Pyrheliometer window spectral transmittance	0.5	1.0
Optical cleanliness (blockage)	0.2	0.1	Optical cleanliness (blockage)	0.25	0.1
Electromagnetic interference and electromagnetic field	0.005	0.005	Electromagnetic interference and electromagnetic field	0.005	0.005
TOTAL Type A**	0.889	1.382	**TOTAL Type B****	0.934	1.938

\# Thermopile detector used for a pyrheliometer.
^ Silicon diode pyranometer detector used for an RSR.
*Typical manufacturer specified accuracy: ± 0.05% of full scale range (typically 50 mV) −25°C to 50°C; assume 10 mV signal so ± 50 microvolts (µV) (0.5%) with 1.67 µV resolution (0.02%).
**Summed under quadrature.

The *combined* uncertainty, U_C, can be determined from the above standard uncertainties for Type A and Type B errors for each detector type:

$$U_{CTP} \quad = \quad [(0.889)^2 + (0.934)^2]^{1/2} \quad = \quad 1.29\%$$

$$U_{CSi} \quad = \quad [(1.382)^2 + (1.938)^2]^{1/2} \quad = \quad 2.38\%$$

The UE with a 95% confidence interval can therefore be computed based on the effective degrees of freedom (greater than 100 for pyrheliometer measurements that can be based on several thousand measurements over the course of a day) and a coverage factor, k, of 2.0:

$$U_{Etp} \quad = \quad 2 \cdot U_{CTP} \qquad\qquad = \quad 2.58\%$$

$$U_{ESi} \quad = \quad 2 \cdot U_{CSi} \qquad\qquad = \quad 4.76\%$$

The expanded uncertainty estimate of DNI from a thermopile pyrheliometer or silicon photodiode-based RSR is ± 2.6% and ± 4.76%, respectively. Measured data should be examined carefully and periodically checked against field reference radiometers to identify conditions that exceed these limits, in which case, problems with the radiometers, data acquisition systems, or other supporting equipment could be affecting the measurements.

Measurement Station Design Considerations

To collect useful DNI resource data, the successful design and implementation of a solar resource measurement station or network of stations requires careful consideration of the elements summarized in this subsection.

Location

The primary purpose of setting up a solar resource measurement station is to collect data that allow an analyst to accurately characterize the solar irradiance and relevant meteorological parameters at a particular location. Ideally, the instruments would be collocated with the targeted analysis area, but in some cases, separation distances may be tolerated depending on the complexities of local climate and terrain variations. Lower variability in terrain and climate generally translates to lower variability in the solar resource over larger spatial scales; however, these effects should be well understood before determining the final location of a measurement station. The proximity to the target area must also be weighed against operational factors, such as availability of power, communications, and access for maintenance as discussed below. One should also consider the possible effects of local sources of pollution or dust, for example traffic on a nearby dirt road that could degrade the measurements.

When measurement stations are constructed in metropolitan or industrial areas, consideration should be given to possible sources of radio frequency signals that could impart unwanted noise in sensors or cables. For example, the same high building that would provide an attractive unobstructed site for solar measurements may also be the ideal location for radio or television broadcast towers, or some other communication apparatus. Such sites should also be investigated for harmful effects of electromagnetic radiation on the health of station maintenance workers.

Instrument selection is a fundamental consideration, as measurements with greater accuracy will better reflect the actual resource; however, instrument placement is also an important consideration. If nearby objects—such as trees or buildings—shade the instruments for some period of time during the day, the resulting measurement will not truly represent the available solar resource. Distant objects—especially mountains—may be legitimate obstructions, as the shadows they cast are likely to produce an influence beyond the area local to the instruments. Conversely, nearby objects can potentially *reflect* solar radiation onto the instruments, likewise resulting in measurements that do not represent the local natural environment. Such cases could include a nearby wall, window, or other highly reflective object. The best practice is to locate instruments away from any objects that are in view of the instrument detector.

The easiest way to determine the quality of solar access is to scan the horizon for a full 360 degrees of azimuth and note the elevation of any objects protruding into the sky above the local horizon. Look for buildings, trees, antennae, power poles, and even power lines. Most locations will have *some* obstructions, but you must determine whether they will be

significant in the context of the necessary measurements. Generally, pyranometers are very insensitive to sky blockage within 5 degrees or so elevation above the horizon. Pyrheliometers, however, will be more sensitive because they can completely block the DNI, depending on the daily path of the sun throughout the year. The amount of blockage time each day will be related the object's width and height above the horizon. The number of blockage days each year will depend on where along the horizon the object lies. To be a concern, it must be in the area of the sun near sunrise or sunset, the time and azimuth of which vary throughout the year. For most of the horizon, objects blocking the sky will not be a factor because the sun rises in a limited range in the east and sets likewise in the west during sunset (e.g., at 40 degrees N latitude, sunrise near the summer solstice occurs at about 60 degrees from true north). However, the further north in latitude the site is located, the greater the range of these sunrise and sunset areas of interest. A solar horizon mapping, or even a sketch of obstructions by elevation and azimuth, will help determine the areas where horizon objects will affect the measurement (see Figure 2-4).

Considerations for locating a station should also include environmental concerns, such as wildlife habitat, migratory paths, drainage, and antiquities or archeological areas.

Station Security and Accessibility

Measurement stations can comprise equipment worth tens of thousands, or even hundreds of thousands of dollars. Although this equipment is typically not the target of thieves seeking property for resale, it is still subject to theft and should be protected. Vandalism may be even more likely than theft. Unlike thieves, vandals typically care less about *what* they're vandalizing and more about their ability to destroy property with high value to its owner. The less visible and accessible the station is to the public, the less likely it will be the target of theft or vandalism. For example, instruments mounted on a rooftop are less likely to attract unwanted attention than those unprotected beside a highway. Lack of visibility is the best defense against vandalism, including damage from bullets or rocks.

Security fences should be used if people or animals are likely to intrude. Fencing should be at least 6 feet tall, topped with barbed wire, and fitted with locking gates in high-profile areas where intrusion attempts are likely. Less elaborate fences may suffice in areas that are generally secure and only the curious need be discouraged from meddling with the equipment. In remote venues with few human hazards, cattle fence paneling (about 4 feet tall) may be advisable if large animals roam the area. The fencing should be sturdy enough to withstand the weight of a large animal that may rub against the compound or otherwise be pushed or fall against the fence. It may not be possible to keep smaller animals out of the station compound, and precautions should be taken to ensure the equipment, cabling, supports, etc., can withstand encounters with these animals. Coyotes, rodents, rabbits, birds, and other wildlife may be able to move through the wires or jump over or burrow under fences. In particular, signal cabling between modules or sensors at or near ground level is prone to gnawing by rodents and should be run through a protective conduit or buried. Any buried cable should either be specified for use underground or run through conduit approved for underground use. Underground utilities and other objects should be investigated before postholes are dug or anchors sunk.

If fences are used, the radiometers must be positioned above the fence line (including barbed wire), if only by a few millimeters, to prevent any shading of the sensor. This assumes that the pyranometer is mounted in a horizontal position and the pyrheliometer is installed in a solar tracker. POA pyranometers should have an unobstructed view of the ground and sky in front of them. If nearby towers are unavoidable, the station should be positioned between the tower and the equator (e.g., to the south of the tower in the northern hemisphere) to minimize shading. The radiometers should be positioned as far as possible from the tower— at least several meters—so the tower blocks as little of the sky as possible (radiometer signal cables should be shorter than 50 meters to avoid losses caused by line resistance). The tower

should also be painted a neutral gray to minimize strong reflections that could contaminate the solar measurement. These guidelines assume the tower is part of the measurement station proper and the site operator has control over placement or modification of the tower. Absent that control, the radiometers should be moved as far as possible from the tower.

Access to the equipment must also be part of a station construction plan. Because routine maintenance is a primary factor affecting data quality, provisions must be made for reasonable and easy access to the instruments. Factors here could include ease of access to cross-locked property, well-maintained all-weather roads, and roof access that might be controlled by other departments. Safety must also be a consideration. Locations that present hazardous conditions—such as rooftops without railings or that require access using unanchored ladders—must be avoided.

Power Requirements

Ongoing measurements require a reliable source of electrical power to minimize system downtime from power outages. In some areas, power from the utility grid is reliable, and downtime is measured in minutes per year. In other areas, multiple daily power interruptions are routine. Depending on the tolerance of the required analysis to missing data, precautions should be taken to ensure gaps in the data stream from power outages do not seriously affect the results. The most common and cost-effective bridge for power outages is an uninterruptible power supply (UPS). A UPS can also filter out unwanted or harmful line voltage fluctuations that can occur for a variety of reasons. It has internal storage batteries that are used as a source of power in the event of an alternating current (AC) power interruption. When the AC power is interrupted, internal circuitry makes an almost seamless switch from grid-connected AC power to AC provided through an inverter connected to the battery bank. When power is restored, the UPS recharges the internal battery from AC line power. Power loss is detected quickly, as is switching to battery, and is measured in milliseconds or partial line cycles. Some equipment may be particularly susceptible to even millisecond power interruptions during switching and should be identified through trial and error to avert unexpected downtime despite use of the UPS.

The UPS is sized according to:

- Operating capacity (amount of power—Watts. It can continuously supply either on or off grid-connected AC power).

- Longevity of battery power (how long the battery can last under anticipated maximum load).

Users should estimate the longest possible power outage and size the UPS for the maximum load of attached devices and the maximum period of battery capacity. Batteries should be tested regularly to ensure the device can still operate per design specifications. Internal battery test functions sometimes report errors only when batteries are near complete failure and not when performance has degraded. A timed full power-off test should be conducted periodically to ensure the UPS will provide backup power for the time needed to prevent measurement system failure.

In remote locations where utility power is not available, local power generation should be devised. Options for on-site electrical power generation include PV or small wind turbine systems (or both) and gasoline- or diesel-fueled generators with battery storage. The renewable energy systems should be sized to provide enough energy for the maximum continuous load and power through several days of cloudy weather when solar generation would be minimal. This would include sites prone to persistent ground fog. The sizing is a function of the extremes of the solar climate and should consider the longest gap during reduced generation, the shortest recharge period available after discharge, and the generation capacity and storage necessary to provide uninterrupted power for the target location. Some oversizing is necessary to accommodate degradation of PV panels and battery storage, and consideration should be

given to ambient temperature, which affects the ability of a battery to deliver energy. Sizing calculators are available to help with this effort (e.g., www.nrel.gov/eis/imby/).

Equipment should be specified and tested for self-power-on capability in the event of a power outage. This ensures that when power is restored, the equipment will automatically resume measurements and logging without operator intervention. This is an important consideration for remote locations where considerable downtime might occur before personnel could be dispatched to restart a system.

Grounding and Shielding

Station equipment should be protected against lightning strikes and shielded from radio frequency interference that could damage equipment or reduce the validity of the measurements. Several books are available that describe techniques for grounding and shielding low-voltage signal cables (e.g., Morrison 1998). The reader is urged to consult available references or seek expert technical advice during the design of a solar resource measurement system.

In general, these steps should be taken when designing and constructing a measurement station:

1. Use a single-point ground (e.g., a copper rod driven several feet into the ground) for all signal ground connections to prevent ground loops that can introduce noise or biases in the measurements.

2. Use twisted pair, shielded cables for low-voltage measurements and connected as double-ended measurements at the data logger. Double-ended measurements require separate logger channels for "+" and "–" signal input conductors. These inputs do not share a common signal ground and therefore significantly reduce the possibilities for electrical noise introduced in the signal cable.

3. Physically isolate low-voltage sensor cables from nearby sources of electrical noise, such as power cables (do not run signal cables in the same bundle or conduit as AC power cables). If a power cable must be near a signal cable, always position the two at right angles to each other. This limited contact will minimize the possibility of induced voltages in the signal cable.

4. Metal structures such as masts and tripods should be connected to the ground to provide an easy path to ground in the event of a lightning strike. This will help protect sensitive instruments. Electronic equipment often has a special ground lug and associated internal protection to help protect against stray voltages from lighting strikes. These should be connected with a heavy gauge wire to ground (12 American wire gauge or larger). Metal oxide varistors, avalanche diodes, or gas tubes can be used to protect signal cables from electrical surges such as lightning. These devices must be replaced periodically to maintain effectiveness. The replacement frequency is a function of the accumulated energy dissipated by the unit.

Data Acquisition

Data logging equipment should have performance specifications that do not degrade the potential measurement of the radiometer signals (e.g., analog-to-digital conversion of low-level direct current voltages, temperature response coefficients, and environmental limits of operation).

Most radiometers output a voltage, current, or resistance that is measured by a voltmeter, ammeter, or ohmmeter. The measured value is subsequently converted to engineering units through a multiplier and/or an offset determined by calibration to a recognized measurement standard. Data loggers should be chosen so that the measurement signal is consistent with the uncertainty of the sensor; e.g., a much smaller uncertainty, perhaps 3 to 10 times smaller than

the estimated measurement uncertainty associated with the radiometer. This is the accuracy ratio between the data logger and the radiometer. For example, typical specifications for a good data logger measuring a 10 mV output from the radiometer accurate to 1%, or 0.1 mV (100 μV) are on the order of total uncertainty (accuracy) of better than (less than) 0.1% of reading (or full scale) for the parameter in question, which would be 0.010 mV, or 10 μV. The logger should also have a range that can measure the voltage or resistance at near full scale to best capture the resolution of the data. For example, a sensor with a full-scale output of 10 mV should be connected to a logger with a range that is at least, but not below, 10 mV. A logger with a 1-V range may be able to measure 10 mV, but not with the desired precision. Most modern data loggers have several range selections, allowing the user to optimize the match for each instrument. Because of the nature of solar radiation, radiometers can sometimes produce 200% or more of clear sky readings under certain passing cloud conditions, and the logger range should be set to prevent over-ranging under unusual sky conditions.

Some radiometers use amplifiers to raise the instrument output to a higher range to better satisfy signal range matching requirements. However, such amplifiers require power and will add some uncertainty to the data with nonlinearity, noise, temperature dependence, or instability. High-quality amplifiers may minimize these effects and allow a reasonable tradeoff between logger cost and data accuracy. Calibrations must be made of these radiometer systems by including the pyranometer or pyrheliometer and its uniquely associated amplifier.

The logging equipment should also have environmental specifications that are compatible with the environment where the equipment will be used. Loggers used inside an environmentally controlled building could have less stringent environmental performance specifications than one mounted outside in a desert or arctic environment. Equipment enclosures can create an internal environment several degrees above ambient air temperature because of solar heating (absorption by the enclosure materials), heat generated by electronic devices mounted inside, and lack of ventilation to help purge heat. Gore Tex vent plugs are available to provide ventilation openings and prevent insects and water from entering the enclosure.

The sampling frequency and time statistics of the solar resource data should be determined from the desired data analysis requirements. For example, monthly means, daily totals, hourly, minute or sub-1-min data records can be useful. Data loggers can generally be configured to produce output of instantaneous or integrated values at any reasonable time period consistent with the radiometer time-response characteristics. The design should consider the current requirements and, if convenient and practical, future needs for additional analyses. A high-temporal resolution data logging scheme can be down-sampled or integrated to longer time periods than the other way around. For example, transforming hourly data to 1-min data with any certainty and accuracy is impossible if a specific data time-series must be reproduced. Data logging equipment, data transfer mechanisms, and data storage can generally handle 1-min data resolution, and this time realm should be considered as the fundamental resolution in the data logger. Because most applications address the solar energy available over time, integrated data of subminute samples within the data logger (e.g., 1-s signal sampling) is a common method of data output regardless of the final data resolution required by the analysis. The output of instantaneous samples is much less likely to represent the available energy and should be avoided when configuring a data logger. If the size of a measured dataset is a defining issue (e.g., limited data communications throughput), the user can determine the lowest temporal resolution necessary for the application and optimize the data collection accordingly.

Data Communications

Provisions should be made for transferring data from the data logger to a data processing facility. Historically, data have been captured, transferred, and processed in various ways. The manual transfer of data recorded on strip charts physically carried or shipped from the observing station to a data center has been replaced by advances in electronics and telecommunications that allow remote data collection from nearly any location. A telephone

modem link that uses conventional dial-up phone lines to connect between station and data center can now be replaced with cellular telephone technology, obviating the need for a physical connection between logger and phone line. The cell phone network is configured to provide virtual Internet links between a measurement station and the data center. Satellite up- and down-links are also available for data transfers in areas that are not served by either wire- or cell-based phone service. Within the area of an observing station, short-distance wireless communications such as Wi-Fi connectivity may be useful to minimize the need for long cables between radiometers and data loggers. (See the Appendix for sources of more detailed information.)

Operations and Maintenance

Proper O&M practices are essential for acquiring accurate solar resource measurements. As addressed in this subsection, there are several elements in the chain that forms a quality system. Collectively, these elements produce accurate and reliable solar resource data: station location, measurement system design, equipment installation, data acquisition, and O&M practices. Proper O&M requires long-term consistency, attention to detail, and a thorough appreciation for the importance of preventative and corrective maintenance of sensitive equipment.

Radiometer Calibrations

To obtain valid solar measurements, the relationship between the radiometer response to solar irradiance and its output signal must be periodically determined. This relationship is defined by the radiometer's Rs ($\mu V/Wm^{-2}$) as determined by calibration with a measurement reference. A calibration provides an Rs or combination of factors that relate sensor response to the solar irradiance. The calibration factor is applied to radiometer output signal to provide a measure of the solar irradiance in the desired engineering units. The calibration is accompanied by an estimate of the measurement uncertainty, either from the calibration process or from the manufacturer, to help determine measurement performance. The regular calibration of pyrheliometers and pyranometers is an important element of measurement station O&M.

As described in Chapter 2 and previously in this chapter, the calibration of broadband radiometers should be traceable to the WRR, the international measurement reference for solar irradiance. The user must determine a calibration interval based on either the manufacturer's recommendations or from instrument history based on stability of periodic calibrations or records indicating a calibration drift with time or exposure. Consideration should also be given to the possibility of instrument error due to factors other than sensor drift. Physical changes or damage can result in marginal changes to radiometer Rs that may still produce seemingly reasonable, but incorrect, measurements. Thus, periodic calibrations are a prudent approach to a defensible measurement protocol. Annual calibrations are common practice for radiometers.

There are two standards for the calibration of pyrheliometers used to measure DNI (ASTM 1997; ISO 1990). Consistent with these standards (and as described in Chapter 2), is the need to include the additional measurement uncertainty associated with each calibration transfer beginning with the use of reference radiometers directly traceable to the World Standard Group (WSG) that is used to define the WRR (Figure 2-11). The lowest measurement uncertainty for the calibration of a field pyrheliometer is generally achieved by direct comparison with an absolute cavity radiometer, with traceability to the WRR, for at least one clear sky daylight interval. A typical estimated measurement uncertainty assigned to the calibration of a field pyrheliometer is ± 1.0% (see Chapter 2 for details). Because of additional sources of error, the uncertainty of the field measurements from a well-calibrated pyrheliometer will be at least twice the calibration uncertainty. Pyrheliometer calibrations are available from the radiometer manufacturer and other providers. (See the Appendix and www.nrel.gov/solar_radiation.)

Instrument Maintenance

Calibrations are performed with clean instrument optics and a carefully aligned detector. To properly apply the calibration factor, the instrument should be kept in the same condition

during field measurements. To maintain the calibration relationship between irradiance and radiometer output, proper cleaning and other routine maintenance are necessary. The maintenance process includes:

- **Checking the alignment of the detector.** Pyrheliometers must be accurately aligned with the solar disk for accurate DNI measurements. Pyranometer detectors must be horizontal for GHI and DHI measurements and accurately aligned with a flat plate collector for POA measurements. The radiometer orientation should be checked periodically using the features described in Chapter 3. (In some cases, a carefully leveled pyranometer may produce GHI readings that are not symmetrical around solar noon under clear skies. If this cannot be attributed to any change in atmospheric composition (aerosols or water vapor), or optical asymmetries can be verified under strict laboratory conditions, the optical axis of the detector is probably not exactly vertical. This is a manufacturing defect.

- **Cleaning the instrument optics.** To properly measure the solar intensity, no contaminant should block or reduce the amount of sunshine falling on the detector. The outdoor environment provides many sources of such contamination, such as dust, precipitation, dew, plant matter, insects, and bird droppings. The sensors should be cleaned regularly to minimize the effect of contaminants on the measurements. Depending on the local conditions, this can require daily maintenance of unventilated or otherwise protected radiometers.

- **Documenting the condition of the radiometer.** For analysts to understand limitations of the data, conditions that affect the measurement must be documented. This includes substandard measurement conditions, but it is just as important to document proper operations to add credibility to the dataset. Observations and notes provide a critical record of conditions that positively and negatively affect data quality.

- **Documenting the environment.** As a consistency check, note the sky and weather conditions at the time of maintenance when interpreting data from the radiometer, including measurements with unusual values.

- **Documenting the infrastructure.** The measurement station as a whole should be examined for general robustness. Any defects should be noted and corrected.

Maintenance frequency depends on prevailing conditions that soil the instruments. This includes dust, rain, snow, birds, and insects. It is also depends on instrument type. Radiometer designs based on optical diffusers (such as LI-COR LI-200) are less susceptible to dust contamination than are instruments with clear optics (Myers et al. 2002). This may be due in part to the area subject to soiling (e.g., a larger dome versus a smaller diffuser). Also, fine dust on the surface of a diffuser can become an integral part of the diffuser, and may lessen the impact of the dust on the diffuser transmittance compared to that on a precision-ground optical dome. Soiling of the windowed or domed radiometers can quickly affect the measurement and increase by many-fold the measurement uncertainty. As described earlier, a pyranometer in a ventilator can reduce this risk of contamination. Thus, the frequency and cost of maintenance should be considerations in instrument specification. If a remote site will be difficult to maintain for extended periods, a higher class windowed instrument might not be optimal, despite its potential for better measurements. The cost of maintenance for a remote site may dominate the estimated cost of setting up and operating a station. This aspect should be anticipated when planning a measurement campaign.

A conservative maintenance schedule will support the credibility of the measurement dataset and provide the analyst a base of justification when assigning confidence intervals for the data. Daily inspection should be scheduled for instruments with clear optics and twice monthly inspections for diffuser instruments. More frequent spot inspections should be conducted after significant weather events. Radiometer optics may not necessarily soil within a 24-hour period, but the effects of soiling can best be mitigated with frequent inspection.

Radiometers should be carefully cleaned at each inspection, even if soiling appears minimal. Cleaning is generally a very short procedure, and removes the possibility of differing interpretations of the need to clean among different technicians. With such a procedure in place, the analyst can claim with confidence that the instruments were kept clean according to the documented schedule.

Maintenance at remote measurement sites away from institutional or corporate employment centers will require finding a qualified person nearby who can perform the necessary maintenance duties. The qualifications for maintenance are generally nontechnical, but require someone with the interest and disposition to reliably complete the tasks. As a rule, compensating these people for time and vehicle mileage—rather than seeking volunteers— becomes a worthwhile investment in the long run, as it sets up a firm contractual commitment to perform all necessary maintenance duties. Absent that formal relationship, it can become difficult to assert the need for reliable and regular attention.

All O&M should be carefully documented with log sheets or electronic databases that contain enough information to reveal problems and solutions, or that assert that the instruments were in good form when inspected. This information enables an analyst to identify potentially bad data, and provides important documentation to determine and defend the overall quality of the measurements.

Data Quality Control and Data Quality Assessment

The data quality is generally established when the measurement is taken. Little can be done after the fact to improve fundamental quality. For example, a poorly maintained station with dirty optics or misaligned instruments will produce data with presumed (or even apparent) errors, and the *magnitude* of those errors is not likely to be discernable until days or weeks later. There is no way to systematically reduce the uncertainty of such a measurement, and one can only guess at which corrections to make. In this context, data quality control involves a well-defined supervisory process by which station operators are confident that, when a measurement is taken with unattended instruments, the instruments are in a state that produces data of known quality. This process largely encompasses the calibration, inspection, and maintenance procedures discussed earlier, along with log sheets and other items that document the condition of the station. It also includes a critical inspection or assessment of the data to help detect problems not evident from physical inspection of the instruments.

Data quality assessment is a method by which data quality can be judged based on criteria for a particular application. Data can be compared with certain physical limits that have been determined to be reasonable, with redundant or complementary measurements, or with physical or empirical models, all of which will provide some degree of independent measure for a quality judgment. One common method for evaluating DNI, GHI, and DHI is a three-component coupling test. As described in Chapter 2, the measurements of DNI and DHI can be combined mathematically to derive a global measurement as described in Equation 2-3 on page 8.

When all three components are measured, measurement redundancy is apparent, because any one component can be derived from the other two. Thus, in the context of quality assurance (QA), expected values for each component can be calculated from the other two. This method helps quantify the relative error among the three components, although it does not necessarily determine strictly which measurement—or measurements—are in error. However, operational knowledge of the instruments and trackers can provide valuable insight into likely errors. For example, a misaligned tracker would cause either a low DNI or high diffuse measurement (low DNI from a poorly aligned pyrheliometer or high diffuse from a poorly aligned shading disk). With this knowledge, and an observation of trends in the magnitude of flagging, a data quality expert can quickly spot common operational errors. The measurement of the three redundant components—rather than just a single measurement or two components of specific interest—is

a significant and important tool for data quality analysis, and it should be strongly considered when specifying instrumentation for a station.

For example, the SERI QC software (NREL 1993) produces flags that can be plotted (see Figure 3-14). The left-hand plot indicates more severe flags with a darker shade, plotted here by day of month (y axis) and hour of day (x axis). In this temporal view, areas of expanding errors are seen over several days, indicating a tracker that has not been adjusted for the changing solar declination, resulting in a longer and more severe error condition as the condition is neglected. Further, the other three plots correspond respectively to a normalized GHI, DNI, and DHI measurements, providing the analyst with additional information to pinpoint the measurement causing the error.
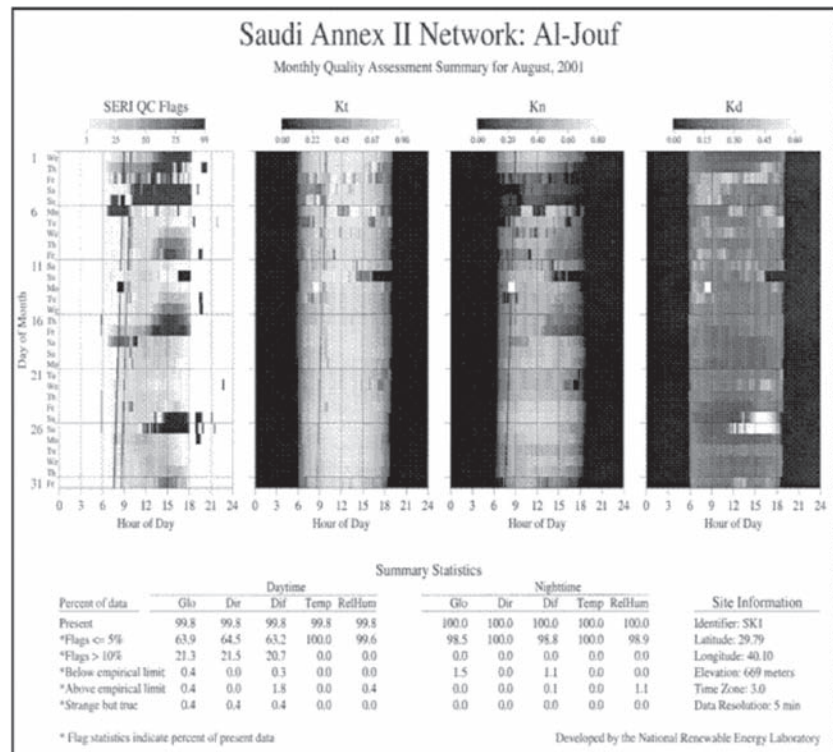
Figure 3-14. Example of SERI quality control data QA reporting

In the case shown in Figure 3-14, the three component data (GHI, DNI, and DHI) were submitted to the SERI QC software, which performs the three component coupling test in the realm of the clearness index, or Kt, Kn, and Kd (see Chapter 2). This K-space value normalizes the solar irradiance values to remove the effect of the SZA of incidence. Thus, in K-space

Kt   =   Kn + Kd.

Or rearranged, the deviation from this equation of component coupling can be quantified as the residual from

ε   =   Kt – Kn – Kd.

Perfect component coupling would result in ε = 0, and any nonzero value indicates some disagreement among the instruments. However, this method does not reveal *which* component or components are in error; only that there is some disagreement. Further, instrument errors in opposing directions could result in a false zero value.

Despite these ambiguities, a knowledgeable analyst can confidently detect measurement errors in most typical measurement scenarios. In the case of Figure 3-14, for each minute data record containing the three components, the residual was plotted as a quality flag, with darker flags

(leftmost column) indicating a greater deviation or apparent error. The actual Kt, Kn, and Kd values are also plotted in the next three columns, with lighter shades roughly correlating to higher irradiance. In the case of days 8–10, darker flags of growing magnitude are evident each day, which correlate with lower Kn (or DNI). This is most likely due to pyrheliometer tracker misalignment. This condition was corrected on day 11. Likewise for days 14–18, a subsequent tracker alignment error was corrected partway through day 18. Days 25 and 26 show significant flags in the afternoon, which are due to diffuse tracker error where the diffuse pyranometer is not adequately shaded, resulting in high diffuse irradiance. Other error conditions are also evident in the plot, including shading from nearby poles, which appear in the flag plot as double-angled stripes each morning. This occurs when the pole shaded individual instruments at slightly different times of the day, resulting in a significant decoupling of the three components.

In each case, examination of the quality flags resulted in feedback to station operators, who corrected tracker alignments.

Data from an RSR consist of GHI, DNI, and DHI, and are derived from a single pyranometer. To some extent, this limitation can be mitigated by including a secondary unshaded (GHI) pyranoemeter on the RSR to provide some redundant measurements. This enhancement is a relatively low-cost method of adding confidence in the measurements and can be included in a two- or three-component quality assessment test.

The three component methods described here are generally more reliable than a simple clear sky data analysis where some conclusions are drawn based on modeled or other expected values of the clear sky data. Significant day-to-day variations in cloudless, clear sky data can occur because of variations in atmospheric constituents such as aerosols or water vapor. Thus, such variation can make it difficult to draw conclusions about possible instrument error without specific information regarding other critical atmospheric components.

A successful quality control process requires elements of quality assessment and feedback. Figure 3-15 depicts a QA cycle that couples data acquisition with quality assessment and feedback.
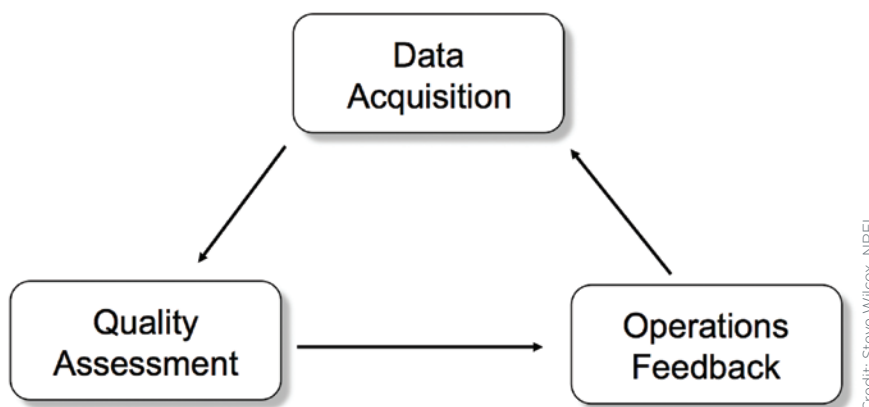
Figure 3-15. Information flow of a QA cycle

In Figure 3-15, the information flows from the Data Acquisition box to Quality Assessment, where some criteria are used to establish data quality. The results of the quality assessment

are analyzed and formed into feedback that goes back to the data acquisition module. The activities in the boxes can take several forms. For example, quality assessment could be the daily site inspection, and the analysis and feedback a simple procedure that corrects equipment malfunctions. Or, the quality assessment could be a weekly summary of data flags, and the analysis provides a determination of specific instrument error that is transmitted back to maintenance personnel with instructions to correct deficiencies or further troubleshoot problems.

The faster the cycle runs, the sooner errors will be detected, and the fewer bad data will collected during failure modes. Conversely, if the site is inspected infrequently, the chances increase that a large portion of the dataset would be contaminated with substandard equipment. More than one QA cycle can—and likely will—run at any time, each with a different period and emphasis as noted above: daily inspection, weekly quality reports, monthly summaries, etc.

One practical aspect of this cycle is the importance of *positive* feedback—a regular report back to site personnel of error conditions and of high-quality operations or datasets exceeding quality thresholds. This positively reinforces a job well done and keeps site operators cognizant that data are being used and that their efforts are an integral part of an ongoing process.

The QA cycle is a deliberate part of the quality control process, *and should be well defined and funded* to maintain a consistency of data quality over time.

Metadata

The interpretation and application of solar resource measurements depend greatly on the efforts to record and include metadata relevant to the observations. This includes site location, local horizon survey, data acquisition system(s), input signal channel assignments, radiometer types, models, serial numbers, calibration histories, installation schemes, and maintenance records. An example of on-line metadata is available from www.nrel.gov/midc/srrl_bms. Such metadata should be included with the archival of the measured solar resource data.

Chapter 4. Modeling Solar Radiation— Current Practices

Introduction

High-quality solar resource assessment accelerates technology deployment by making a positive impact on decision making and reducing uncertainty in investment decisions. GHI and DNI are the two quantities of interest for resource assessment and characterization at a particular location. GHI is defined as the total energy from sunlight, both direct and diffuse, that reaches unit area horizontal to the surface of the Earth. DNI is the amount of energy from direct sunlight that reaches unit area normal to the sun. Surface based measurements of DNI and GHI are best measured using well calibrated pyrheliometers and pyranometers, but such measurements can only be made on a sparse network given the costs of operation and maintenance. For example, currently there are only seven National Oceanic and Atmospheric Administration (NOAA) measurement sites under the SURFRAD (Surface Radiation) Network (Augustine et al. 2000). Nevertheless, observations from ground networks have been used in conjunction with models to create maps of surface solar radiation.

Another option is to use information from geostationary satellites to estimate GHI and DNI at the surface (e.g., Perez and Ineichen 2002; Pinker and Laszlo 1992). As geostationary satellite coverage is available at regular intervals on a fixed grid surface, radiation can be available for the entire globe at temporal and spatial resolution representative of the particular satellite.

This chapter contains a summary of available ground-based techniques, discussions of satellite-based methods, currently operational models that have surface radiation data available for current or recent periods, a summary of two radiative transfer models used in the operational models, and a discussion of uncertainty in solar-based resource assessment.

Surface-Based Methods

The sunshine recorder, in which the direct beam is focused to create burn marks during clear periods, has been used for more than a century to measure solar radiation around the world (Iqbal 1983). The monthly mean global solar radiation is measured using a regression fit to the number of clear hours measured by the burn marks where the regression coefficients are calculated using GHI measurements. Sunshine recorder data are often more widely available than GHI measurements, so the spatial coverage is expanded by using the regression fits. The exact method to calculate GHI using sunshine recorder information is empirical and therefore specific to each geographical area and not standardized. Moreover, the meteorological services of some countries, such as the United States and Canada, have stopped measuring sunshine because of the limited quality and significance of this measurement, which is not standardized and varies from country to country.

In the absence of surface measurements, estimates of surface radiation can also be made using meteorological information such as cloud cover, temperature, and water vapor in a radiative transfer model (Marion and Wilcox 1994). Reliable methods have been developed over the years and have been used to create the NSRDB, for instance (George et al. 2007). Initially created for the period between 1961 and 1990 for 239 stations in the United States, the NSRDB is an hourly dataset created using the meteorological-statistical (METSTAT) radiative transfer model of Maxwell (1998). The METSTAT model uses information about cloud cover, water vapor, ozone, and aerosol optical depth to compute atmospheric transmittance extinction under both clear and cloudy sky conditions. Ideally, surface-based cloud information comes from human-observed cloud cover, which includes total and opaque cloud amounts. More recently, automated cloud observations are derived from vertical ceilometer data, mainly for airport locations, reducing the accuracy of cloud cover observations. The atmospheric transmittance extinction is then used to produce DNI, GHI,

and diffuse irradiance at the surface. A modification of the METSTAT model called the Climatological Solar Radiation Model (Maxwell et al. 1998) is used to calculate monthly average daily totals of DNI, GHI, and diffuse irradiance using cloud information derived from the U.S. Air Force Real-Time Nephanalysis data. This cloud information is derived on a 40-km resolution grid from surface observations and satellite estimates (from polar orbiting satellites). The NSRDB was updated to create GHI and DNI for the period between 1991 and 2005 (Wilcox et al. 2007). Although the period between 1991 and 1997 was covered using METSTAT model runs, with cloud observations similar to the original NSRDB, the years 1998 through 2005 were processed in parallel, using hourly satellite-based model outputs.

Satellite Coverage and Satellite-Based Methods

Satellite-based retrievals of GHI have primarily been used for climate studies for three decades (Justus et al. 1986). Their goal is to use observed information about TOA radiances and albedos to calculate GHI and DNI. These methods can primarily be divided into statistical and empirical methods and physical methods (Pinker et al. 1995; Schmetz 1989). The empirical methods are based on developing relationships between satellite- and ground-based observations; the physical methods estimate surface radiation directly from satellite information using retrieval schemes to determine the atmospheric properties important to radiative transfer. Empirical methods generally produce only GHI and require additional models to calculate DNI from GHI.

Global Coverage

Geostationary Satellites

Geostationary satellites near the equator provide continuous global coverage (measurements are usable up to 66 degrees north and south latitudes because of the Earth's curvature) (see Figure 4-1). As an example of satellite coverage the Geostationary Operational Environmental Satellite (GOES) series covers North and South America every 3 hours and the Northern Hemisphere, including the United States, every 30 minutes. Two GOES satellites (GOES-East or GOES-12 and GOES-West or GOES-11) operate concurrently and provide 30-minute coverage for the entire United States. The Imager instrument on the current GOES satellites measures at 5 wavelength bands. The visible channel (0.64 µm) has a nominal 1-km resolution; the infrared channels (3.9 µm, 6.5 µm, 10.7 µm, and 12 µm) have 4-km resolution. The next (future) series of GOES satellites that are expected in 2015 will have a new instrument called the Advance Baseline Imager with 5 minutes coverage at 1-km resolution for 16 channels (6 in the visible and near-infrared). The European Organisation for the Exploitation of Meteorological Satellites Union owned the METEOSAT series of satellites that covered Europe and Africa as well as the Indian Ocean. The Visible and Infrared Imager on the METEOSAT first-generation satellites (up to METEOSAT 7) had 3 channels in the visible, water vapor, and infrared. The visible channel had a 2.5 that produced 8-km nadir resolution; the infrared channel's nadir resolution is 5 km. Repetition frequency is imagery every 30 minutes. The Spin Enhance Visible and Infrared Imager on the MSG satellites (METEOSAT 8 onward) provide satellite imagery every 15 minutes at a nominal 3-km resolution for 11 channels (Schmetz et al. 2002). The twelfth channel, a high-resolution visible channel, has a nadir resolution of 1 km. The Japanese Multifunctional Transport Satellite covers East Asia and the Western Pacific at 4 km spatial and 30-minute temporal resolution taking measurement in 5 channels. It replaced the GMS series of satellites, which has been in operation since 1977.
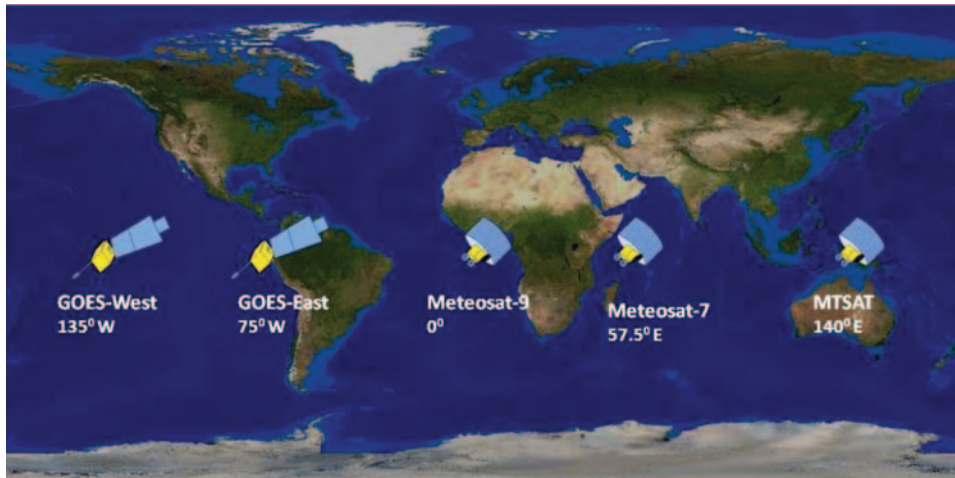
Figure 4-1. The location of the current geostationary satellites that provide coverage about the globe
(Image courtesy NOAA)

Polar-Orbiting Satellites

Polar-orbiting satellites are also used to continuously sense the Earth and retrieve cloud properties and solar radiation at the surface. An example of such instruments is the Advanced Very High Resolution Radiometer on the NOAA series of polar orbiting platforms. Another recent example is the Moderate Resolution Imaging Spectroradiometer instrument on NASA's Aqua and Terra satellites. Although polar orbiters provide global coverage, their temporal coverage is limited because of their orbit where they essentially cover a particular location only once a day at the lower latitudes.

Satellite-Based Empirical Methods

Solar radiation reflects to space and is well correlated to radiation reaching the surface of the Earth. The empirical methods create regression relationships between what is simultaneously observed by a satellite and ground-based instruments (e.g., Cano et al. 1986; Hay et al. 1978; Paris and Tarpley 1986; Tarpley 1979). Hay et al. created a regression model that relates atmospheric transmittance to the ratio of incoming to outgoing radiation at TOA. The transmittance is then used to compute GHI. In this method, the coefficients of the regression model change significantly based on location and need to be trained with surface observations (Nunez 1990) to produce accurate results. The Tarpley method also used the well known relation between surface radiation, the TOA radiation (both upwelling and downwelling) and atmospheric transmittance to create three separate regression equations. The regression equations were classified based on sky conditions labeled as clear, partly cloudy, and cloudy and used accordingly.

Satellite-Based Physical Models

Physical models generally use radiative transfer theory to directly estimate surface radiation. These can be classified as either broadband or spectral, depending on whether the radiative transfer calculations involve a single broadband calculation or multiple calculations in different wavelength bands.

The broadband method of Gautier et al. (1980) used thresholds depending on multiple days of satellite pixel measurements to determine clear and cloudy skies. Separate clear sky and cloudy sky models were then used to compute surface DNI and GHI. The clear sky model initially included water vapor and Rayleigh scatter but progressively added ozone (Diak and Gautier 1983) and aerosols (Gautier and Frouin 1984). Assuming attenuation caused by the

atmosphere does not vary from clear to cloudy conditions, Dedieu et al. (1987) created a method that combines the impact of clouds and the atmosphere. This method again uses a time series of images to determine clear sky for computing surface albedo. Darnell et al. (1988) created a parameterized model to calculate surface radiation using a product of the TOA insolation, atmospheric transmittance, and cloud transmittance. Developed with data from polar orbiting satellites, this model used collocated surface and satellite measurements to create relationships between cloud transmittance and planetary albedo.

Möser and Raschke (1983) created a model based on the premise that GHI is related to fractional cloud cover and used it with Meteosat data to estimate solar radiation over Europe (Möser and Raschke 1984). The fractional sky cover is determined to be a function of satellite measurements in the visible channel. This method uses radiative transfer modeling (Kerschegens et al. 1978) to determine the clear and overcast sky boundaries. Stuhlmann et al. (1990) have since enhanced the model to include elevation dependence, and additional constituents as well as multiple reflections in the all sky model. An important spectral model developed by Pinker and Ewing (1985) divided the solar spectrum into 12 intervals and applies the Delta-Eddington radiative transfer (Joseph et al. 1976) to a three-layer atmosphere. The primary input to the model is cloud optical depth that can be provided from various sources. This model was enhanced by Pinker and Laszlo (1992) and used in conjunction with cloud information from the International Satellite Cloud Climatology Project (ISSCP) (Schiffer and Rossow 1983). Another physical method involves the use of satellite information from multiple channels to derive cloud properties (Stowe et al. 1999) and then computing DNI and GHI using the cloud properties in a radiative transfer model. This method, called Clouds (from an advanced very high resolution radiometer), was originally developed for the polar orbiting. It is an advanced, very high-resolution radiometer instrument on NOAA satellites (Stowe et al. 1999) and has been modified and enhanced to obtain cloud properties from the GOES satellites (Heidinger 2003; Pavlonis et al. 2005). The cloud information is then input to the Pinker and Laszlo (1992) model to produce surface radiation.

Empirical and semi-empirical models (discussed in next subsection) have been used to produce good estimates of surface radiation as they are computationally less expensive. Although physical models are computationally more intensive, they can use additional channels from new satellites (such as MSG) to improve cloud property retrieval, and hence, surface radiation.

Semi-Empirical Models

Semi-empirical models are so classified because of their hybrid approach to retrieving surface radiation from satellite observations where normalized satellite-observed reflectance is related to GHI at the surface.

Cloud cover indices that use visible satellite imagery are first created with budget equations between TOA and surface radiation. Those indices are then used to modify clear sky GHI and estimate GHI at the ground consistent with the cloud scene. The Cano model was modified by Diabate et al. (1988) and Moussu et al. (1989), who used METEOSAT data to develop the Heliosat model to create solar resource. These data are available commercially from Ecole des Mines de Paris (see Chapter 5). Models such as those developed by Perez et al. (2002) also evolved from Cano et al. (1986) and are currently being used to estimate GHI and DNI. For the United States, datasets created using the Perez et al. (2002) model, for the period between 1998 and 2005, are available for free from NREL. Beyond 2005 the datasets are commercially available.

Currently Available Operational Models

NASA/GEWEX Surface Radiation Budget

To serve the needs of the World Climate Research Programme (WCRP), Whitlock et al. (1995) developed a global Surface Radiation Budget (SRB) dataset using cloud information from the ISCCP C1 dataset at a 250 km × 250 km (approximately 2.5 degrees × 2.5 degrees) resolution

every 3 hours (Schiffer and Rossow 1983; Zhang et al. 2004). Information from the ISCCP-C1 dataset is used as input into the Pinker and Laszlo (1992) model and the Darnell et al. (1988) model.

The currently available version is the NASA/GEWEX SRB Release-3.0 datasets that contain global 3-hourly, daily, monthly/3-hourly, and monthly averages of surface longwave and shortwave radiative parameters on a 1 degree × 1 degree grid (http://eosweb.larc.nasa.gov/PRODOCS/srb/table_srb.html). Primary inputs to the models include:

- Visible and infrared radiances, and cloud and surface properties inferred from ISCCP pixel-level (DX) data

- Temperature and moisture profiles from GEOS-4 reanalysis product obtained from the NASA Global Modeling and Assimilation Office

- Column ozone amounts constituted from Total Ozone Mapping Spectrometer and TIROS Operational Vertical Sounder archives, and Stratospheric Monitoring-group's Ozone Blended Analysis, an assimilation product from NOAA's Climate Prediction Center.

The SRB dataset are also available from the Surface Meteorology and Solar Energy Web site (http://eosweb.larc.nasa.gov/sse/) in a version that is more applicable to renewable energy. SRB datasets are also available from the Clouds and the Earth's Radiant Energy System project (http://eosweb.larc.nasa.gov/PRODOCS/ceres/table_ceres.html). Additionally, the Fast Longwave and Shortwave Radiative Fluxes (FLASHFlux) project makes real-time SRB data available from http://eosweb.larc.nasa.gov/PRODOCS/flashflux/table_flashflux.html. Both projects use global observations from Clouds and the Earth's Radiant Energy System and moderate-resolution imaging spectroradiometer instruments. Table 4-1 shows the estimated bias and root-mean-square (RMS) error between measured WMO Baseline Surface Radiation Network (BSRN) monthly averages of the three solar radiation components. The NASA SSE accuracy and methodology are documented on the SSE Web site.

Table 4-1. Regression Analysis of NASA SSE Versus BSRN Bias and RMS Error for Monthly Averaged Values for July 1983 Through June 2006

Parameter	Region	Bias (%)	RMS (%)
GHI	Global	−.01	10.25
	60° Poleward	−1.18	34.37
	60° Equatorward	0.29	8.71
DHI	Global	7.49	29.34
	60° Poleward	11.29	54.14
	60° Equatorward	6.86	22.78
DNI	Global	−4.06	22.73
	60° Poleward	−15.66	33.12
	60° Equatorward	2.40	20.93

DLR-ISIS Model

Similar to the NASA SSE datasets discussed in Chapter 5, the DLR-ISIS dataset (available at www.pa.op.dlr.de/ISIS/) is a 21-year DNI and GHI dataset (280 km × 280 km every 3 hours) based on the ISCCP cloud product covering the period between July 1983 through December 2004. The cloud products are used in a 2-stream radiative transfer model (Kylling et al. 1995) to compute DNI and GHI. The correlated-k method of Kato et al. (1999) is used to compute atmospheric absorption in the solar spectrum. Scattering and absorption in water clouds are analyzed using the parameterization of Hu and Stamnes (1993); ice cloud properties are obtained from Yang et al. (2000) and Key et al. (2002). Fixed effective radii of 10 µm and 30 µm

are used for water and ice clouds, respectively. The radiative transfer algorithm and parameterizations are included in the radiative transfer library libRadtran (Mayer and Kylling 2005, available at www.libradtran.org/doku.php). The complete method for creating the DLR-ISIS dataset using the ISCCP cloud products and the libRadtran library is outlined in Lohmann et al. (2006). The cloud data used for the derivation of the DLR-ISIS dataset are taken from the ISCCP FD input dataset (Zhang et al. 2004), which is based on ISCCP D1 cloud data (see ISCCP homepage at http://isccp.giss.nasa.gov for more information about cloud datasets). It provides 3-hourly cloud observations on a 280 km × 280 km equal area grid. The whole dataset consists of 6,596 grid boxes on 72 latitude steps of 2.5 degrees. This grid is maintained for the DLR-ISIS dataset.

ISCCP differentiates between 15 cloud types. The classification includes three intervals of optical thickness in three cloud levels: low, middle and high clouds. Low and middle cloud types are further divided into water and ice clouds; high clouds are always ice clouds.

For DLR-ISIS, optical thickness, cloud top pressure, and cloud phase given in the ISCCP dataset are processed to generate clouds for the radiative transfer calculations. One radiative transfer calculation is carried out for each occurring cloud type assuming 100% cloud coverage, plus one calculation for clear sky. For the final result, irradiances are weighted with the cloud amount for each cloud type and for clear sky, respectively.

HelioClim

The Heliosat method based on Cano et al. (1986) is used to produce the HelioClim database (Rigollier et al. 2004) that uses METEOSTAT data (www.soda-is.com/eng/help/helioclim_eng.html). HelioClim covers Europe, Africa, the Mediterranean Basin, the Atlantic Ocean, and part of the Indian Ocean. Mines Paristech - Armines produces that can be accessed through the SoDa Service (www.soda-is.com/eng/index.html). Mines ParisTech produced the method Heliosat-2 in November 2002, partly with the support of the European Commission; Heliosat-4 is being developed by Mines Paris Tech and the German Aerospace Agency DLR. Table 4-2 shows representative differences in comparisons of HelioClim modeled data and ground measurements in Europe and Africa between 1994 and 1997 (Lefe`vre 2007).

**Table 4-2. HelioClim Versus Ground Bias and RMS Error for
Monthly Averaged Values for 1994–1997**

Parameter	Region	Bias (%)	RMS (%)
GHI	Europe	−9% to −1%	25%
	Africa	−3% to +4%	18%

Solar Energy Mining

Solar Energy Mining (SOLEMI) is a service provided by DLR (Deutsches Zentrum für Luft- und Raumfahrt) German Aerospace Center that provides irradiance data commercially. The data are derived from Meteosat satellite images. GHI and DNI datasets are available every hour at 2.5-km resolution and cover Europe and Africa (1991 to 2005) and Asia (1999 to 2006). SOLEMI uses the Heliosat method of Cano et al. (1986), modified by Beyer et al. (1996) at http://wdc.dlr.de/.

Perez/Clean Power Research

The Perez et al. (2002) method (herein referred to as the Perez State University of New York [Perez SUNY] model) for computing GHI and DNI is based on the concept that atmospheric transmittance is directly proportional to the TOA planetary albedo (Schmetz 1989). This method is being applied to the GOES satellites and is currently available from Clean Power Research (www.cleanpower.com). The concept of using satellite-based measurements of

radiance assumes the visible imagery demonstrates cloud cover for high levels of brightness and lower levels for more clear sky conditions (e.g., dark ground cover). The method is outlined below and readers are referred to Perez et al. (2002) for additional details. The method:

- Normalizes the satellite measurement with the SZA to remove effects of solar geometry.
- Creates a dynamic range of satellite measurements using time series information for each pixel.
- Calculates cloud index for every pixel in an image by scaling with the dynamic range for the corresponding pixel that was created in Step 3.
- Uses the SOLIS model (Mueller et al. 2004) to create a GHI map for clear sky (GHIclr).
- Calculates GHI by scaling GHIclr with the cloud index.
- Calculates clear sky DNI (DNIclr) and DNI from GHIclr and GHI, respectively, using the DIRINT model (Perez et al. 1992).
- Calculates clear sky DNI from the Bird Model (DNIclr, Bird) using water vapor, ozone, and aerosol optical depths as inputs (DNIclr, Bird is estimated to be more accurate than DNIclr).
- Scales DNIclr, Bird with ratio of DNI and DNIclr from Step 6 to calculate the DNI.

The above steps are used to calculate DNI and GHI from satellite visible imagery. Some additional corrections and ancillary data are used to make the product more accurate. These include:

- Using snow cover information from the National Snow and Ice Data Center to reset the lower bound of the dynamic range
- Using surface elevation from the U.S. Geological Survey's digital elevation models (DEMs) to adjust for atmospheric optical depth based on elevation
- Adjusting the lower bound of the dynamic range for high AM effects
- Adjusting for specular reflection caused by the angle between the sun and satellite
- Adjusting the cloud index to a clearness index using a nonlinear conversion process and applying the clearness index to GHI calculations.

3-TIER Solar Dataset

A new dataset, the 3-TIER dataset, has become available. It follows the method of Perez et al. (2002). Datasets for the Western Hemisphere are available at 3-km resolution from 1997 (White paper 2009a). Also available are data for India (White paper 2009b) at the same resolution from 1999. Data for Australia are available (White paper 2009c) from 1998 at 3-km resolution.

SolarGIS

A new model for high-performance calculation of global and direct irradiances has been implemented for the region covered by the MSG, the satellite covering Europe, Africa, and the Middle East. The model philosophy is based on the principles of Heliosat-2 calculation scheme (Hammer et al. 2003) and the model by Perez et al. (2002), and it is implemented to operationally process MSG data at full spatial and temporal resolution.

The model was developed by GeoModel (Cebecauer et al. 2010). The enhancements include:

- Multispectral satellite information to improve classification of snow/land/cloud signals
- A new algorithm to find lower bound values preserving diurnal variability
- Implementation of backscatter correction

- Variable upper bound for dynamic range and cloud index calculations
- Simplified SOLIS clear sky model
- Downscaling with high-resolution DEM to include local variability of solar irradiance.

In particular, the following algorithms are implemented:

- Clear sky model: broadband simplified Solis (Ineichen 2008)
- Satellite model: modified version of Heliosat by Perez et al. (2002), adapted for multispectral MSG data, with improvements of snow classification and cloud index determination
- Snow detection: Dürr and Zelenka (2009)
- DHI: Perez model, Perez et al. (1987)
- DNI: DirIndex, Perez et al. (1992, 2002)
- Terrain disaggregation: Ruiz-Arias et al. (2010).

NOAA Global Surface Insolation Project

NOAA is currently running a physical model (www.osdpd.noaa.gov/ml/land/gsip/index.html) that produces GHI at approximately 12-km resolution for the northern hemisphere. Its output is called the *GOES Surface Insolation Product*. The GOES Surface Isolation Product algorithm follows a 2-step process:

1. Uses multichannel GOES satellite information and ancillary datasets, including snow cover, surface albedo, and digital elevation to retrieve cloud properties (Heidinger 2003).

2. Uses the cloud properties from Step 1 to produce GHI (Lazslo and Pinker 1992; Laszlo et al. 2008).

Although the GOES Surface Isolation Product was primarily developed to estimate sea surface temperature for coral bleaching and numerical weather prediction applications, it can be tailored to CSP needs as DNI is currently produced, but not saved, in the official product (Istvan Laszlo, personal communication).

Clear Sky Models Used in Operation Models

Bird Clear Sky Model

The Bird Clear Sky Model (Bird and Hulstrom 1981) is a broadband algorithm that produces estimates of clear sky direct beam, hemispherical diffuse, and total hemispherical solar radiation on a horizontal surface. The model is based on parameterization built using radiative transfer computations and is composed of simple algebraic expressions. Model results are expected to agree within ± 10% with radiative transfer models. The model computes hourly average solar radiation for every hour of the year, based on the 10-user input parameters; however, variable atmospheric parameters such as aerosol optical depth, ozone, and water vapor, are fixed for the entire year. The Bird Clear Sky Model also forms the basis of the clear sky part of METSTAT, with only minor modifications. The performance of these two models has been assessed rigorously and compared to other algorithms (Gueymard 1993, 2003a, 2003b; Gueymard and Myers 2008).

European Solar Radiation Atlas Model

The European Solar Radiation Atlas (ESRA) model is another example of a clear sky model. Used in the Heliosat-2 model that retrieves GHI from satellites, this model computes DNI, GHI, and DHI using Rayleigh optical depth, elevation, and the Linke Turbidy factor as its inputs.

SOLIS Model

The SOLIS model (Mueller et al. 2004) is a simple clear sky model that can calculate DNI, GHI, and diffuse radiation based on an approximation to the Lambert-Beer relation for computing DNI:

$$I = I_0 e^{(-\tau)}$$

where

τ is the atmospheric optical depth,

I_0 is the TOA direct radiation, and

I is the DNI at the surface for a monochromatic wavelength.

This equation is modified to account for slant paths and adapted for GHI and diffuse. The modified Lambert-Beer relation (Mueller et al. 2004) is

$$I(SZA) = I_0 exp\ (-\tau_0 / Cos^a\ (SZA)$$

where

I(θz) is the irradiance associated with the empirical factor, a, used to compute the DNI, DHI, or GHI (a = 1 for DNI),

τ_0 is the vertical broadband optical depth of the atmosphere, and

SZA is the solar zenith angle.

The Beer-Lambert equation is a simple relationship as it accounts for monochromatic DNI and is impacted only by atmospheric attenuation. On the other hand, DHI and GHI are broadband values that contain energy that is scattered by the atmosphere. The empirical factor a is used as an adjustment factor to compute GHI and DHI, as explained in Mueller et al. (2004).

Model Uncertainty and Validation

It is important to understand the accuracy of satellite measurements compared to surface data. A satellite pixel provides an estimate of surface radiation based on cloud and aerosol information spread over a certain area; the surface observations are based on an instrument viewing the sky from a point. If the satellite pixel size is small enough, parallax errors enter into the comparison. Terrain effects may also influence a comparison where cloudiness may vary within a short distance. According to Perez et al. (1987), satellite-based retrievals are accurate to 10%–12%. According to Renné et al. (1999) and Zelenka et al. (1999), the target-specific comparison with ground-based observations will have a root mean square error (RMSE) of at least 20%; the time specific pixel wide accuracy is 10%–12% on an hourly basis.

The various empirical and theoretical methods discussed above have been tested for accuracy. Although there is no standardized method for accuracy assessment, the authors have mostly reported root mean square deviation (RMSD) and bias error either as a percent or in energy units. As an example, the physical model of Darnell et al. (1988) was used to compute surface radiation using cloud information from the ISCCP-C1 data. The results were then compared to surface observations collected by the WRDC by Darnell and Staylor (1992). The RMSD from this comparison was found to be about 16 W/m^2 and the mean bias was about 4 W/m^2 (See Tables 4-3 through 4-6). It should also be noted that interpretation of reported errors is dependent on the spatial and temporal resolution of the data being compared.

**Table 4-3. Summary of Applications and Validation Results of Satellite Models—
Empirical/Statistical Models**
(after Renné et al. 1999)

References	Objective	Satellite Data/ Study Period	Location/ Resolution	Methodology	Accuracy
Nullet 1987	GHI over tropical Pacific	ESSA 1,3,5,7; ITOS I, NOAA 1,2/Feb 1965– Jan 1973	Tropical Pacific/ monthly, 2.5 km × 2.5 km	Cloud cover by Sadler et al. 1976; 2 irradiance models	Three islands (annual) −0.5% to +4.4%
Shaltout and Hassen 1990	Seasonal maps of daily GHI and DHI	METEOSAT 1100 LST cloud cover images	Egypt, one obser- vation/day, 2.5 km × 2.5 km (visible) and 5 km × 5 km (in- frared)	Linear regression with 24 ground stations	GHI ± 7.0% DHI ± 12.5%
Delorme et al. 1992	Real-time daily images	METEOSTAT visible Mar 15 – Jun 30, 1990	Southern France/ daily 367 km × 725 km	"Gistel" model applied to WEFAX images	Generally high inaccuracies
Ben Djemaa and Delorme 1992	Compari- son with 7 ground stations	METEOSAT B2/ Oct 1985–Sept 1986	Tunisia/ daily 30 km × 30 km	"Gistel" model applied to B2 data for daily values	0%–10% (51% of data) −10% to 0% (38% of data)

**Table 4-4. Summary of Applications and Validation Results of Satellite Models—
Empirical/Physical Models**
(after Renné et al. 1999)

References	Objective	Satellite Data/ Study Period	Location/ Resolution	Methodology	Accuracy
Nunez 1990	Solar energy for Australian cities	GMS/ 1986–1988	8 Australian cities/ daily 219 km × 177 km	Simple physical model by author	< 10% (6 cities) > 10% (2 cities)
Tarpley 1979	GHI from GOES	Summer 1997	USA Great Plains/ daily totals from hourly images 50 km × 50 km	Empirical relation with ground stations coupled with physical models	RMSE < 10% (daily) RMSE < 20% (1 image/day)
Klink and Dollhopf 1986	Resource assessment for Ohio	GOES 1982	8 stations in Ohio/ 50 km × 50 km	Tarpley 1979	10%–12% RMSE (snow-free) −3.5% MBE
Czeplak et al. 1991	Comparisons of Tarpley method	METEOSAT visible/ Nov 1986	Western Germany/ 8 km × 8 km	Tarpley 1979	21% RMSE (daily) 11% RMSE (monthly)
Frulla et al. 1988	Solar radiation over Argentina	GOES-E/ 1982–1983	Northern Argentina/ daily 1 km × 1 km	Tarpley 1979	RMSE 10%–15% (daily) RMSE 25% (hourly)
Diabate et al. 1989	Establish a HELIOSAT station	METEOSAT 1983–1985	European and eastern Mediterranean/ hourly	HELIOSAT (Cano et al. 1986; Moussu et al. 1989)	RMSE 0.06 kWh/m²

**Table 4-5. Summary of Applications and Validation Results of Satellite Models —
Broadband Theoretical Models**
(after Renné et al. 1999)

References	Objective	Satellite Data/ Study Period	Location/ Resolution	Methodology	Accuracy
Frouin et al. 1988	Compare Gautier's method with five empirical models	GMS/ 1986–1988	8 Australian cities/daily 219 km × 177 km	Gautier et al. 1980, with refinements	RMSE 12.0 Wm² (daily) MBE −4.9 Wm²
Gautier 1988	GHI over oceanic regions	Summer 1997	USA Great Plains/ daily totals from hourly images 50 km × 50 km	Gautier et al. 1980, with refinements	RMSE 12 Wm² or 5% (daily) MBE −6 Wm²
Darnell et al. 1988	GHI estimates using sun-synchronous satellites	GOES 1982	8 stations in Ohio/ 50 km × 50 km	GHI technique from sun-synchronous satellites	RMSE 19.2% (daily) 2.7% (monthly)
Dedieu et al. 1987	Calculate GHI and albedo from METEOSAT	METEOSAT visible/ Nov 1986	Western Germany/ 8 km × 8 km	Physical relationship between computed TOA and satellite values	RMSE 19.5% (hourly, noon) RMSE 6.7% (monthly)

A rigorous method that is currently gaining acceptance for benchmarking satellite-retrieved GHI and DNI with ground-based observations is the Kolmogorov-Smirnov test (Massey Jr. 1951). This test has the advantage of being nonparametric and is therefore not distribution dependent. It compares the distributions of GHI and DNI obtained from the two sources.

A detailed analysis of uncertainty is beyond the scope of this handbook; however, it is important to indicate possible sources of these uncertainties. One important issue to DNI and GHI assessments is the aerosol optical depth of the atmosphere. Depending on its composition, an aerosol can scatter, absorb, or scatter and absorb the DNI. This interaction is called *atmospheric extinction*. The proportion of absorption and scattering is determined by the aerosol type. As an example, mineral dust is a mostly scattering aerosol; black carbon is highly absorbing. To calculate the DNI, we need only the aerosol extinction, but GHI calculations are more accurate if the scattering and absorption components are available. Aerosol optical depths vary over the wavelength range and the use of a single broadband aerosol optical depth results in additional uncertainties. Climatological aerosol optical depths can be used for resource assessment but sometimes lead to large DNI errors. This happens in areas of biomass burning, urban air pollution, and dust storms where the use of climatology results smoothes out episodic events, ultimately leading to an underestimation of DNI.

It is difficult to discriminate between clouds and snow cover on the ground by using the satellite visible imagery. As snow results in elevated reflection of sunlight, the satellite image may be interpreted as cloud covered. This results in underestimation of GHI and DNI. The use of multiple satellite channels in the visible and infrared can solve this issue.

Specular reflection, especially from sandy desert surface during certain times of the day, may result in the satellite image being interpreted as cloudy and result in underestimation of GHI and DNI. This issue can be resolved by theoretically estimating the probability of specular reflection and factoring that into the calculation of surface radiation.

Table 4-6. Summary of Applications and Validation Results of Satellite Models—Spectral Theoretical Models
(after Renné et al. 1999)

References	Objective	Satellite Data/Study Period	Location/ Resolution	Methodology	Accuracy
Möser and Raschke 1984	Solar radiation over Europe	METEOSAT-I-II Jun 1979 and Apr 1982	Europe/ daily (3–6 images/ day) 25 km × 25 km	Normalized reflected radiance; 2-stream radiative transfer model	RMSE 5% – 6% (monthly) RMSE 10% – 14% (daily) Daily RE < 20% (no snow) > 20% (snow)
Stuhlmann et al. 1990	Improve IGMK model of Möser and Raschke 1983 (cloud transmittance)	METEOSAT ISCCP B2	Europe, Africa, Western South Africa 30–50 km	Explicitly account for multiple reflections between surface and atmospheric layers; improved clear sky algorithm	Monthly means generally within ± 10% (better over Europe)
Pereira et al. 1996	Surface GHI	METEOSAT-II 1985–1986	Brazil monthly	IGMK model (Sthuhlman et al. 1990)	RMSE 13% MBE –7%
Raschke et al. 1991	Solar radiation atlas for Africa	METEOSAT ISSCP B2 1985–1986	Africa: 30–50 km (IGMK), 2.5 km (HELIOSAT) monthly (derived from 3-hourly values)	IGMK (HELIOSAT for selected areas over western Africa)	RMSE –8% to 16% (monthly) MBE –2% to 8% (monthly)
Pinker and Laszlo 1992	Global SRB estimates	ISCCP C1 (based on ISSCP B3) July 1983	Global 2.5 degrees latitude × 2.5 degrees longitude	Pinker and Ewing 1985	High level of consistency on global scale

Chapter 5: Historical Solar Resource Data

Introduction

Understanding the long-term spatial and temporal variabilities of available solar resources is fundamental to any assessment of CSP potential. Information derived from historical solar resource data can be used to make energy policy decisions, select optimum energy conversion technologies, design systems for specific locations, and operate and maintain installed solar energy conversion systems. Historical solar resource data can be the result of in-situ measurement programs, satellite-remote sensing methods, or meteorological model outputs. As described in the previous chapters, each type of data has different information content and applicability.

This chapter summarizes historical solar resource data available for the United States and selected international locations. It is an inventory of representative sources of solar radiation data and provides a summary of important data characteristics associated with each data source (e.g., period of record, temporal and spatial resolutions, available data elements, and estimated uncertainties).

NREL and other agencies have made every effort to make data products that are as useful, robust, and as representative as possible; however, the responsibility for applying the data correctly resides with the user. A thorough understanding of the data sources, how they are created, and their limitations is vital to proper application of the resource data to analyses and subsequent decision-making. Discussion and examples of the use of several of these datasets for CSP applications are presented here. Users are encouraged to read the pertinent sections of this chapter before applying solar resource and meteorological data.

Measured solar irradiance data can provide detailed temporal information for a specific site. Because solar radiation measurement stations are challenging to operate and the data collected are not used for routine weather forecasts, they are few in number and have limited data collection records. The largest national measurement network for obtaining hourly solar resource data in the United States was the 39-station NOAA Network, which operated from 1977 through 1980 (see section on the NOAA network, page 69). Currently, measured solar irradiance of some form is available from more than 3,000 sites in the United States that are operated by various interests producing data with a wide range of data quality (see section on the PVGIS, page 73).

Satellite-based observations and mesoscale meteorological models address the needs for understanding the spatial variability of solar radiation resources over a range of distances. Present state-of-the-art models provide estimates for GHI and DNI at spatial resolutions of 10 km or less for the United States. The rapidly growing needs for more accurate solar resource information over shorter temporal and smaller spatial scales require the user to fully appreciate the characteristics of all available data, especially those from historical sources.

Solar Resource Data Characteristics

Characterizing the available solar resources for CSP applications is important for all aspects of realizing the full potential of this utility-scale energy source. Energy policy decisions, engineering designs, and system deployment considerations require an accurate understanding of the relevant historical solar resource data, the ability to assess the accuracy of current solar measurement and modeling techniques, and to forecast the levels of solar irradiance for various temporal and spatial scales.

Solar resource data can be the result of in-situ measurement programs, remote sensing instruments, or meteorological modeling outputs. Each type of data product has different information content and applicability.

Measured solar irradiance data can provide information about the temporal variability at a specific site. Practical radiometer designs were developed in the early 1900s to determine the sun's energy output based on high-altitude measurements of DNI made with pyrheliometers (Hulstrom 1989). To address the needs of agriculture for monitoring such quantities as evapotranspiration, the U.S. Weather Bureau deployed a national radiometer network in the 1950s to collect GHI. Since then, radiometer design and data acquisition system performance have seen many advancements. The earliest records of solar flux measurements were based on thermopile-type pyranometer signals stored on analog strip chart recordings to determine daily amounts of solar flux on a horizontal surface. Today, 1-minute (or shorter) digital recordings are available from fast-response silicon photodiodes and improved thermopile-type pyranometers and pyrheliometers that are deployed in regional measurement networks to provide solar energy resource data for a variety of applications.

Historically, there have been four radiometer calibration reference scales: Ångström Scale (ÅS 1905), Smithsonian Scale (SS 1913), International Pyrheliometric Scale (IPS 1956), and the WRR (1979). The relative differences among these scales can introduce a data bias on the order of 2%. The user should be aware of this potential bias in data measured before 1979.[3]

Modeled solar resource data derived from available surface meteorological observations and satellite measurements provide estimates of solar resource potential for locations lacking actual measurements. These modeling methods address the needs for improved spatial resolution of the resource data. The first national effort to model solar resources in the 1970s advanced our understanding of solar radiation distributions based on the then available historical measurements at 26 locations to an additional 222 meteorological observing stations with detailed records of hourly cloud amounts and other relevant data (see SOLMET/ERSATZ section, page 58). Today, satellite-based observations of clouds are used to model hourly surface solar fluxes with 10-km spatial resolution (see 1991–2005 NSRDB, page 80).

Long-Term and Typical Meteorological Year Datasets

Understanding the timeframe, or period of record, associated with solar resource and other meteorological data is important for conducting useful analyses. These weather-driven data have fluctuations that can range from seconds to years and longer. Long-term data can be representative of the climate if the period of record is at least 30 years. By convention, the 30-year interval has been deemed sufficient to reflect longer term climatic trends and filter the short-term interannual fluctuations and anomalies.[4] Climate normals are recomputed each decade to address temperature, pressure, precipitation, and other surface meteorological variables. The most recent climatic normals are based on data from 1971 to 2000.

A TMY dataset provides designers and other users with a reasonably sized annual dataset that holds 8,760 hourly meteorological values that typify conditions at a specific location over a longer period, such as the 30-year climatic normal. The TMY dataset is composed of 12 TMMs selected on the basis of their similarity of individual cumulative frequency distributions for selected data elements. The longer term distributions are determined for that month using data from the full period of record. The TMMs are then concatenated, essentially without modification, to form a single year with a serially complete data record. The resulting TMY dataset contains measured and modeled time-series solar radiation and surface meteorological data, although some hourly records may contain filled or interpolated data for periods when original observations are missing from the data archive.

TMY datasets are widely used by building designers and others for modeling renewable energy conversion systems. Although not designed to provide meteorological extremes, TMY data have natural diurnal and seasonal variations and represent a year of typical climatic conditions for a

---

[3] WRR = 1.026 (åS 1905) = 0.977 (SS 1913) = 1.022 (IPS 1956)
[4] International Meteorological Conference in Warsaw, 1933.

location. The TMY should not be used to predict weather or solar resources for a particular period of time, nor is it an appropriate basis for evaluating real-time energy production. Rather, a TMY represents conditions judged to be typical over a long period, such as 30 years. Because they represent typical rather than extreme conditions, they are not suited for designing systems and their components to meet the worst-case weather conditions that could occur at a location.

The next section describes the three versions of TMY data for the United States. In 1978, Sandia National Laboratories produced the first TMY for 248 locations using long-term weather and solar data from the 1952–1975 Solar Meteorological (SOLMET)/ERSATZ database (Hall et al. 1978). In 1994, NREL developed the TMY2 using data from the 1961–1990 NSRDB (Marion and Urban 1995). In 2007, NREL released a 15-year updated NSRDB for 1991–2005 (Wilcox 2007) that formed the basis of the TMY3 dataset.

Solar Resource Data

An inventory of solar resource data sources is presented in chronological order, based on the first data record.
The attributes of each data source are presented using the list of key considerations (see sidebar). DNI data are available from these sources or can be estimated by using available models and the data elements present in each dataset.

NCEP/NCAR Global Reanalysis Products

Products from National Center for Environmental Prediction/National Center for Atmospheric Research (NCEP/NCAR) Reanalysis Project are archived in the dataset called ds090.0. The resolution of the global Reanalysis Model is 209 km with 28 vertical levels. Results are available at 6-hour intervals. Although the initial plan was to reanalyze the data for a 40-year period (1957–1996), production has gone back to 1948 and is going forward continuously. Plans call for rerunning the entire period as next generation models are ready (Kalnay et al. 1996; Kistler et al. 2001).

Key Considerations

Applying solar and meteorological data from different sources requires attention to these key considerations:

- **Period of record.** Influenced by many factors, solar resource data vary from year to year, seasonally, monthly, weekly, daily, and on timescales down to a few seconds. Thus, climate normals are based on 30 years of meteorological data. Another popular approach is to determine a TMY dataset from a statistical analysis of multiyear data to derive a single year of data that are representative of a longer term record. Comparative analyses must account for any natural differences that result from the periods when the data were acquired.

- **Temporal resolution**. Solar resource data can range from annually averaged daily-integrated power (kWh/m^2/day) typically used for mapping resource distributions to 1-s samples of irradiance (W/m^2) for operational time-series analyses.

Other considerations depend on the data type:

- **Spatial coverage.** The area represented by the data can range from a single station to a sample geographic region to a global perspective.

- **Spatial resolution.** Ground-based measurements are site specific. Current satellite-remote sensing estimates can be representative of 10-km × 10-km or smaller areas.

- **Data elements and sources of the data.** The usefulness of solar resource data may depend on the available data elements (e.g., DNI) and whether the data were measured, modeled, or produced in combination.

- **Data quality control and quality assessments.** Descriptions of the measurement operations, model validation methods, and data adjustments or corrections are key metadata elements.

- **Estimated uncertainties.** Stated uncertainties should include a description of the methodology used to provide this information.

- **Availability.** Data are distributed in the public domain, for purchase, or license.

- **Updates.** The need to include the most recent data and other revisions can require regular database updates.

There are more than 80 variables, including incoming solar radiation (GHI), temperature, relative humidity, and wind components, in several coordinate systems. They are organized as different subgroups in the archive. Some special periods are analyzed more than once to provide data for special research studies.

The Research Data Archive is maintained by the Computational and Information Systems Laboratory at NCAR. NCAR is sponsored by the National Science Foundation. The original data are available from the Research Data Archive (http://dss.ucar.edu) in dataset number ds090.0.

Period of record: 1948–2009.

Temporal resolution: 6 hours (W/m²).

Spatial coverage: Global.

Spatial resolution: 2.5 degrees (nominal).

Data elements and sources: GHI and more than 80 variables, including geopotential height, temperature, relative humidity, and U and V wind components, in several coordinate systems, such as a 17 pressure level stack on 2.5 × 2.5 degree grids, 28 sigma level stacks on 192 × 94 Gaussian grids, and 11 isentropic level stacks on a 2.5 × 2.5 degree grid.

Data quality control and assessment: No information.

Estimated uncertainties: None stated.

Availability: University Center for Atmospheric Research, Computational and Information Systems Laboratory Research Data Archive, http://dss.ucar.edu/datasets/ds090.0.

Updates: Monthly.

SOLMET/ERSATZ

In response to the energy crisis in the mid-1970s, NOAA and the Energy Research and Development Administration (later the U.S. Department of Energy [DOE]) funded the "rehabilitation" of surface meteorological and solar measurement data to create the SOLMET hourly dataset. SOLMET data were derived from the best available solar radiation measurements from 26 stations operated by the National Weather Service (NWS) (NCDC 1978, 1979). Additional ERSATZ data, literally "inferior substitute," were modeled from available hourly and 3-hourly cloud and other surface meteorological observations to expand the data coverage by an additional 222 NWS stations. The SOLMET/ERSATZ database was created to address the needs of the solar energy R&D community. The database provided:

- A single source of merged suitable solar measurements and meteorological data

- Data consistent with SI

- Time-series data so users can access the information in true solar and standard time

- Time-series data so users will be aware of the selected meteorological observation that is closest to the time of the solar observation (e.g., selected to be the observation nearest to the midpoint of the solar hour)

- Data recorded in local standard time for conversion to solar time

- A data format with additional solar radiation parameters (direct and tilted, normal incidence, diffuse, and net), as well as additional measurements (ultraviolet and other spectral regions) to be available from stations in the future

- Historical solar radiation data (including the ETR field) converted to the same international scale based on a solar constant value of 1,377 W/m²

- Eliminated undesirable format features that were inherent in the past data sources such as over punches and blanks

- Missing observations and observations that were estimated via models (e.g., bright sunshine duration and cloud regression models)

- Solar GHI data as they were originally observed and provided the user with data corrected for all known scale, instrument, and calibration problems in addition to a dataset corrected via a model.

This database provides some of the earliest measurements of solar irradiance from a national network.

Period of record: December 1951 through December 1976.

Temporal resolution: Hourly (hour ending in local solar time).

Spatial coverage: United States and territories (Figure 5-1).

Spatial resolution: 26 measurement stations and 222 modeled stations.

Data elements and sources: ETR, GHI (observed-SOLMET or modeled-ERSATZ, engineering corrected, standard year corrected), direct normal radiation (estimated from global), minutes of sunshine, clouds (ceiling height, total and opaque cloud fractions, and information for up to four cloud layers), and surface meteorological conditions (temperature, wind speed, pressure, snow cover, horizontal visibility, sky condition, and current weather).

Estimated uncertainties: Based on comparisons with subsequent NOAA Network measurements from 1977 to 1980, the monthly mean daily total SOLMET GHI and DNI accuracies are ± 7.5% and ± 10% respectively. Similarly, the monthly mean daily total ERSATZ GHI and DNI accuracies are ± 10% and ± 20%. The modeling method eliminated any evidence for long-term trends in atmospheric opacity resulting from volcanic eruption, urbanization, or other causes. The uncertainty of individual hourly values is higher than the monthly mean daily statistics.

Availability: National Climatic Data Center (NCDC), NESDIS, NOAA, U.S. Department of Commerce, www.ncdc.noaa.gov/.

Updates: Released in 1978, the SOLMET/ERSATZ database was replaced in 1992 by the 1961–1990 NSRDB.
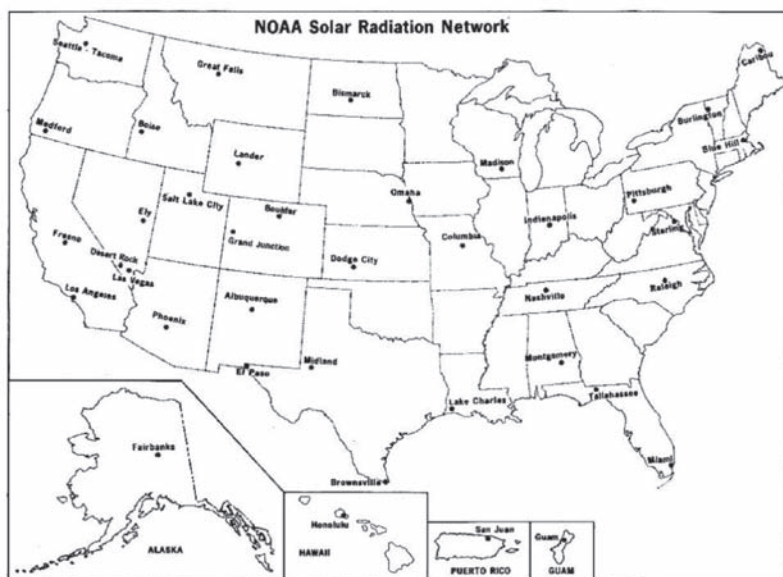
Figure 5-1. SOLDAY and SOLMET measurement stations (26 each)

SOLDAY

SOLDAY is the second of two data rehabilitation projects completed for NOAA and the Energy Research and Development Administration (now DOE) to produce a solar resource dataset with merged suitable solar measurements and meteorological data consistent with SI (NCDC 1979b). The daily GHI data were reformatted by removing all known procedural and instrumental errors and included all available meteorological elements. Rehabilitated hourly solar measurement stations used in SOLMET were not selected for the SOLDAY format to eliminate data redundancy. Daily GHI data were based on recorded solar radiation on strip charts and daily amounts obtained for a part of the time by summing hand-computed hourly values. For the remainder of the time, daily sums were obtained from a mechanical integrator. This dataset provides some of the earliest measurements of solar radiation and complements the geographic distribution of the SOLMET measurement stations.

Period of record: January 1952 through December 1976.

Temporal resolution: Daily.

Spatial coverage: Continental United States (Figure 5-1).

Spatial resolution: 26 measurement stations.

Data elements and sources: Computed times of daily sunrise and sunset, ETR (based on solar constant = 1,377 W/m²), measured GHI from mechanical integrators and strip charts and daily amounts calculated by summing hand-computed hourly values, minutes, and percent of possible sunshine, temperature (maximum, minimum, mean), precipitation, snowfall, snow depth, weather codes, and sky cover from hourly observations. None of the 26 SOLDAY measurement stations are in the hourly SOLMET dataset.

Data quality control and assessment: Individual station histories note pertinent information, making it possible to properly interpret the data. If more than 60 days elapsed between clear solar noon irradiance values, no sky cover/sunshine model was used to fill the irradiance data gaps.

Estimated uncertainties: Based on the known measurement characteristics of the Eppley Laboratory, Inc., Model 50 and Model PSP pyranometers used to measure GHI at SOLDAY stations, the estimated daily total irradiances are expected to be within ± 10%. Measured data from Model PSP radiometers were not corrected for thermal offsets that were discovered much later.

Availability: NCDC, NESDIS, NOAA, U.S. Department of Commerce, www.ncdc.noaa.gov/.

Updates: Released in 1979, the SOLDAY database was replaced in 1992 by the 1961–1990 NSRDB.

Typical Meteorological Year

A TMY dataset provides a single year of hourly data for solar radiation and other meteorological elements that permit performance comparisons of system types and configurations for one or more locations. A TMY is not necessarily a good indicator of conditions over the next year, or even the next 5 years. Rather, it represents conditions judged to be typical over a long period, such as 30 years. Because they represent typical rather than extreme conditions, TMYs are not suited for designing systems and their components to meet the worst-case weather conditions that could occur at a location.

The first TMY dataset[5] is a subset of the hourly SOLMET measurement and ERSATZ model estimates for 248 locations in the United States and territorial possessions. The TMY data consists of typical months concatenated to form a complete year of 8,760 hourly records. The TMMs were selected in part by comparing weighted cumulative distribution functions of nine

---

[5] Subsequent TMY datasets are described in other sections.

data elements as shown in Table 5-1 with the long-term distributions. Examining the weighted sum of the 13 Finkelstein-Schafer statistics for each year and persistence characterized by frequency and run length above and below fixed long-term percentiles resulted in 5 "candidate years" for the month in question. The final selection of a TMM was somewhat subjective; years with small weighted sum statistics, small deviations, and "typical" run structures were chosen.

TMY data provide hourly GHI and DNI solar data and other surface meteorological elements.

Table 5-1. Weighting Factors Applied to Cumulative Distributions

| Version | Temperature | | | | | | Wind Velocity | | Solar Radiation | |
| | Dry Bulb | | | Dew Point | | | | | | |
	Max.	Min.	Mean	Max.	Min.	Mean	Max.	Mean	GHI	DNI
TMY	1/24	1/24	2/24	1/24	1/24	2/24	2/24	2/24	12/24	N/A
TMY2-3	1/20	1/20	2/20	1/20	1/20	2/20	1/20	1/20	5/20	5/20

Period of record: One year representative of the SOLMET/ERSATZ data period 1952–1976.

Temporal resolution: Hourly.

Spatial coverage: United States and territories (Figure 5-1).

Spatial resolution: 26 measurement stations and 222 modeled stations.

Data elements and sources: ETR, GHI (observed-SOLMET or modeled-ERSATZ, engineering corrected, standard year corrected), direct normal radiation (estimated from global), minutes of sunshine, clouds (ceiling height, total and opaque cloud fractions, and information for up to four cloud layers), and surface meteorological conditions (temperature, wind speed, pressure, snow cover, horizontal visibility, sky condition, and current weather).

Data quality control and assessment: Measured hourly GHI determined from strip chart recordings and labeled as "observed" data. Known instrument corrections for temperature response were applied to observed GHI and labeled as "engineering corrected" data. Measured data from single-black thermopile radiometers were not corrected for thermal offsets that were discovered much later. Clear sky model estimates of pyranometer calibration changes were applied to observed GHI and labeled as "standard year irradiance corrected" data. The clear sky model was also used to fill missing GHI observations. Only the standard year irradiance data field is serially complete. All SOLMET DNI data were computed based on a regression relationship between observed hourly global and direct normal irradiance measurements taken at five measurement stations: Livermore, California; Raleigh, North Carolina; Maynard, Massachusetts; and Fort Hood, Texas. All ERSATZ GHI and DNI data were estimated from clear sky models and available cloud observations.

Estimated uncertainties: Based on comparisons with subsequent NOAA Network measurements from 1977 to 1980, the monthly mean daily total SOLMET GHI and DNI accuracies are ± 7.5% and ± 10%, respectively. Similarly, the monthly mean daily total ERSATZ GHI and DNI accuracies are ± 10% and ± 20%, respectively. The modeling method destroyed any evidence for long-term trends in atmospheric opacity resulting from volcanic eruption, urbanization, or other causes. The uncertainty of individual hourly values is certainly higher than the monthly mean daily statistics.

Availability: NCDC, NESDIS, NOAA, U.S. Department of Commerce, www.ncdc.noaa.gov/.

Updates: TMY was released in 1978. TMY Version 2 (TMY2) is based on the 1961–1990 NSRDB and was available in 1994. TMY Version 3 (TMY3) is based on input data for 1976–2005 from the 1961–1990 NSRDB, Version 1.1 and the 1991–2005 NSRDB update. TMY3 was available in 2008.

1961–1990 National Solar Radiation Database

NREL completed the 1961–1990 NSRDB in 1992 (NREL 1992). The database consists of serially complete hourly modeled (93%) and measured (7%) solar radiation data for 239 locations in the United States. Data records include associated meteorological measurements such as temperature, humidity, cloud cover, and visibility. Measured solar radiation data are included in the datasets when available for 52 NSRDB primary stations, but among those, no station has more than a few years of measured data. All remaining GHI solar data were modeled using a METSTAT solar radiation model. The METSTAT model was designed to accept hourly cloud information from the then readily available data from trained NWS observers. DNI measurements were available from primary stations; otherwise, these data were modeled from available meteorological data.

The NSRDB contains statistical summaries computed from the hourly data for the entire period of record for all stations. For the solar radiation data, these statistics include the average and standard deviations of the daily total solar energy (DNI, DHI, and GHI) for each station-year-month and each station-year. The 30-year averages and the standard deviations of monthly and annual means from 1961 through 1990 are also provided. For the meteorological elements, only monthly, annual, and 30-year averages were computed.

The hourly statistical products include monthly, annual, and 30-year averages and standard deviations for each hour of the day for GHI, DNI, and DHI. The averages can be used to prepare average diurnal profiles of hourly solar energy. The hourly values have also been binned in 24, 50-Wh/m^2 bins from 0 to 1200 Wh/m^2. The mean number of hourly values falling into each bin has been determined for each station-month for the 30-year period of record from 1961 through 1990. These statistics can be used to plot histograms and determine cumulative frequency distributions.

A solar radiation persistence product was created for each station-month by calculating the number of times the daily total solar radiation energy persisted above or below set thresholds for periods from 1 to 15 days. These calculations were performed for the entire 30-year period from 1961 to 1990.

Period of record: 1961–1990.

Temporal resolution: Hourly.

Spatial coverage: United States, Guam, and Puerto Rico (Figure 5-2).

Spatial resolution: 239 stations (56 stations have some measurements).

Data elements and sources: Hourly GHI, DNI, DHI, ETR, direct normal ETR, total sky cover, opaque sky cover, ceiling height, dry-bulb temperature, dew point temperature, relative humidity, atmospheric pressure, horizontal visibility, wind speed, wind direction, present weather, aerosol optical depth, total precipitable water, snow depth, number of days since last snowfall. About 93% of the irradiance data were modeled from cloud observations. Measured DNI are available from primary stations.
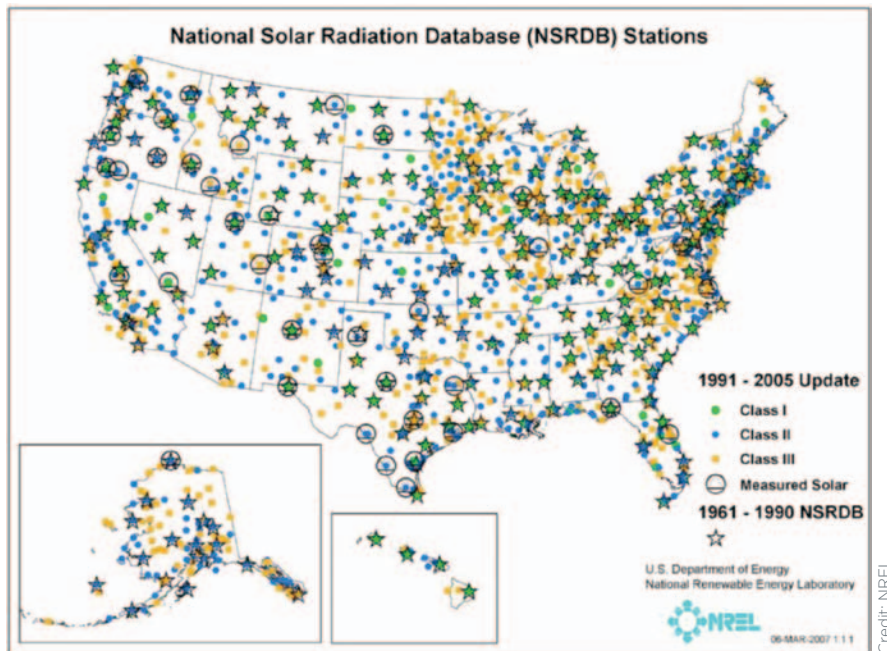
Figure 5-2. Original 239 stations in the 1961–1990 NSRDB released in 1992 and the 1,454 stations in the 1991–2005 NSRDB released in 2007

Data quality control and assessment: An automated data processing method was developed to apply quality flags to each hourly solar radiation and meteorological element. These flags provide information on the source and uncertainty of a data element, allowing the user to evaluate its usefulness. Because of the difficulties frequently encountered when measuring solar radiation and the resultant unknown quality of some solar radiation data, a major effort was undertaken to develop procedures and software for performing post-measurement quality assessment of these data. Such assessments were needed to ensure that the data selected for model development and other applications were of the highest quality available. The assessments also were needed to calculate the uncertainty of measured solar radiation data. A quality assessment software package (SERI QC) was developed to address these needs (NREL 1993). SERI QC is based on the establishment of boundaries or limits within which acceptable data are expected to lie. This is similar to previous quality assessment procedures that used extraterrestrial values for the upper limit and zero for the lower limit within which solar radiation data were expected. SERI QC increased the sophistication of this approach by establishing much more restrictive boundaries specific to each station-month. Measured data from single-black thermopile radiometers were not corrected for thermal offsets that were discovered much later.

Estimated uncertainties: Statistics on the quality of the solar radiation data were determined by calculating the percentage of the hourly values to which each source and uncertainty flag was assigned. These percentages were calculated for each station-year and for the 30-year period of record and are available as a separate product.

Availability: NCDC, NESDIS, NOAA, U.S. Department of Commerce Renewable Energy Data Sources at www.ncdc.noaa.gov/oa/reds/index.html.

Solar data only and documentation are maintained by the NREL Renewable Resource Data Center (RRDC) at http://rredc.nrel.gov/solar/old_data/nsrdb/1961-1990.

Updates: Released in 1992; updated in 2007 (see 1991–2005 NSRDB, page 80).

Typical Meteorological Year Version 2

TMY provides a single year of hourly data for solar radiation and other meteorological elements that permit performance comparisons of system types and configurations for one or more locations. A TMY is not necessarily a good indicator of conditions over the next year, or even the next 5 years. Rather, it represents conditions judged to be typical over a long period of time, such as 30 years. Because they represent typical rather than extreme conditions, they are not suited for designing systems and their components to meet the worst-case conditions occurring at a location.

TMY2 was developed from the 1961–1990 NSRDB. Succeeding the older 1952–1975 SOLMET/ERSATZ database, the NSRDB accounted for any 1975–1990 climate changes and provided more accurate values of solar radiation for several reasons:

- Better model for estimating values (more than 90% of the solar radiation data in both databases are modeled)

- More measured data, some of which are DNI

- Improved instrument calibration methods

- Rigorous procedures for assessing data quality.

A comparison of the older and newer databases provided an incentive for developing the TMY2s. On an annual basis, 40% of the NSRDB and SOLMET/ERSATZ stations were in disagreement for values of GHI by more than 5%; some stations showed disagreement of up to 18% (Marion and Myers 1992). For DNI, 60% of the NSRDB and SOLMET/ERSATZ stations were in disagreement by more than 5%; some showed disagreement of up to 33%. Disagreement between the two databases is even greater when compared on a monthly basis.

An analysis of cloud cover data indicated little or no change for the two periods; consequently, most of the disagreement for NSRDB and SOLMET/ERSATZ data is attributed to differences in reconstructing the instrument calibrations and differences in the solar radiation models (NSRDB Vol. 2 1995). Because of differences in the databases from which they were derived, the old TMYs and the new TMY2s will differ. For some stations the differences may be minor, but others will be significant.

For the TMY2 and the more recent TMY3 data (see Solar Radiation Research Laboratory section, page 71), selection of the months in the typical year included a weighting index for DNI radiation (see Table 5-1). This improves the agreement between annual DNI for the TMY and the 30-year annual average by about a factor of 2 (based on 20 geographically representative NSRDB stations) as follows. When only GHI is used for the solar index, the TMY annual direct radiation values for the 20 stations were within 4% (95% confidence level) of the 30-year annual average. Using both GHI and DNI indices reduced the differences to 2%, with no adverse effect on GHI comparisons.

Because they represent typical rather than extreme conditions, TMYs are not suited for designing systems and their components to meet the worst-case conditions at a location.

Period of record: One year representative of the 1961–1990 NSRDB data period.

Temporal resolution: Hourly.

Spatial coverage: United States and territories (Figure 5-1).

Spatial resolution: 239 stations representing the 1961–1990 NSRDB.

Data elements and sources: Hourly GHI, DNI, DHI, ETR, direct normal ETR, total sky cover, opaque sky cover, ceiling height, dry-bulb temperature, dew point temperature, relative humidity, atmospheric pressure, horizontal visibility, wind speed, wind direction, present weather, aerosol optical depth, total precipitable water, snow depth, number of days since last

snowfall. About 93% of the irradiance data were modeled from surface observations of clouds. Measured DNI is available from primary stations. The format of the TMY2 data files is different from the format used for the NSRDB and the original TMY data files.

Data quality control and assessment: The data are serially complete; each hourly record in the file contains values for solar radiation, illuminance, and meteorological elements. A two-character source and uncertainty flag is attached to each data value to indicate whether the data value was measured, modeled, or missing, and to provide an estimate of the uncertainty of the data value. Measured data from single-black thermopile radiometers were not corrected for thermal offsets that were discovered much later.

Estimated uncertainties: The TMY2 data were compared with 30-year NSRDB datasets to show differences in mean values between TMY2 data and long-term data for the same stations. Comparisons were made on a monthly and an annual basis for GHI, DNI, and south-facing latitude tilt radiation; and for heating and cooling degree-days. These comparisons give general insight into how well, with respect to long-term conditions, the TMY2s portray the mean solar resource and the dry-bulb temperature environment for simulations of solar energy conversion systems and building systems. On an annual basis, the TMY2s compare closely to the 30-year datasets. The monthly comparisons are less favorable than the annual comparisons (Table 5-2).

Table 5-2. Comparisons of TMY2 Data With 30 Years of NSRDB Data

Data Element	Confidence Interval (kWh/m^2 per day)	
	Monthly	Annual
GHI	± 0.20	± 0.06
DNI	± 0.50	± 0.16
Global on tilted surface (tilt angle = site latitude)	± 0.29	± 0.09

Availability: NREL RRDC at http://rredc.nrel.gov/solar/old_data/nsrdb/1961-1990/tmy2/.

Updates: TMY2 was released in 1994. TMY3 is based on input data for 1976–2005 from the 1961–1990 NSRDB, Version 1.1 and the 1991–2005 NSRDB update. TMY3 was available in 2008 (see page 82).

World Meteorological Organization World Radiation Data Center

Established in 1962, the WRDC is one of the recognized World Data Centers sponsored by the WMO. Located at the Main Geophysical Observatory in St. Petersburg (formerly Leningrad), Russian Federation, the WRDC has collected, archived, and published solar radiation data from observing stations from around the world in accordance with Resolution 31 of WMO Executive Committee XVIII, which ensures the availability of these data for research by the international scientific community. Daily total GHI measurements comprise most of the data from the more than 1000 sites that have contributed to the archive. Some diffuse, sunshine duration, and radiation balance observations are also submitted. Data are submitted mainly by National Meteorological Services of contributing countries. Some recent hourly measurements are present for a few measurement stations. Dense coverage is available for the western European continent, whereas the South American continent has large unrepresented areas.

Period of record: 1964–present.

Temporal resolution: Daily totals with some hourly measurements at a few sites.

Spatial coverage: Global (Figure 5-3).

Spatial resolution: 1000+ measurement stations.

Data elements and sources: Primarily daily total GHI, radiation balance, and sunshine duration, but some DHI and DNI. Some hourly measurements are available from a few sites.

Data quality control and assessment: In an effort to ameliorate the differing practices among submitting countries, the WRDC has a long-term practice of processing data arrays from many stations. However, the processing of data, and especially quality control, is carried out without knowledge of in-situ weather conditions.

Estimated uncertainties: No information.

Availability: http://wrdc-mgo.nrel.gov and http://wrdc.mgo.rssi.ru.

For more detailed information, contact:
Voeikov Main Geophysical Observatory
World Radiation Data Centre
7, Karbyshev Str.
194021, St. Petersburg, Russian Federation
tel.: (812) 297-43-90
fax: (812) 297-86-61

Please direct any comments or suggestions regarding the Web site to
Dr. Anatoly V. Tsvetkov, Head of WRDC
tel: (812) 295-04-45
e-mail: wrdc@main.mgo.rssi.ru
e-mail: tsvetkov@main.mgo.rssi.ru
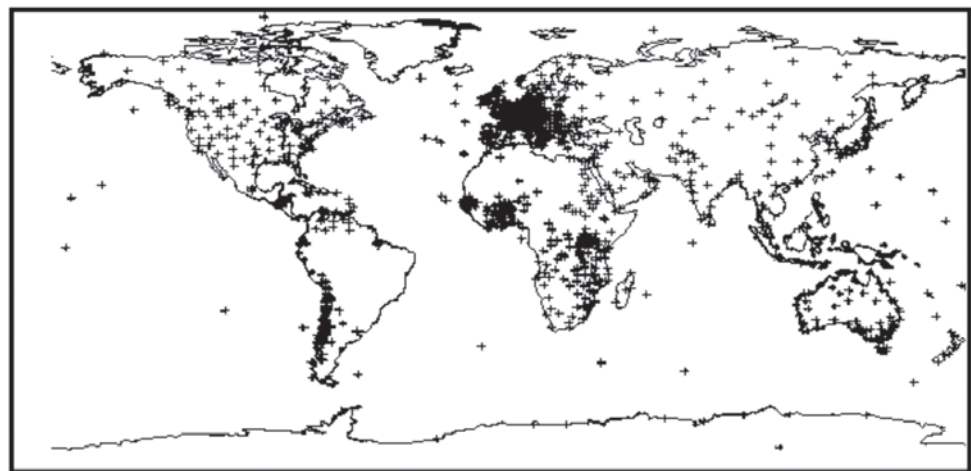
Credit: NREL

Figure 5-3. WRDC measurement stations

Western Energy Supply and Transmission Associates Solar Monitoring Network

In the mid-1970s, Southern California Edison submitted a proposal to Western Energy Supply and Transmission Associates to expand the solar monitoring effort outside the Southern California Edison service territory in an effort to establish an accurate solar resource database. The resulting Western Energy Supply and Transmission Solar Monitoring Network eventually included 52 stations in 6 western states (Arizona, California, Colorado, Nevada, New Mexico, and Wyoming). The network operated for 5 years during 1976–1980 collecting 15-minute GHI, and solar DNI, as well as dry-bulb temperatures. Not all stations were in operation all 5 years, nor did all collect all data parameters. Thirteen stations reported data in the first West Associates Network publication in 1976. All told, during the approximately 4½ years of network operation, 52 stations gathered data on GHI and ambient temperature. Twenty-six also reported DNI measurements.

Period of record: 1976–1980.

Temporal resolution: 15 min.

Spatial coverage: Arizona, California, Colorado, Nevada, New Mexico, and Wyoming.

Spatial resolution: 52 measurement stations (Figure 5-4).

Credit: NREL

Figure 5-4. Western Energy Supply and Transmission Associates Solar Monitoring Network of 52 measurement stations (1976–1980)

Data elements and sources: GHI, DNI, and dry-bulb temperature measured with pyranometers (Eppley Black and White, Eppley PSP, and the Spectrolab Spectrosun SR75) and pyrheliometers (Eppley NIP) in automatic solar trackers. DNI was measured at 26 of the 52 stations.

Data quality control and assessment: Southern California Edison instituted a rigorous program of radiometer maintenance and calibration for the Western Energy Supply and Transmission Associates Solar Monitoring Network. Procedures included maintenance to be performed once per week at stations that monitored GHI and dry-bulb temperature. The pyranometer dome was cleaned and the electronics package checked for correct operation. At stations that also monitored DNI, additional procedures called for maintenance to be performed three times per week. During this maintenance, the pyrheliometer was cleaned and the semiautomatic solar tracker was adjusted for changes in declination and azimuth. All network radiometers were calibrated twice per year to the WRR. Measured data from single-black thermopile radiometers were not corrected for thermal offsets that were discovered much later.

Estimated uncertainties: Accounting for the frequency of maintenance and radiometer calibrations, the daily total GHI and DNI are likely accurate to ± 5% and ± 8%. (DNI uncertainty estimate accounts for semiautomatic operation of the solar tracker requiring manual adjustment for changing solar declination.)

Availability: Data and documentation are maintained by the NREL RRDC at http://rredc.nrel. gov/solar/pubs/wa/wa_index.html.

Updates: Released in 1981.

Pacific Northwest Solar Radiation Data Network

The University of Oregon's Pacific Northwest Solar Data Network has the longest continuous record of measured DNI in the United States. Beginning in 1977 with an 11-station network, the goal has remained to provide high-quality scientific data for solar energy resource evaluation and long-term climate studies. The work is made possible by the Bonneville Power Administration, Energy Trust of Oregon, Eugene Water and Electric Board, Emerald People's Utility District, NREL, Northwest Power and Conservation Council, and Oregon BEST. Information about the monitoring stations, solar data, software tools, and educational material is available from the University of Oregon's Solar Radiation Monitoring Laboratory at http://solardat.uoregon.edu/index.html.

Period of record: 1977–present.

Temporal resolution: 5 min.

Spatial coverage: Idaho, Montana, Oregon, Utah, Washington, and Wyoming.

Spatial resolution: 39 measurement stations (Figure 5-5).

Data elements and sources: GHI, DNI, DHI, global irradiance on tilted surfaces (various), spectral irradiance (various), and surface meteorological data (temperature, relative humidity, dew-point temperature, barometric pressure, precipitation, cloud cover, snow depth, etc.).

Data quality control and assessment: A two-digit data quality control flag is assigned to each data value to identify the type of data (observed, corrected, interpolated, computed, missing or rejected). Radiometers are calibrated annually with periodic on-site checks with traveling references.

Estimated uncertainties: Based on the instrument selections, installation, O&M practices, the estimated uncertainties for corrected daily total irradiances are: DNI ± 2%, GHI ± 5%, and DHI ± 15% + 5 W/m^2.

Availability: The University of Oregon's Solar Radiation Monitoring Laboratory operates and maintains the measurement network and provides the data online at http://solardat.uoregon.edu/SolarData.html.

Updates: Continuous.

Figure 5-5. Pacific Northwest Solar Radiation Data Network operated by the University of Oregon

NOAA Network

Coincident with the rehabilitation of historical data from NWS in the 1970s, DOE and NOAA cofunded the reconstruction of the NWS solar measurement network. The new network of 39 stations was instrumented with new Eppley Laboratory, Inc., model PSP pyranometers and model NIP pyrheliometers for measuring GHI and DNI. Seven stations had shaded PSP pyranometers for measuring DHI. New data acquisition systems were installed to digitally sample the radiometer signals at 1-min intervals and provide strip chart records as a backup medium. Radiometers were calibrated annually at NOAA's solar research facility in Boulder, Colorado, using references traceable to the WRR. Network data were processed and disseminated on 9 track magnetic tape reels by NCDC. These data represent the most complete set of solar resource measurements from the largest federally operated measurement network ever fielded in the United States.

Period of record: 1977–1980.

Temporal resolution: Hourly.

Spatial coverage: United States and territories (Figure 5-6).

Spatial resolution: 39 NWS measurement stations.

Data elements and sources: GHI, DNI, DHI (7 stations), air temperature, relative humidity, cloud amounts, barometric pressure, wind speed and direction at 10 meters, precipitation, snow cover, weather codes measured according to standard NWS operating procedures. Radiation measurements digitally recorded from 1-min instantaneous samples with redundant strip chart recordings.

Data quality control and assessment: Data processing performed at the NCDC using standard procedures that included visual inspection of strip chart records. Radiometers were calibrated annually in Boulder, Colorado, with reference radiometers traceable to the WRR. Monthly data reports and digital data files were produced by the NCDC. Measured data from single-black thermopile radiometers were not corrected for thermal offsets that were discovered much later.

Estimated uncertainties: Based on the instrument selections, installation, and O&M practices, the estimated uncertainties for corrected daily total irradiances are: DNI $\pm$ 2%, GHI $\pm$ 5%, and DHI $\pm$ 15% + 5 W/m².

Availability: NCDC; National Environmental, Satellite, Data, and Information Service; NOAA; U.S. Department of Commerce at www.ncdc.noaa.gov/.

Updates: Final release of TD-9736 occurred in 1983.
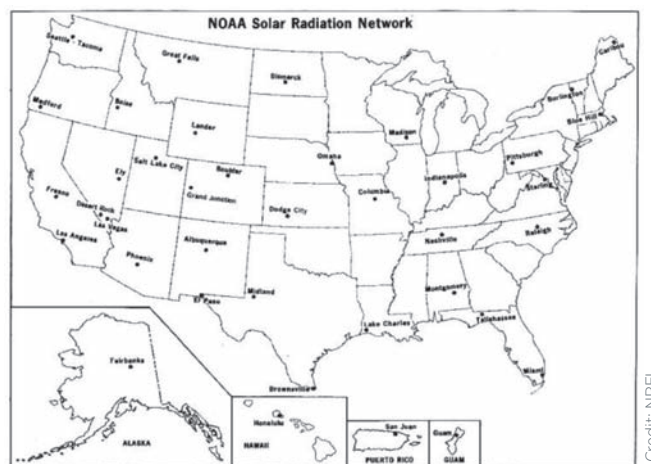
Figure 5-6. NOAA Solar Monitoring Network of 39 stations (1977–1980)

Solar Energy and Meteorological Research Training Sites

Recognizing the need to provide an educated workforce and advance the knowledge of solar radiation and meteorological measurements, DOE and the Solar Energy Research Institute (now NREL) solicited responses from U.S. universities and colleges to participate in what became the Solar Energy and Meteorological Research Training Sites (SEMRTS) Program. Central to the multiyear effort was the requirement to produce a minimum of 12 months of solar resource data from precision instruments with measurements collected at 1-min maintains the data from four of the original six participants as part of its RRDC (data from Davis, California, and Honolulu, Hawaii, were never made available).

Period of record: 1979–1983.

Temporal resolution: 1-min.

Spatial coverage: Fairbanks, Alaska; Atlanta, Georgia; Albany, New York; San Antonio, Texas (see Figure 5-7).

Spatial resolution: Four measurement stations.

Data elements and sources: GHI, DNI, and DHI; global irradiance on tilted surfaces (varies), infrared irradiances, ultraviolet and other spectral irradiance (varies), and surface meteorological conditions (temperature, relative humidity, pressure, visibility, wind speed and direction at 10 meters, precipitation, etc.).

Data quality control and assessment: Research-quality data from proper instrument selection, installation, and maintenance. Data were used to develop automated quality assessment methods. Measured data from single-black thermopile radiometers were not corrected for thermal offsets that were discovered much later.

Estimated uncertainties: Based on radiometer types, installation, and O&M practices, the data uncertainties for daily irradiances were GHI $\pm$ 7%, DNI $\pm$ 3%, DHI $\pm$ 15% + 5 W/m^2.

Availability: Data and documentation are maintained by NREL's RRDC at http://rredc.nrel.gov/solar/old_data/semrts/.

Updates: Released in 1985.

Credit: NREL

Figure 5-7. SEMRTS provided the first 1-min measurements of multiple solar resource parameters for the United States

DAYMET

DAYMET generates daily surfaces of temperature, precipitation, humidity, and GHI over large regions of complex terrain. The model was developed at the University of Montana, Numerical Terradynamic Simulation Group, to meet the needs for high-resolution, daily meteorological and climatological data necessary for plant growth model inputs (Thornton et al. 2000; Thornton and Running 1999). A DEM and daily observations of minimum and maximum temperatures and precipitation from ground-based meteorological stations were used to produce an 18-year daily dataset (1980–1997) as a continuous surface at 1-km resolution. A wide range of summary and point daily data over the conterminous United States is available.

Period of record: 1980–1997.

Temporal resolution: Daily.

Spatial coverage: Continental United States.

Spatial resolution: 1 km.

Data elements and sources: GHI, air temperature (minimum and maximum), relative humidity, and precipitation.

Data quality control and assessment: No information.

Estimated uncertainties: No information.

Availability: www.daymet.org.

Solar Radiation Research Laboratory

The SRRL was established at the Solar Energy Research Institute (now NREL) in 1981 to provide continuous measurements of the solar resources, outdoor calibrations of pyranometers and pyrheliometers, and to characterize commercially available instrumentation. The SRRL is an outdoor laboratory located on South Table Mountain, a mesa providing excellent solar access throughout the year, overlooking Denver. Beginning with the basic measurements of DNI, GHI, and DHI at 5-minute intervals, the SRRL Baseline Measurement System now produces more than 130 data elements at 1-min intervals that are available from the Measurement & Instrumentation Data Center Web site (www.nrel.gov/midc/srrl_bms).

Period of record: 1981–present.

Temporal resolution: 5 min (beginning 15 July 1981), 1 min (beginning 13 January 1999).

Spatial coverage: Golden, Colorado (Figure 5-8).

Spatial resolution: Research measurement station.

Data elements and sources: GHI, DNI, DHI (from shadowband and tracking disk), global on tilted surfaces, reflected solar irradiance, ultraviolet, infrared (upwelling and downwelling), photometric and spectral radiometers, sky imagery, and surface meteorological conditions (temperature, relative humidity, barometric pressure, precipitation, snow cover, wind speed and direction at multiple levels).

Data quality control and assessment: Daily instrument maintenance (M–F) with automated data quality control based on real-time examinations of redundant instrumentation and internal consistency checks using the SERI-QC methodology (NREL 1993). Operators are notified of equipment problems by automatic e-mail messages generated by the data acquisition and processing system. Radiometers are recalibrated at least annually with reference instruments traceable to the WRR. An instrument characterization study is available (Wilcox and Myers 2008). Beginning in 2000, measured data from single-black thermopile radiometers are corrected for thermal offsets that were discovered at that time.

Estimated uncertainties: Based on the instrument selections, installation, and O&M practices, the estimated uncertainties for corrected daily total irradiances are: DNI ± 2%, GHI ± 5 %, and DHI ± 15% + 5 W/m² (GHI data from thermopile-based detectors under clear sky conditions can exhibit a bias of up to –2.5% if not corrected for thermal offsets).

Availability: NREL Measurement & Instrumentation Data Center at www.nrel.gov/midc/srrl_bms.

Updates: Data are updated at least hourly.
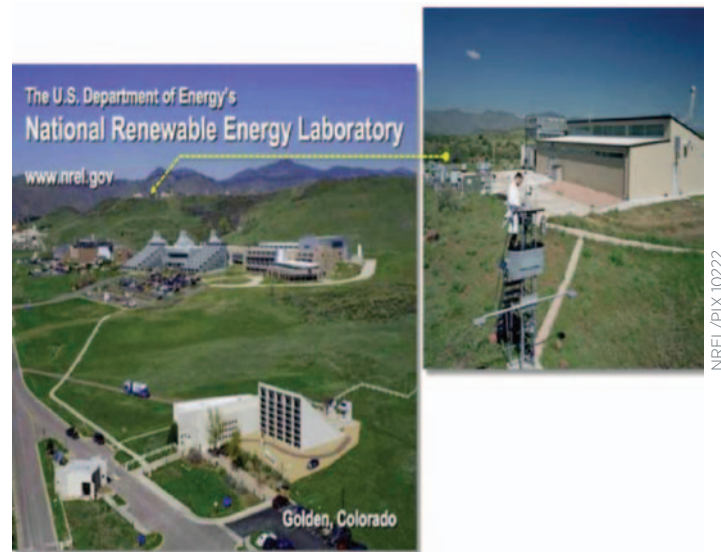
Figure 5-8. The SRRL on South Table Mountain

European Solar Radiation Atlas

This atlas is a software package offering solar resources for Europe in a broad sense, from Ural to Azores and from Northern Africa to Polar Circle. It is a powerful tool for architects, engineers, meteorologists, agronomists, local authorities, tourism professionals, researchers, and students. It covers the period 1981 through 1990. The volume containing the CD-ROM database offers spatial (every 10 km approximately) and temporal knowledge for different time scales (from climatologically means—more than 700 stations—to hourly values—7 stations) on the solar resources: irradiation (global and its components), sunshine duration, as well as air temperatures, precipitation, water vapor pressure, and air pressure in a number of stations.

The software uses the database in either a map or a station mode at user choice. More than 50 maps provide information about the global irradiation, direct and diffuse components, and clearness index. Once a station is selected, the program looks for all the data available for this station. The software includes algorithms covering solar geometry, optical properties of the atmosphere, estimation of hourly slope irradiation under cloudless skies, estimation of solar irradiation values (from daily to hourly values, conversion from horizontal to titled surfaces), spectral irradiance, illuminance, and daily mean profiles of temperature and other statistical quantities (central moments, extremes, probability, cumulative probability, and utilization curves). Graphics can be displayed in 2 or 3 dimensions.

Period of record: 1981–1990.

Temporal resolution: Monthly and annual average daily totals (kWh/m²/day).

Spatial coverage: Europe.

Spatial resolution: 10 km.

Data elements and sources: GHI, DNI, and DHI, sunshine duration, air temperatures, precipitation, water vapor pressure, air pressure in a number of stations.

Data quality control and assessment: No information.

Estimated uncertainties: No information.

Availability: Les Presses Mines Paris Tech.: http://www.ensmp.fr/Presses/?livreplus=54--col3#54. Also see: www.soda-is.com/eng/index.html.

Updates: No information.

Photovoltaic Geographical Information System

PVGIS provides a map-based inventory of solar energy resource and assessment of the electricity generation from PV systems in Europe, Africa, and southwestern Asia. It is a part of the SOLAREC action that contributes to the implementation of renewable energy in the European Union as a sustainable and long-term energy supply. As the basis for PVGIS, the Joint Research Council (JRC) European Commission has developed a solar radiation database from climatologic data homogenized for Europe and available in the European Solar Radiation Atlas, using the r.sun model and the interpolation techniques s.vol.rst and s.surf.rst. These GRASS GIS routines are described with references available from http://re.jrc.ec.europa.eu/pvgis/solres/solresref.htm.

The model algorithm estimates beam, diffuse, and reflected components of the clear sky and real-sky global irradiance/irradiation on horizontal or inclined surfaces. The total daily irradiation (Wh/m^2) is computed by the integration of the irradiance values (W/m^2) calculated at regular time intervals over the day. For each time-step during the day, the computation accounts for sky obstruction (shadowing) by local terrain features (hills or mountains), calculated from the DEM.

The database consists of raster maps representing 12 monthly averages and 1 annual average of daily sums of global irradiation for horizontal surfaces, as well as those inclined at angles of 15, 25, and 40 degrees. Besides these data, raster maps of clear-sky irradiation, the Linke turbidity,[6] and the ratio DHI/GHI were computed.

Period of record: 1981–1990.

Temporal resolution: Annual average (kWh/m^2).

Spatial coverage: Europe.

Spatial resolution: 1 km aggregated to 5 arc-minutes (~8 km).

Data elements and sources: GHI, DNI, DHI, and POA irradiance based on these inputs for the For the European subcontinent:

- Monthly averages of daily sums of global and diffuse irradiation, measured or calculated for 566 ground meteorological stations distributed over the region. The averages represent the period 1981–1990; the data were collected within the ESRA project.

- Linke turbidity derived from the global database (Remund et al. 2003), available also at the SoDa.

- DEM with a grid resolution 1 × 1 km; derived from the USGS SRTM data.

- CORINE land cover with grid resolution 100 m × 100 m.

- Global land cover 2000 with grid resolution 1-km × 1-km GISCO database (© EuroGeographics Association for the administrative boundaries).

- VMAP0 and ESRI data.

---

[6] The Linke turbidity factor is an approximation to model the atmospheric absorption and scattering of clear sky DNI solar radiation due to water vapor and aerosols.

For the Mediterranean Basin, Africa, and southwestern Asia:

- HelioClim-1 database, consisting of daily sums of GHI calculated from Meteosat Prime images over the whole disc. The values represent the period 1985–2004, the original spatial resolution is 15- × 15-arc minute, (about 30 km × 30 km on the equator); the data were processed by the Heliosat-2 method (Rigollier et al. 2000).

- Linke turbidity derived from the global database (Remund et al. 2003), available also at the SoDa.

- DEM with original grid resolution 1 km × 1 km; derived from the USGS SRTM data.

- Global Land Cover 2000 with original grid resolution 1 km × 1 km.

- VMAP0 data.

Data quality control and assessment: A cross-validation was applied to estimate the predictive accuracy of the modeling approach that better explains the distribution of errors further from the locations with known measurements. The cross-validation error shows the maximum possible error that might occur at the given point if it was not taken into consideration in the interpolation. The average yearly mean bias error (MBE) from cross-validation is smaller: 1 Wh/m^2 (0.03%), but the range of monthly averages of MBE is higher – from –3 Wh/m^2 in January to 4 Wh/m^2 in August. The cross-validation RMSE is higher, within the interval of 97 to 299 Wh/m^2/day (4.7% to 11.2%), and the yearly average is 146 Wh/m^2 (4.5%).

Estimated uncertainties: The model accuracy of the PVGIS values in the database was evaluated against the input meteorological data used in the computation. Comparing the yearly averages of the daily GHI, the MBE is 8.9 Wh/m^2 (0.3%) and the RMSE is 118 Wh/m^2 (3.7%). The average RMSE of the PVGIS data is almost the same as for ESRA, the PVGIS approach shows better performance from October to April. Its advantage is linking the terrain features with changes in radiation fields and considering the shadowing effects. Comparisons of GHI data from 563 measurement stations with PVGIS (version 2) and ESRA raster maps respectively indicate the RMSE of the results to the original measurements of daily global irradiation occur within an interval of 68 to 209 Wh/m^2. In relative terms, it is within the interval of 3.2% to 7.8%; the RMSE values peak in winter months. The comparison of the ESRA interpolation approach shows that, although the overall accuracy is practically the same (the yearly average of the RSME for ESRA is 113 Wh/m^2, i.e., 3.5%), the PVGIS modeled values are slightly better in period from October to April and poorer in summer months.

Availability: European Commission, JRC, Institute for Energy, Renewable Energy Unit. http://re.jrc.ec.europa.eu/pvgis/download/download.htm.

METEONORM

METEONORM 6.1 (Edition 2009) is a comprehensive meteorological reference, incorporating a catalogue of meteorological data and calculation procedures for solar applications and system design at any desired location in the world. METEONORM addresses the needs of engineers, architects, teachers, planners, and anyone interested in solar energy and climatology by providing access to a unified set of data, models, and software tools.

Database Properties

- Climatological data from more than 8,055 weather stations (1,422 recording GHI)

- Measured parameters: monthly means of global radiation, temperature, humidity, precipitation, days with precipitation, wind speed and direction, and sunshine duration

- Time periods 1961–1990 and 1996–2005 for temperature, humidity, precipitation, and wind speed selectable

- Updated global radiation database for period 1981–2000

- Use of satellite data for areas with low density of weather stations
- Inclusion of climate change projections (Hadley CM3 model).

Models Overview

- Interpolation models to calculate mean values for any site in the world
- One-minute time resolution for radiation parameters
- Calculation of radiation for inclined surfaces with updated models
- Enhanced temperature and humidity generation for building simulation.

Software Functions

- Import of user data (including current data by Internet)
- Effects of high horizon considered in radiation calculation (high horizon calculated automatically for all mountain regions)
- Twenty-eight output formats as well as user-definable output format
- Five languages supported: English, French, German, Italian, and Spanish
- Manual in English, maps and illustrations included on CD-ROM.

Period of record: 1981–2000 (GHI database); current user data also accepted by the software.

Temporal resolution: 1-minute and hourly modeled data.

Spatial coverage: Global.

Spatial resolution: Data from 8,055 meteorological stations are interpolated to establish weather data at any specified point.

Data elements and sources: Measured: monthly means of GHI, temperature, humidity, precipitation, wind speed and direction, and bright sunshine duration. Modeled: 1-minute and hourly typical years radiation parameters (GHI, DNI, DHI, global on a tilted surface, downwelling infrared, luminance, and ultraviolet-A and -B), precipitation, and humidity parameters (dew point, relative humidity, mixing ratio, psychrometric temperature).

Data quality control and assessment: With the Version 6.1 database, solar energy systems can be consistently simulated in all parts of the world. The interpolation errors are within the variations of climate from one year to the next. Extensive testing and validation of the radiation models are documented in the "Handbook Part II: Theory" available from www.meteonorm.com/pages/en/downloads.php.

Estimated uncertainties: Interpolation of GHI – MBE = 0 W/m^2; RSME = 15 W/m^2; for yearly mean GHI – 17 W/m^2 (10%).

Availability: METEOTEST GmgH, Bern, Germany at www.meteonorm.com/pages/en/meteonorm.php.

Updates: Periodic.

NASA Surface Meteorology and Solar Energy

The Prediction of Worldwide Energy Resource (POWER) project was initiated in 2003 to improve subsequent releases of SSE, and to create new datasets applicable to other industries from new satellite observations and the accompanying results from forecast modeling. The POWER Web interface (http://power.larc.nasa.gov) currently encompasses the SSE dataset, tailored for the renewable energy industry, as well as parameters tailored for the sustainable buildings community and the bioenergy/agricultural industries. In general, the underlying data behind the parameters used by each of these industries are the same: solar radiation and meteorology, including surface and air temperatures, moisture, and winds.

The data are on a 1-degree longitude × 1-degree latitude equal-angle grid covering the entire globe (64,800 regions). The data are generated using the NASA GEOS, Version 4 (GEOS 4) Multiyear Assimilation Time Series Data. The GEOS 4 dataset has a spacing of 1.25 degrees of longitude by 1 degree of latitude. Bilinear interpolation is used to produce 1- degree × 1-degree regions.

The solar energy data are generated using the Pinker and Laszlo shortwave algorithm (Pinker and Laszlo 1992). Cloud data are taken from the ISCCP DX dataset. These data are on an equal area grid with an effective 30-km × 30-km pixel size. The output data are generated on a nested grid containing 44,016 regions. The nested grid has a resolution of 1 degree latitude globally, and longitudinal resolution ranging from 1 degree in the tropics and subtropics to 120 degrees at the poles. This in turn is regridded to a 1-degree equal-angle grid (360 longitudes × 180 latitudes). The regridding method is by replication, wherein any grid region that is larger than 1 × 1 degree is subdivided into 1 × 1 degree regions, each with the same value as the original.

SSE estimates were compared with ground site data on a global basis. Radiation parameters were compared with data from the BSRN (NASA 2008). The summary results are presented in Table 5-3.

Table 5-3. Regression Analysis of SSE Versus BSRN Monthly Averaged Values for July 1983 Through June 2006

Parameter	Region	Bias (%)	RMS (%)
GHI	Global	−.01	10.25
	60 degrees poleward	−1.18	34.37
	60 degrees equatorward	0.29	8.71
DHI	Global	7.49	29.34
	60 degrees poleward	11.29	54.14
	60 degrees equatorward	6.86	22.78
DNI	Global	−4.06	22.73
	60 degrees poleward	−15.66	33.12
	60 degrees equatorward	2.40	20.93

See the NASA SSE Web site at http://eosweb.larc.nasa.gov/sse/. The source data were downloaded from the SSE Web site at Data Retrieval: Meteorology and Solar Energy > Global datasets as text files. The tabular data were then converted to the shapefile format.

Period of record: July 1983–June 2005.

Temporal resolution: Monthly and annual average daily totals (kWh/m²/day).

Spatial coverage: Global.

Spatial resolution: 1 degree.

Data elements and sources: GHI, DNI, and DHI from a satellite remote sensing model. Also available: Estimates of clear sky GHI, DNI, and DHI and tilted surface irradiance, temperature, pressure, humidity, precipitation, and wind speed.

Estimated uncertainties: Based on comparisons with surface measurements available from the BSRN, the 23-year, monthly mean daily total irradiance uncertainties (Bias%/RMSE%) for mid-latitudes have been determined for GHI (0.29%/8.71%), DHI (6.86%/22.78%), and DNI (2.40%/20.93%).

Availability: NASA SSE Web site at http://eosweb.larc.nasa.gov/sse/.

Updates: Release 6.0 Dataset (January 2008).

DLR ISIS

The Deutsches Zentrum für Luft-und Raumfahrt Irradiance at the Surface derived from ISCCP cloud data (DLR-ISIS) dataset gives an overview of the available total solar irradiance worldwide based on radiative transfer model results using cloud properties and cloud amount data supplied from the ISCCP – http://isccp.giss.nasa.gov. The radiative transfer model also uses atmospheric aerosol optical thickness determined from the NASA-GISS dataset (Lohmann et al. 2006).

With more than 21 years of model estimates, the data can be used to derive stable long-term averages, evaluate the variability of irradiance from year to year, and study the effects of extreme atmospheric conditions on the irradiance at the surface; e.g., after a volcano eruption. The 3-hourly temporal resolution of ISIS enables the study of daily cycles. However, the spatial resolution of 280 km by 280 km is too coarse for site selection (see SOLEMI on page 94).

Period of record: July 1983–December 2004.

Temporal resolution: 3-hourly.

Spatial coverage: Global.

Spatial resolution: 280 km × 280 km.

Data elements and sources: DNI and GHI from radiative transfer model using cloud and aerosol inputs.

Data quality control and assessment: Comparison of monthly mean daily total DLR-ISIS DNI with data from 78 stations shows an average underestimation of 3% for monthly means. For DLR-ISIS GHI, validation with data from 89 stations indicates an overestimation of monthly means by 3%.

Estimated uncertainties: No information.

Availability: http://www.pa.op.dlr.de/ISIS.

Historically Black Colleges and Universities Solar Measurement Network

The Historically Black Colleges and Universities (HBCU) Solar Radiation Monitoring Network operated from July 1985 through December 1996. Funded by DOE, the six-station network provided 5-minute averaged measurements of global and diffuse horizontal solar irradiance. The data were processed at NREL to improve the assessment of the solar radiation resources in the southeastern United States (Marion 1994). Three of the stations also measured the DNI with a pyrheliometer mounted in an automatic sun tracker. Historical HBCU data available online include quality assessed 5-min data, monthly reports, and plots.

In January 1997 the HBCU sites became part of the CONFRRM solar monitoring network.

Period of record: 1985–1996.

Temporal resolution: 5 min.

Spatial coverage: Southeastern United States (Daytona Beach, Florida; Savannah, Georgia; Itta Bena, Mississippi; Elizabeth City, North Carolina; Orangeburg, South Carolina; Bluefield, West Virginia).

Spatial resolution: Six measurement stations (Figure 5-9).

Figure 5-9. HBCU Solar Monitoring Network (1985–1996)

Data elements and sources: GHI, DNI (at three stations), DHI (shadowband) from measurements by the Eppley Laboratory, Inc. Model PSP pyranometers and Model NIP pyrheliometers mounted in automatic solar trackers (LI-COR Model 2020). Radiometers were maintained daily and calibrated annually at NREL using the broadband outdoor radiometer calibration process (Myers et al. 2002) with reference standards traceable to the WRR.

Data quality control and assessment: The station operators inspected the instrumentation daily to ensure the radiometers were clean and properly aligned. Data were processed at NREL using SERI-QC software to assign each data value a two-digit quality flag. Measured data from single-black thermopile radiometers were not corrected for thermal offsets that were discovered much later.

Estimated uncertainties: Based on the instrument selections, installation, and O&M practices, the estimated uncertainties for corrected daily total irradiances are: measured DNI ± 2%, computed DNI from measured GHI and DHI ± 8%, GHI ± 5%, and DHI ± 15% + 5 W/m^2.

Availability: NREL RRDC, http://rredc.nrel.gov/solar/old_data/hbcu/ (includes quality assessed monthly data files, monthly summary reports, and monthly irradiance plots).

Updates: Final data released in 1997. Measurements from the Elizabeth City State University station continue to be available from the NREL Measurement & Instrumentation Data Center, www.nrel.gov/midc/ecsu/.

Solar and Wind Energy Resource Assessment

The Solar and Wind Energy Resource Assessment (SWERA) Programme provides easy access to high-quality renewable energy resource information and data to users around the world. Its goal is to help facilitate renewable energy policy and investment by making high-quality information freely available to key user groups. SWERA products include geographic information systems and time series data, along with links to energy optimization tools needed to apply these data. To view additional information about the available resources or tools, select one of the links in the Resource Information or Analysis Tools section (http://swera.unep.net/index.php?id=7). These products are being offered through a team of international experts and their in-country partners.

Period of record: Moderate resolution: 1985–1991 and high resolution: 1998–2002.

Temporal resolution: Monthly and annual average daily totals (kWh/m^2/day).

Spatial coverage: Moderate resolution: South America, Central America, Africa, South and East Asia, Caribbean, Mexico, Middle East (Israel, Palestine/Jordan, Lebanon, Syria, Iraq, Yemen, Saudi Arabia [partial], and Kuwait). High resolution: Guatemala, Belize, El Salvador, Honduras, Nicaragua, partial Mexico (Oaxaca), Cuba, Afghanistan, Pakistan, partial Mexico (Chiapas, Vera Cruz, northern Mexico to 24 degree latitude), Dominican Republic, Bhutan, India (NW), Ethiopia, Ghana, Ethiopia, Kenya, Sri Lanka, Nepal, Bangladesh, Western China, United Arab Emirates.

Spatial resolution: Moderate resolution = 40-km high resolution = 10 km.

Data elements and sources: GHI, DNI (DHI), and POA from model estimates based on surface meteorological observations and/or satellite remote sensing input data.

Data quality control and assessment: No information.

Estimated uncertainties: No information.

Availability: SWERA designed and maintained by UNEP/GRID-Sioux Falls:

- http://swera.unep.net/index.php?id=ghi_nrel_mod&no_cache=1&dataprovider=8&datatype=4,70,79&energycategory=83&resolution=medium
- http://swera.unep.net/index.php?id=ghi_suny_high&no_cache=1&dataprovider=10&datatype=4,70,79&energycategory=83&resolution=high
- http://swera.unep.net/index.php?id=metainfo&rowid=109&metaid=226.

Products for Brazil were developed by Brazil's National Institute of Space Research and Laboratory of Solar Energy/Federal University of Santa Catarina. More information about INPE is available at www.inpe.br/ingles/index.php. Products developed by the Deutsches Zentrum für Luft- und Raumfahrt are available from http://swera.unep.net/index.php?id=metainfo&rowid=109&metaid=226. Maps of solar power potential in Latin America countries also available from www.temasactuales.com/tools/solarmaps.php.

Updates: New datasets are made available on a continuing basis.

HelioClim

HelioClim is a family of databases comprising solar irradiance and irradiation values available at ground level. HelioClim data are modeled from Meteosat imagery covering Europe, Africa, the Mediterranean Basin, the Atlantic Ocean, and part of the Indian Ocean. Three databases on the HelioClim server are presently operated by the Ecole des Mines de Paris/Armines Center for Energy and Processes. The Center Mines Paristech - Armines receives Meteosat data from Eumetsat and processes them in real-time. It produces the databases HelioClim that can be accessed through the SoDa Service.

Period of record: 1985–present.

Temporal resolution: 15 min.

Spatial coverage: Europe and Africa.

Spatial resolution: 5 km.

Data elements and sources: Hourly and daily GHI from satellite remote sensing model.

Data quality control and assessment: Web-based data quality programs compare the data against the extraterrestrial irradiation and data provided by a clear sky model for the day or hour and generate a data quality report. The report explains anomalies in the HelioClim data.

Estimated uncertainties: No information.

Availability: Ecole des Mines de Paris - Armines, Center for Energy and Processes. It is a companion to the SoDa Service. www.helioclim.org/radiation/index.html. Also see: www.soda-is.com/eng/index.html.

Updates: There are presently three databases: HC-1, HC-2, and HC-3. Work continues on the most recent database HC-3. An improved method Heliosat-4 to process Meteosat images is under preparation; it will create the database HC-4.

Solar Data Warehouse

The Solar Data Warehouse accesses climate data from more than 30 measurement networks across the United States, providing hourly and daily data from more than 3000 stations. Measurements from these networks are converted to a uniform format and combined into a consistent dataset.

Period of record: Varies from 5 to 25 years ago to the present.

Temporal resolution: Hourly and daily.

Spatial coverage: Continental United States.

Spatial resolution: 3000+ measurement stations.

Data elements and sources: GHI.

Data quality control and assessment: Most of the radiometers are medium-quality pyranometers. Spatial and temporal comparisons of data among multiple nearby stations are used to identify anomalous data. Continual (weekly) adjustments to quality control routines due to addition, relocation, and discontinuation of measurement stations.

Estimated uncertainties: Data from 13 NSRDB Class 1 measurement stations were compared with 16 Solar Data Warehouse stations separated by less than 40 km for the period 2003–2005. The average daily error was 9.85% and the RMSE was 19.0 W/m².

Availability: http://solardatawarehouse.com.

1991–2005 National Solar Radiation Database

The 1991–2005 NSRDB update contains hourly solar radiation (including GHI, DNI, and GHI) and meteorological data for 1,454 stations. This update builds on the 1961–1990 NSRDB, which contains data for 239 stations (see Figure 5-3). The update includes the conventional time series for NSRDB ground stations as well as a 1/10-degree gridded dataset from SUNY-Albany that contains hourly solar records for 8 years (1998–2005) for the United States (except Alaska above 60 degrees latitude) for about 100,000 pixel locations (at a nominal 10-km × 10-km pixel size). To increase data quantity, developers relaxed the standard of serial completeness mandated by the 1961–1990 NSRDB. In the update, the stations were classified by data quality. The 221 Class I stations have a complete hourly dataset for the 1991–2005 period and were produced with the best available input data. The 637 Class II stations have a complete hourly data record, but they have a higher uncertainty because of lower quality input data (due to NWS automation of weather observations in the mid-1990s). The 596 Class III stations contain gaps in the data period but contain at least 3 years of data that may be useful for some applications.

A significant difference between the 1961–1990 and 1991–2005 NSRDBs involves data storage. In the original database, measured data were merged with modeled data such that a seamless dataset of solar radiation values was produced, i.e., the model essentially filled gaps in the measured data. The updated database includes separate fields for both modeled and measured data, which allows users the flexibility to chose modeled, or, if available, measured data for an application.

The NSRDB user manual is available at www.nrel.gov/docs/fy07osti/41364.pdf.

Period of record: 1991–2005.

Temporal resolution: Hourly.

Spatial coverage: United States.

Spatial resolution: 1,454 locations and 10-km × 10-km grid (1998–2005) (Figure 5-3).

Data elements and sources: Computed or modeled data: ETR on surfaces horizontal and normal to the sun, GHI, DNI, and DHI. Measured or observed data: total sky cover, opaque sky cover, dry-bulb temperature, dew point temperature, relative humidity, station pressure, wind speed and direction, horizontal visibility, ceiling height, precipitable water, aerosol optical depth, surface albedo, and precipitation.

Data quality control and assessment: Each data element has been assigned flags indicating the source and estimated uncertainty. Thirty-three measurement sites were used for the model evaluation based on their instrumentation, period of record, and proximity to NWS sites (Figure 5-10).
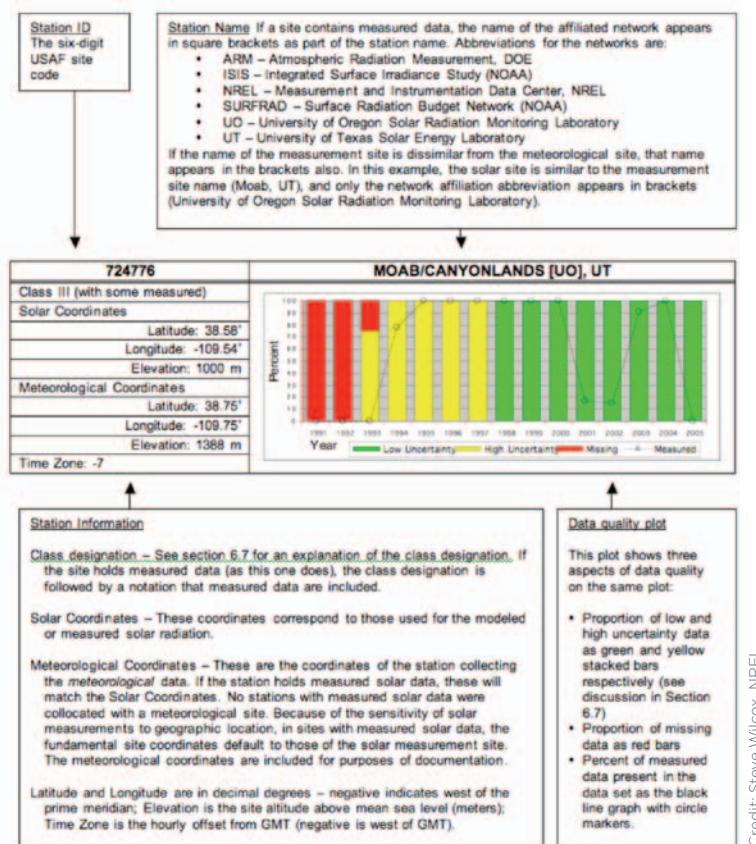
Figure 5-10. Example data quality summary for one of the 239 stations in the 1961–1990 NSRDB

Estimated uncertainties: Base uncertainty estimates were made for the two models used to generate the database. The base uncertainty of the surface model, METSTAT (Maxwell 1998), was determined from results that used high-quality model input data and compared the model output with measured data. Measured data from single-black thermopile radiometers were not corrected for thermal offsets that were discovered much later. This base uncertainty was then modified for the increased uncertainty of filled meteorological or the Automated Surface Observing System data when such input data were used. Similarly, the base uncertainty of the satellite remote sensing model (Perez et al. 2002) was determined in the model evaluation and then increased for periods of snow cover or high latitude—

circumstances known to degrade model performance. Hourly uncertainties for modeled data range from 8% under optimal conditions to more than 25% for less-than-optimal input data. Additional information is available from Zelenka et al. (1999).

Availability: Data are available from the NREL and NCDC as shown in Table 5-4.

Updates: Released in 2007.

Table 5-4. NSRDB Data Access Options

Dataset	Distributor	URL
NSRDB solar and filled meteorological fields	NCDC	ftp://ftp3.ncdc.noaa.gov/pub/data/nsrdb[a]
NSRDB solar and Integrated Surface Database meteorological fields (no data filling)	NCDC	http://cdo.ncdc.noaa.gov and http://gis.ncdc.noaa.gov[a]
NSRDB solar fields (no meteorological data)	NCDC	ftp://ftp.ncdc.noaa.gov/bup/data/nsrdb-solar[b]
SUNY 10-km gridded data	NCDC	ftp://ftp.ncdc.noaa.gov/bup/data/nsrdb-solar[b]
NSRDB statistical summaries	NCDC	ftp://ftp.ncdc.noaa.gov/bup/data/nsrdb-solar[b]
NSRDB research solar fields (no meteorological data)	NREL	http://rredc.nrel.gov/solar/old_data/nsrdb/1991-2005[b]

[a] No-cost access is domain-restricted to .edu, .gov, .k12, and .mil. A fee-access restriction applies to all other domains.
[b] No fee.

Typical Meteorological Year Version 3

The TMY3 data were produced using input data for 1976–2005 from the 1961–1990 NSRDB, Version 1.1 and the 1991–2005 NSRDB update. Because the 1961–1990 NSRDB has 239 sites and the 1991–2005 NSRDB update has more than 1400 sites, production of the TMY3 data was designed to maximize both the number of stations and the number of years from which to characterize the typical conditions (Wilcox and Marion 2008). At sites where data are available for 30 years, the base time period for the TMY algorithm spans 1976–2005. For the remaining sites, the base time period spans 1991–2005.

Except for a few changes to the weighting criteria, which account for the relative importance of the solar radiation and meteorological elements, the TMY2 and TMY3 datasets were created using procedures similar to those developed by Sandia National Laboratories to create the original TMYs from the 1952–1975 SOLMET/ERSATZ data (Table 5-1). Minor changes to the algorithm were made between the TMY2 and TMY3 production runs. A small change to the persistence criteria better accommodates selecting a TMY month for periods of records with fewer years. Also, computer code was removed that prioritized the selection of months with measured solar data because less than one percent of the data records in the 1991–2005 NSRDB update contain measured data. The effects of these changes between the TMY2 and TMY3 algorithm were evaluated as part of the TMY3 production process. In the context of producing datasets with similar characteristics, these effects were small (Wilcox and Meyers 2008). In practice, however, there are differences in the apparent solar resources among the data available as TMY2, TMY3, and the 8-year annual means of the NSRDB/SUNY model. Figure 5-11 illustrates the differences of annual mean daily total DNI for 8 years of NSRDB/SUNY model estimates and the TMY3 data based on data from 1976 to 2005.

Annual DNI Estimates from NSRDB/SUNY and TMY3 Data Sets

Grid = NSRDB/SUNY (kWh/m² per Day)
Circles = NSRDB/SUNY minus TMY3 (%)

Credit: Ray George, NREL
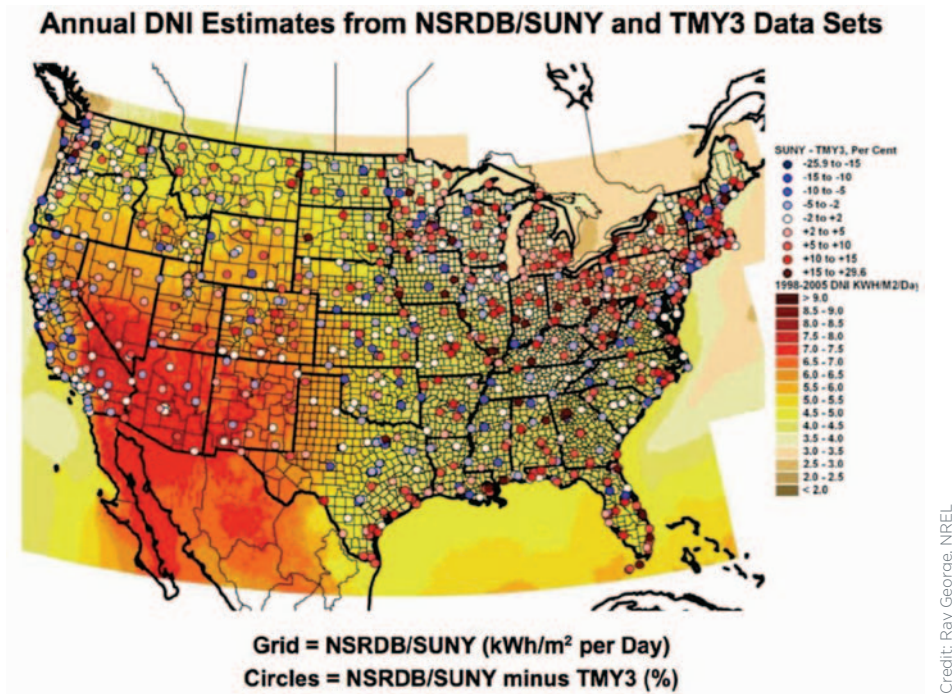
Figure 5-11. Annual mean daily total DNI distribution based on NSRDB/SUNY model results for 1998–2005 and the corresponding differences between the model and TMY3 (red circles indicate DNI values from TMY3 < NSRDB/SUNY and blue circles indicate TMY3 > NSRDB/SUNYA)

Missing meteorological data have been filled to provide serially complete records as input for modeling the TMY3 solar radiation fields. Filled meteorological data fields (which are flagged in the data file) may also be useful for certain renewable energy applications. However, the filled data are not suitable for climatological studies.

To help guide the development and process validation for the TMY3, a 1961–1990 TMY was created with the updated software using data from the TD3282 NSRDB dataset distributed by the NCDC. This dataset was created solely for algorithm evaluation purposes and no data have been released. Missing meteorological fields were filled according to methods used for the 1991–2005 NSRDB update. To evaluate the effects of drawing from differing periods of time for the input dataset, we compared each of the following year-span subgroups using the original 1961–1990 TMY dataset as a benchmark:

- 1961–1990 (30 years for evaluating software algorithm changes)
- 1976–2005 (for evaluating an updated TMY from a 30-year dataset)
- 1991–2005 (for evaluating an updated TMY from a 15-year dataset)
- 1998–2005 (for evaluating an updated TMY from an 8-year dataset).

The TMY software was run on each dataset to create TMYs for the 233 sites common to all subgroups (several sites among the 239 in the TMY2 dataset did not have sufficient data for this analysis). We calculated a mean value for each parameter by site for each subgroup TMY.

Although mean values of any data element are only a minor consideration in the TMY algorithm, they are one characteristic of climate and are a simple method of detecting large shifts or errors in the results. The ranges of the mean differences (the largest possible mean difference at any one site) in DNI for all stations, except Alaska and Hawaii, between the original 1961 through 1990 TMY2 and TMY3 data interval subgroups) are shown in Table 5-5.

Table 5-5. Ranges of Mean Station Differences for Hourly DNI

Data Interval	Range of Station-Mean DNI Differences* (W/m^2)
1961–1990	± 15
1975–2005	± 25
1991–2005	± 40
1998–2005	± 45

* Differences computed as "new TMY3" minus original TMY2 hourly DNI values at each of the 233 stations. Larger mean differences in DNI, approaching -100 W/m^2, were computed for stations in Alaska and Hawaii and require further study.

The mean biases and standard deviations for these comparison datasets are shown in Tables 5-6 and 5-7. The statistics are found by determining the mean of sun-up data for the solar parameters and the mean of all data for meteorological parameters. Biases are determined as the test TMY dataset minus the original 61-90 TMY. This information may give the user some indication of the increased uncertainty in the data (particularly noticeable in Table 5-7) with the smaller source datasets. The years corresponding to the eruptions of volcanoes El Chichón and Mount Pinatubo (1982–1984 and 1992–1994, respectively) are not represented among the selected years. The TMY algorithm explicitly excluded these years because the effects of increased aerosols on solar radiation for those years are considered atypical.

Table 5-6. Bias Differences (Test Data Minus Original 1961–1990 TMY)

Parameter	1961–1990	1976–2005	1991–2005	1998–2005
Direct normal W/m^2	−5.9	−1.1	−7.9	−1.7
Global horizontal W/m^2	−4.0	−5.7	−15.2	−11.7
Dry-bulb temperature °C	0.07	0.39	0.77	0.94
Dew point temperature °C	0.08	0.33	0.81	1.08
Wind speed m/s	0.02	−0.1	−0.3	−0.4

Table 5-7. Standard Deviations of Hourly Data

Parameter	1961–1990	1976–2005	1991–2005	1998–2005
Direct normal W/m^2	6.7	11.9	21.0	32.5
Global horizontal W/m^2	2.8	5.3	10.0	15.1
Dry-bulb temperature °C	0.22	0.37	0.49	0.77
Dew point temperature °C	0.28	0.43	0.57	0.82
Wind speed m/s	0.12	0.20	0.30	0.34

Data quality flags were assigned to each hourly data value to indicate the source and uncertainty, except for the computed values for extraterrestrial horizontal and extraterrestrial direct normal radiation. The source flag indicates whether the data were measured, modeled, or missing, and the uncertainty flag provides an estimate of the uncertainty of the data. Usually, the source and uncertainty flags are the same as those in the NSRDB, from which the TMY files were derived. In the case of the TMY3 data files, the uncertainties are expressed as plus-minus

percent rather than the coded uncertainty used in the TMY2 files. Uncertainty values apply to the data with respect to actual values at the time stamp, and not to how typical a particular hour is for a future month and day. The uncertainty values represent the plus or minus interval about the data value that contains the true value 95% of the time.

The uncertainty assigned to modeled solar radiation data includes primarily the model bias error and, to a lesser extent, the random error component, which could be several times larger for partly cloudy skies (Wilcox 2007). For partly cloudy skies, an hour can be composed of large or small amounts of sunshine, depending on whether the sun is mostly free of or occluded by the clouds. Consequently, modeled hourly values may depart significantly from true values for partly cloudy skies. The uncertainty assigned to modeled solar radiation data represents the average uncertainty for a large number of model estimates (such as for a month). When averaging large datasets, random errors tend to cancel, leaving only the bias error.

Period of record: 1991–2005.

Temporal resolution: Hourly.

Spatial coverage: United States and territories.

Spatial resolution: 1020 locations (Figure 5-12).
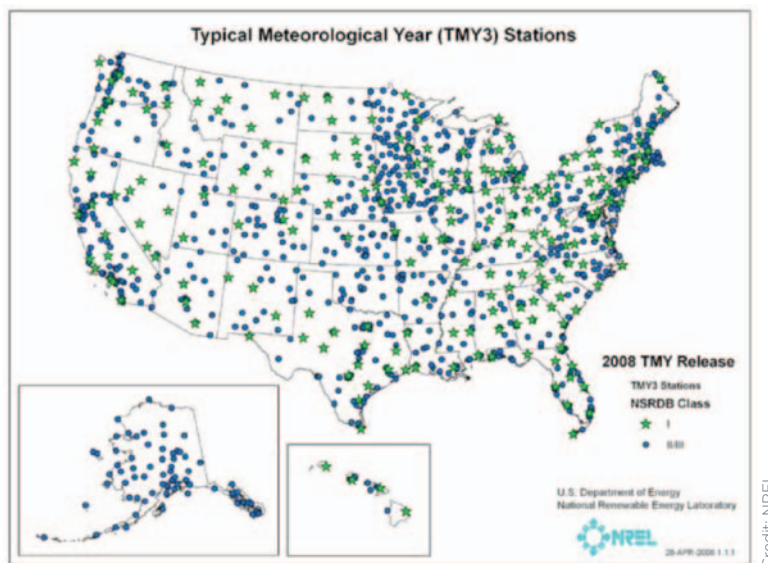
Figure 5-12. TMY3 stations

Data elements and sources: Computed or modeled data: ETR on surfaces horizontal and normal to the sun, GHI and illuminance, DNI and illuminance, DHI and illuminance, zenith luminance. Measured or observed data: total sky cover, opaque sky cover, dry-bulb temperature, dew-point temperature, relative humidity, station pressure, wind speed and direction, horizontal visibility, ceiling height, precipitable water, aerosol optical depth, surface albedo, and precipitation.

Data quality control and assessment: Each data element has been assigned flags indicating the source and estimated uncertainty.

Estimated uncertainties: Base uncertainty estimates were made for the two models used to generate the database. The base uncertainty of the surface model was determined from results that used high-quality model input data and compared the model output with measured hourly data. This base uncertainty was then modified for the increased uncertainty of filled meteorological or the Automated Surface Observing System data when such hourly input data were used. Similarly, the base uncertainty of the satellite remote sensing model was determined

in the model evaluation and then increased for periods of snow cover or high latitude—circumstances known to degrade model performance. Hourly uncertainties for modeled data range from 8% under optimal conditions to more than 25% for less-than-optimal input data.

Availability: The NREL RRDC, http://rredc.nrel.gov/solar/old_data/nsrdb/1991–2005/tmy3.

Updates: Released in 2008 (revision expected in 2010).

Management and Exploitation of Solar Resource Knowledge

The Management and Exploitation of Solar Resource (MESoR) Project started in June 2007 for the purpose of removing the uncertainty and improving the management of solar energy resource knowledge. The results of past and present large-scale initiatives in Europe will be integrated, standardized, and disseminated uniformly to facilitate their effective exploitation by stakeholders. The project will contribute to preparation of the future roadmap for research and development (R&D) and strengthening of the European position in the international field. The project includes activities in user guidance (benchmarking of models and datasets; handbook of best practices), unification of access to information (use of advanced information technologies; offering one-stop-access to several databases), connecting to other initiatives (INSPIRE of the EU, POWER of the NASA, SHC and PVPS of the IEA, GMES/GEO) and to related scientific communities (energy, meteorology, geography, medicine, ecology), and information dissemination (stakeholders involvement, future R&D, communication). MESoR is supported as a Coordination Action by the European Commission.

Period of record: 1991–2005: Europe and Africa; 1999-2006: Asia.

Temporal resolution: Hourly.

Spatial coverage: Europe, Western Asia, Africa, parts of Australia, South America.

Spatial resolution: 2.5 km.

Data elements and sources: GHI, DNI, DHI from ground measurements and modeling results.

Data quality control and assessment: Benchmarking data include ground measurements available from BSRN, International Daylight Measurement Program, Global Atmospheric Watch, and others. Time-series data analyzed for MBE, RMSE, and Kolmogrov-Smirnov Test statistics.

Estimated uncertainties: Sample MBE and RSME results for eight BSRN stations are shown in Table 5-8.

Table 5-8. Sample MBE and RSME Results for Eight BSRN Stations

Time Scale	GHI				DNI			
	Mean (Wm⁻²)	MBE (%)	RMSE (%)	R^2	Mean (Wm⁻²)	MBE (%)	RMSE (%)	R^2
Hour	387.3	1.93%	18.79	0.97	467.8	−0.73	36.83	0.87
Day	n/a	n/a	11.08	0.99	n/a	n/a	23.58	0.95
Month	n/a	n/a	4.95	0.99	n/a	n/a	9.69	0.99
Year	n/a	n/a	3.66	0.99	n/a	n/a	4.92	0.99

Availability: Deutsches Zentrum für Luft- und Raumfahrt www.mesor.org/.

International Daylight Measurement Program

The International Daylight Measurement Program was initiated in the framework of Technical Committee 3.07 of the CIE (Commission Internationale de l'Eclairage) by Derrick Kendrick of the University of Adelaide, Australia. The year 1991 was designated the International Daylight

Measurement Year on the occasion of the CIE quadrennial conference. Researchers from around the world took this opportunity to start measurement stations based on standard conventions developed by the program. In conjunction with the International Energy Agency Solar Heating and Cooling Program, the International Daylight Measurement Program measurements and modeling of spectral radiation continued through 1994.

Period of record: 1991–1994.

Spatial coverage: Australia, Canada, China, France, Germany, Greece, India, Indonesia, Israel, Japan, Korea, The Netherlands, New Zealand, Portugal, Russia, Singapore, Slovakia, Spain, Sweden, Switzerland, United Kingdom, and the United States.

Spatial resolution: 43 measurement stations.

Data elements and sources: GHI, DNI, DHI, zenith luminance, illuminance (including vertical surfaces), air temperature, relative humidity (or dew point), wind speed and direction, bright sunshine duration, sky imagers, and sky scanners.

Data quality control and assessment: International Daylight Measurement Program guidelines address the use of physical limits (acceptance thresholds), and comparisons of measurements with validated models that account for various sky conditions and solar position. The stand-alone program, AQCCIE, is available from http://idmp.entpe.fr/.

Estimated uncertainties: No information

Availability: Ecole Nationale des Travaux Publics de l'Etat, http://idmp.entpe.fr/.

Baseline Surface Radiation Network

In 1992, the WCRP Radiative Fluxes Working Group initiated a new BSRN to support the research projects of the WCRP and other scientific programs needing high-quality and continuous measurement of the irradiances at the Earth's surface. Some years later the BSRN incorporated into the WCRP Global Energy and Water Cycle Experiment (GEWEX) Radiation Panel.

The objective of the BSRN is to provide, using a high sampling rate, observations of the best possible quality, for short- and long-wave surface radiation fluxes. These readings are taken from a small number of selected stations, in contrasting climatic zones, together with collocated surface and upper air meteorological data and other supporting observations. The uniform and consistent measurements throughout the BSRN network are used to:

- Monitor the background (least influenced by immediate human activities that are regionally concentrated) short-wave and long-wave radiative components and their changes with the best methods currently available.

- Provide data to validate and evaluate satellite-based estimates of the surface radiative fluxes.

- Produce high-quality observational data for comparison with climate model calculations and to develop local and regionally representative radiation climatological analyses.

At present, about 40 BSRN stations are in operation. These stations measure different sets of radiation values. Some carry out only basic measurements according to the BSRN Technical Plan (Hagner et al. 1998). Other stations carry out other measurements in addition to the basic measurements. Some stations also perform synoptic observations, upper air soundings, ozone measurements, and expanded measurements. More stations are being established. Some should be in operation within the current year.

The BSRN database is based on PANGAEA (named after the PANGAEA theory). This Publishing Network for Geoscientific & Environmental Data is an Open Access library aimed at archiving, publishing, and distributing georeferenced data from Earth system research. Data can be found by using the PANGAEA search engine or www.pangaea.de/PHP/BSRN_Status.php. Data descriptions (metadata) of all datasets are visible and include the principal investigator's name

and e-mail for contact. The online data access is offered to anybody who accepts the data release guidelines.

In addition to the Web-based PANGAEA access, the original station-to-archive files (without derived quantities and quality flags) can be obtained via the ftp-server: ftp.bsrn.awi.de (contact Gert.Koenig-Langlo@awi.de).

The BSRN data have become widely known for their research quality and used for model development and validation.

Period of record: 1992–present.

Temporal resolution: 1 min.

Spatial coverage: Global.

Spatial resolution: 40 measurement stations (Figure 5-13). A list of stations is available at www.pangaea.de/ddi?request=bsrn/BSRNEvent&format=html&title=BSRN+Stations.
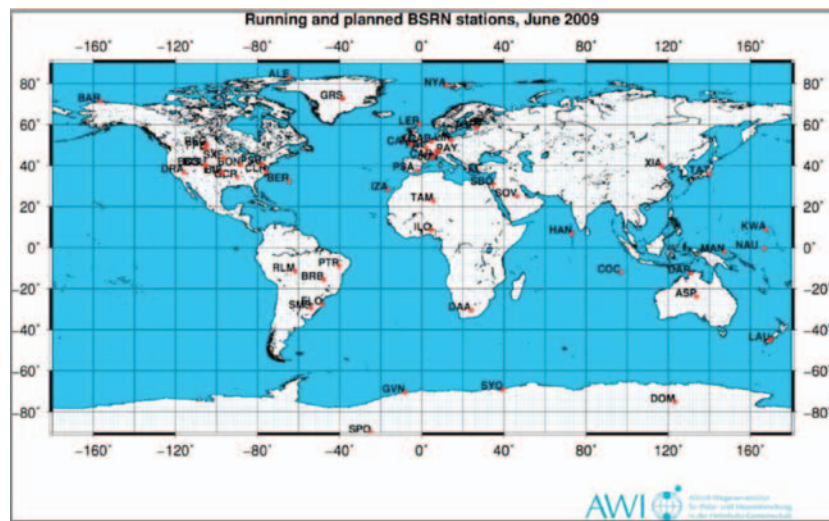
Figure 5-13. Baseline Surface Radiation Network

Data elements and sources: The number and type of measurements vary with station. Basic radiation measurements include GHI, DNI, DHI, downwelling infrared irradiance, upwelling infrared irradiance, and upwelling (reflected) shortwave irradiance. Measurements are from radiometers of various manufacturers. Synoptic meteorological observations, upper air measurements, and numerous expanded and supporting measurements are available. (Details are available from www.bsrn.awi.de/en/data/measurements/.)

Data quality control and assessment: Measurement station design and O&M practices must conform to established BSRN requirements. The station scientist is responsible for measurements and data quality. For each month, the station scientist produces a station-to-archive file according to Hegner (1998). (Details are available from www.bsrn.awi.de/en/data/data_input/).

Estimated uncertainties: The WCRP of the WMO established the standards of measurement for the BSRN. The stated accuracies are 15 W/m^2 for broadband solar measurements and 110 W/m^2 for thermal infrared measurements.

Availability: The WRMC provides Web-based and ftp data access (www.bsrn.awi.de/en/home/).

Updates: The BSRN data archive is maintained by the WRMC and updated regularly (www.bsrn.awi.de/en/home/wrmc/).

Surface Radiation Network

SURFRAD was established in 1993 through the support of NOAA's Office of Global Programs to support climate research with accurate, continuous, long-term measurements of the SRB over the United States.

Currently seven SURFRAD stations operate in climatologically diverse regions: Montana, Colorado, Illinois, Mississippi, Pennsylvania, Nevada, and South Dakota. This represents the first time that a monitoring network in the United States was designed to measure the complete SRB. The site selection process for SURFRAD was a collaborative effort between NOAA, NASA, and university scientists. Locations were chosen with the intent of best representing the diverse climates of the United States. Special consideration was given to places where the landform and vegetation are homogeneous over an extended region so the point measurements would be qualitatively representative of a large area.

Each station is equipped to measure broadband solar and infrared irradiances, including DNI, to compute the net surface fluxes. Measurements of the spectral irradiance are collected to provide the relative amounts of ultraviolet and photosynthetically active radiation. Photometric measurements at selected solar irradiance wavelengths can be used to estimate the aerosol optical depth (important for determining DNI and amounts of forward scattering—circumsolar irradiance), total column ozone, and precipitable water vapor. Surface meteorological measurements, including all-sky digital cameras for measuring cloud cover, complete the instrumentation.

Data are downloaded, quality controlled, and processed into daily files that are distributed in near real-time by anonymous FTP and the Internet. Observations from SURFRAD have been used to evaluate satellite-based estimates of surface radiation, and to validate hydrologic, weather prediction, and climate models. QA built into the design and operation of the network, and good data quality control, ensure continuous high-quality product.

The station at Boulder is an operating SURFRAD station and serves as a calibration facility for network instruments, as well as for spectroradiometers operated by several North American agencies that monitor ultraviolet radiation.

Period of record: 1993–present.

Temporal resolution: Data are reported as 3-min averages of 1-s samples before 1 January 2009, and 1-min averages on and after 1 January 2009.

Spatial coverage: United States.

Spatial resolution: Seven stations: Montana, Colorado, Illinois, Mississippi, Pennsylvania, Nevada, and South Dakota (Figure 5-14).

Figure 5-14. The SURFRAD network is operated by the Global Monitoring Division, Earth Systems Research Laboratory, NOAA

Data elements and sources: GHI, DNI, DHI, downwelling infrared irradiance, upwelling infrared irradiance, and upwelling (reflected) shortwave irradiance. Photosynthetically active radiation, solar net radiation, infrared net radiation, air temperature, relative humidity, wind speed and direction (10 m AGL), and all-sky images (details available from www.srrb.noaa.gov/surfrad/).

Data quality control and assessment: The stations are regularly maintained and data are downloaded, quality controlled, and processed into daily files that are distributed in near real-time by anonymous FTP and the World Wide Web (www.srrb.noaa.gov). Radiometers are recalibrated annually and field measurements compared with standards as part of the instrument exchange procedure. Data elements are assigned an individual quality assessment flag. The redundancy of three component solar measurements (global, direct, and diffuse) provides a useful tool for quality control of the SURFRAD data by examining the internal consistency of these measurements at any time interval.

Estimated uncertainties: Based on the instrument selections, installation, and O&M practices, the estimated uncertainties for corrected daily total irradiances are measured DNI ± 2%, computed DNI from measured GHI and DHI ± 8%, computed GHI from measured DNI and DHI ± 5%, measured GHI corrected for unshaded pyranometer thermal offsets ± 5%, and DHI ± 15% + 5 W/m². SURFRAD has adopted the standards for measurement set by the BSRN as developed by the WCRP of the WMO. The stated accuracies are 15 W/m² for broadband solar measurements and 110 W/m² for thermal infrared measurements. To achieve these ambitious goals, the broadband solar instruments are calibrated at NREL against standards traceable to the WWC in Davos, Switzerland.

Availability: NOAA, Earth Systems Research Laboratory, Global Monitoring Division, Boulder, Colorado. ftp://ftp.srrb.noaa.gov/pub/data/surfrad and www.srrb.noaa.gov.

SURFRAD data are also submitted to the BSRN archives, www.bsrn.awi.de/.

Updates: Continuous data updates accommodate the latest measurements.

Integrated Surface Irradiance Study

The Integrated Surface Irradiance Study (ISIS) is a continuation of earlier NOAA surface-based solar monitoring programs. ISIS addresses questions of spatial distributions and time trends at sites selected to be regionally representative and long-term continuous records of observations. Data from 1995 to 2008 are archived at the NCDC from 10 stations: Albuquerque, New Mexico; Bismarck, North Dakota; Desert Rock, Nevada; Hanford, California; Madison, Wisconsin; Oak Ridge, Tennessee; Seattle, Washington; Salt Lake City, Utah; Sterling, Virginia; and Tallahassee, Florida. Data consist of 15-min-averaged measurements with standard deviations and minimum/maximum values based on 1-s samples of GHI using The Eppley Laboratory, Inc., Model PSP pyranometer, DNI using a Model NIP pyrheliometer, diffuse irradiance using Models PSP or 8-48 pyranometers, ultraviolet-B (UV-B) irradiance using a solar light ultraviolet biometer, GHI using a silicon cell pyranometer, plus its maximum, minimum, photosynthetically active radiation, and GHI using RSRs with photodiode detectors, and SZA.

The network ceased operation in January 2006 because of funding limitations.

Period of record: 1995–2006.

Temporal resolution: 15 min.

Spatial coverage: Continental United States.

Spatial resolution: 9 stations (Figure 5-14).

Data elements and sources: GHI, DNI, DHI, and Global UVB.

Data quality control and assessment: These data are provisional. The NOAA Solar Radiation Research Branch (SRRB) has attempted to produce the best dataset possible; however, the data quality is constrained by measurement accuracies of the instruments and the quality of the

calibrations. Regardless, SRRB attempts to ensure the best quality possible through QA and quality control. The data were subjected to automatic procedures as the daily files were processed. Data were subjected only to this first-level check and a daily eye check before being released.

QA methods were in place to ensure against premature equipment failure in the field and postdeployment data problems. For example, all instruments at each station were exchanged annually for newly calibrated instruments. Calibrations were performed by world-recognized organizations with pyranometers and pyrheliometers calibrated at NREL to the WRR. Calibration factors for the UVB instrument were transferred from three standards maintained by SRRB's National UV Calibration Facility in Boulder. In general, all of the standards collected by SRRB and NREL were traceable to NIST or its equivalent.

Estimated uncertainties: Based on the instrument selections, installation, and O&M practices, the estimated uncertainties for corrected daily total irradiances are: Measured DNI $\pm$ 2%, computed DNI from measured GHI and DHI $\pm$ 8%, GHI $\pm$ 5%, and DHI $\pm$ 15% + 5 W/m².

Availability: NOAA Earth Systems Research Laboratory, Global Monitoring Division, Boulder, Colorado (see ftp://ftp.srrb.noaa.gov/pub/data/isis/).

Updates: First released in 1995 and updated through 2005 with subsequent measurements.

Satel-Light

The European database of daylight and solar radiation is based on Meteosat images and a model that uses an estimation of cloud cover to produce a cloud index to produce GHI data. The DNI data are derived from GHI using the Page model (Page 1996). The Satel-Light server provides these data in map form for all of Europe.

Period of record: 1996–2000.

Temporal resolution: 30 min.

Spatial coverage: Europe.

Spatial resolution: ~5 km.

Data elements and sources: DNI, GHI, DHI, POA, horizontal illuminance, tilted illuminance, and sky luminance distribution.

Data quality control and assessment: The satellite-based model results have been compared with measurements from 25 stations. End user products generated from the satellite estimates were also compared to those generated from ground measurements at five stations (Dumortier 1998; Olseth and Skartveit1998).

Estimated uncertainties: Measurements of GHI from 25 sites in Europe were used to evaluate model performance for all sky conditions. The resulting annual mean bias deviation for GHI ranged from −1% to 3% and a RMSD ranged from 20% (south of Europe with a high frequency of sunny skies) to 40% (north of Europe with a high frequency of cloudy skies).

Availability: www.satellight.com/indexgS.htm.

Atmospheric Radiation Measurement

The ARM (Atmospheric Radiation Measurement) Climate Research Facility is a DOE national user facility for the study of global change by the national and international research community. Research at this facility includes the study of alterations in climate, land productivity, oceans or other water resources, atmospheric chemistry, and ecological systems that may alter the capacity of the Earth to sustain life. Measuring solar and infrared irradiances is an important source of data for this research. Continuous measurements of surface radiative flux are made in three geographic areas of the world. Beginning in 1997, ARM began operating 23 solar infrared stations (SIRS) in the southern Great Plains located in parts of Kansas and Oklahoma. GNDRAD and SKYRAD stations are located at three sites in the tropical western Pacific and two sites in the

north slope of Alaska. Known for the research quality of these measurements, the data are used for a variety of atmospheric model validations.

Important ancillary data, such as aerosol optical depth, precipitable water vapor, cloud cover and optical depth, surface albedo, spectral irradiance, and atmospheric profiles of temperature, pressure, and water vapor are also available from the ARM facility.

Period of record: 1997–present.

Temporal resolution: 20-s instantaneous samples and 1-min averages of 2-s scans.

Spatial coverage: Southern Great Plains, north slope of Alaska, and tropical western Pacific (Figure 5-15).
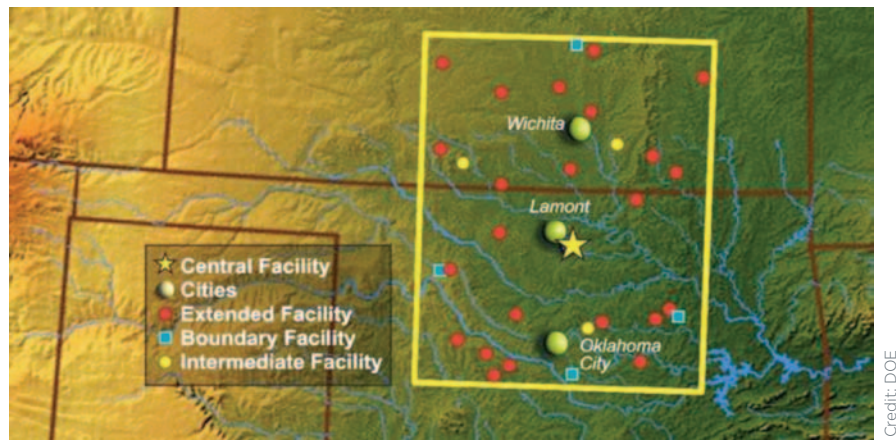

Figure 5-15. DOE has operated the 23 ARM stations in the southern Great Plains since 1997

Spatial resolution: 23 stations (southern Great Plains), 2 stations (north slope of Alaska), and 2 stations (tropical western Pacific).

Data elements and sources: GHI, DNI, DHI, DIR, UIR, and upwelling (reflected) shortwave irradiance (USI). Measurements from The Eppley Laboratory, Inc., Model PSP (GHI, DHI, and USI), Model 8-48 (DHI after 2000), Model NIP (DNI), and Model PIR (DIR and UIR).

Data quality control and assessment: Measurement stations are inspected daily (north slope Alaska and tropical western Pacific stations) to biweekly (southern Great Plains, except for central facility stations that are maintained daily) for preventative and corrective maintenance. Data are processed using data quality assessment methods based on SERI-QC, checked visually as time-series plots, and compared with relevant ancillary measurements and model outputs (e.g., clear sky solar irradiance model results). The pyranometer data are corrected for known thermal offsets. The ARM Data Quality Office reports on the health and status of the data at hourly and daily intervals. Each measurement is assigned a data quality flag. Radiometers are calibrated annually at the Radiometer Calibration Facility near Lamont, Oklahoma, and control and reference radiometers are compared with standards maintained by NREL. All pyranometers and pyrheliometer calibrations are traceable to the WRR.

Estimated uncertainties: Based on the instrument selections, installation, and O&M practices, the estimated uncertainties for corrected daily total irradiances are measured DNI ± 2%, GHI ± 5%, and DHI ± 15% + 5 W/m^2.

Availability: DOE, ARM Climate Research Facility, www.arm.gov. Datasets are labeled SIRS, SKYRAD, and GNDRAD. SIRS data are also submitted to the BSRN archives, www.bsrn.awi.de/.

Updates: Continuous data updates accommodate latest measurements and value-added products are available.

3-TIER Solar Time-Series

The dataset over the Western Hemisphere is based on more than 12 years of half-hourly high-resolution (roughly 1-km) visible satellite imagery from GOES data (GOES East, GOES West, and GOES South) using the broadband visible wavelength channel. The satellite dataset was collected from January 1997 through March 2009) and has been processed to create more than 12 years of hourly values of GHI, DNI, and DIF at a horizontal resolution of roughly 3 km.

3-TIER processes the satellite images based on a combination of in-house research and algorithms published in peer-reviewed scientific literature. These algorithms contain parameters and coefficients that are based on empirical fits to observational data. To develop and validate their model, 3-TIER used observations from the SURFRAD, BSRN, NSRDB, Bureau of Meteorology (Australia), National Institute of Water and Atmospheric Research (New Zealand), Indian Meteorology Department, Linke Turbidity Database from Ecole des Mines de Paris, and snow data from the 24-km dataset developed by the National Snow and Ice Data Center.

The basic processing scheme follows the SUNY model (Perez et al. 2002) with a few key improvements made within the 3-TIER algorithms. These include a higher spatial and temporal resolution, an in-house developed seasonal variability correction factor, an in-house developed empirical fitting of the data to ground station measurements, and the integration of instantaneous irradiance values to determine the hourly value. Each improvement results in a lower RMSE compared to the NREL/NSRDB Update/SUNY dataset (1998–2005).

Period of record: January 1997–March 2009.

Temporal resolution: ~30-min instantaneous and 1-h averages.

Spatial coverage: Western Hemisphere and much of Asia and Oceania.

Spatial resolution: 2 arc-min (~ 3 km).

Data elements and sources: GHI, DNI, and DHI from model estimates based on satellite remote sensing input data.

Data quality control and assessment: The irradiance data are based on the model developed by Perez et al. (2002) with proprietary improvements for increased spatial and temporal resolution, seasonal variability correction factor, empirical fitting of the modeled data to ground station measurements, and integration of instantaneous irradiance values to determine the hourly value. Surface radiation measurements from ground stations operated for the BSRN, SURFRAD, and other regional networks as identified by the NSRDB were used to validate the 3-TIER model.

Estimated uncertainties: Analyses of continental United States based on 36 observing stations for the years 1998 through 2005 indicate the following RSME and Bias values in W/m^2 for each irradiance component: GHI [77/4], DNI [181/4] and DHI[63/4].

Availability: 3-TIER, 2001 Sixth Avenue, Suite 2100, Seattle, Washington 98121 USA. www.3tier.com/products/.

Updates: Released in 2008 (Western Hemisphere) with updates through November 2009 (India, Australia, and Japan).

Clean Power Research – SolarAnywere

SolarAnywhere is a Web-based service that provides hourly estimates of the solar irradiance based on satellite images and atmospheric data using algorithms developed and maintained by Dr. Richard Perez and the State University of New York at Albany (Perez et al. 2002).

Period of record: 1998–present.

Temporal resolution: Hourly.

Spatial coverage: Continental United States and Hawaii.

Spatial resolution: 10 km.

Data elements and sources: GHI, DNI, wind speed, and ambient air temperature.

Data quality control and assessment: The Perez/SUNY model was developed and has been validated using surface irradiance measurements from selected SURFRAD stations.

Estimated uncertainties: Based on comparisons with measured data from 10 stations in the United States (Perez et al. 2002), the annual average hourly RSME and MBE for GHI are 14.0% and 0.8%, respectively, and for DNI, 29.8% and 0.9%, respectively.

Availability: Clean Power Research, www.cleanpower.com/SolarAnywhere.

Updates: Model version control information available.

Solar Energy Mining

SOLEMI is a new service set up by Deutsches Zentrum für Luft- und Raumfahrt (DLR) providing high-quality irradiance data based on Meteosat-data with a nominal spatial resolution of 2.5 km and half-hourly temporal resolution. Solar radiation maps and hourly time series will be available for almost half the Earth's surface.

Period of record: No information.

Temporal resolution: 30 min.

Spatial coverage: Europe, Africa, and Asia.

Spatial resolution: 2.5 km.

Data elements and sources: No information.

Data quality control and assessment: No information.

Estimated uncertainties: No information.

Availability: Deutsches Zentrum für Luft- und Raumfahrt: www.solemi.com/home.html.

Updates: No information.

GeoModel

The GeoModel database is derived from MSG satellite data and atmospheric parameters using in-house algorithms and computing infrastructure.

Period of record: April 2004–present.

Temporal resolution: 15 min.

Spatial coverage: Europe, Africa, and Middle East.

Spatial resolution: ~5 km down scaled to ~80 m using DEM SRTM-3.

Data elements and sources: DNI, GHI, DHI, and air temperature (2 m AGL).

Data quality control and assessment: Model data compared with measurements from 50 stations in Europe and North Africa.

Estimated uncertainties: See Table 5-9 for summary statistics based on comparisons with measurement stations in Europe and North Africa.

Availability: http://geomodel.eu/index.php.

Table 5-9. GeoModel Validation Summary

Component	Number of Stations	MBE	RMSE
GHI	50	−1.4%	20% (hourly) 10.7% (daily) 4.7% (monthly)
DNI	30	−2.5%	38.2% (hourly) 24.4% (daily) 10.7% (monthly)

Chapter 6: Applying Solar Resource Data to Concentrating Solar Power Projects

This chapter provides a summary of the tools and techniques for evaluating specific CSP sites based on all available information, as well as guidance on steps to improve the on-site determination of the solar resource relevant to the type of CSP technology that is being considered. The overall goal is to help the project developer and investor obtain the best estimates of the solar resource and weather information to address four stages of a CSP project evaluation and operation (see Figure 6.1).
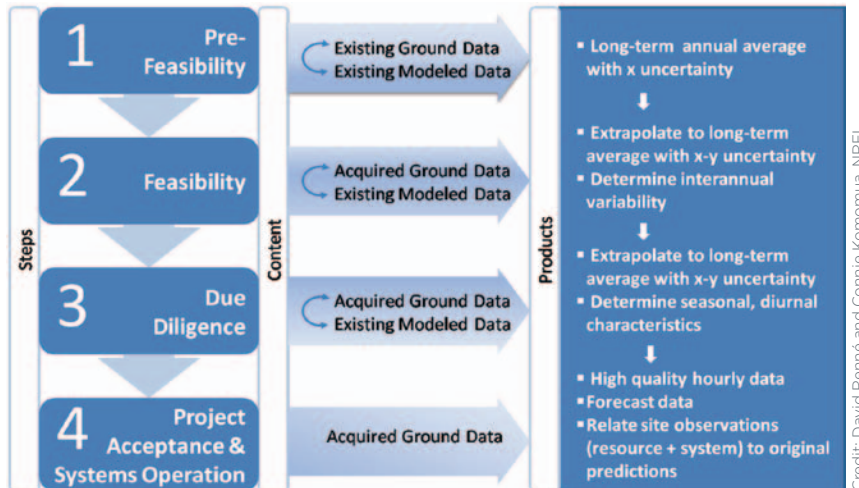

Figure 6-1. The four stages of a CSP project

Ideally, a potential CSP site will have several years of high-quality on-site data, using the measurement and metrology procedures described in Chapter 3, in formats directly relevant to the type of technology being considered. However, in the current CSP market, such data are not usually available, and project developers must rely on a number of techniques to provide the most accurate determination of site resource characteristics based on any available information sources. In the United States, these data sources might include some limited on-site measurements of varying quality, access to nearby measurements that may or may not be precisely applicable to the site because of spatial and temporal variability, access to satellite-derived DNI estimates, or access to nearby modeled ground stations, such as found in the NSRDB. In the latter case, both hourly statistics over the entire length of the NSRDB period, and TMY data representing either 15 or 30 years of solar resource data modeled from ground observations, might be available. Most ground stations in the NSRDB provide modeled estimates of the solar resource based on cloud cover and other weather observations obtained at the station, and not on actual solar measurements (see Chapter 5).

We assume that during the site-screening and prefeasibility stages, no high-quality on-site data are available, and that annual energy estimates must be derived from historical datasets such as the Perez SUNY satellite data and the NSRDB. During feasibility assessments, including engineering analysis and due diligence, some periods of high-quality measurements are assumed to be available at the site; however, these relative short-term measurements must be extrapolated to long-term records that capture seasonal trends and the interannual variability of solar resources for the site. During the system acceptance and site operation stages, reliance should be on high-quality ground-based measurements, perhaps supplemented to some extent by ongoing satellite-derived measurements for the region.

The project developer should consult Table 6-1 when evaluating sites through the various stages of project development.

Table 6-1. Site Evaluations

Evaluation Step	Question	Solutions and Insights
Site selection	What proposed site location(s) need to be evaluated?	
	Has a single site been chosen?	If not, is the developer making a choice among two or more sites, or "prospecting" over a wider area? If choosing among multiple sites, the developer will benefit from using maps and graphical techniques to evaluate both the estimated resource and the uncertainty of those resource estimates. See examples below.
Predicted plant output over its project life	How can short-term datasets that provide projections over the next few years be extended to long-term (30-year) projections so cash flow projections through the life of the project can be made?	Different locations may have different interannual variability, e.g., locations more subject to a monsoon effect will have higher interannual variability in the summer months. Typically, on-site data cover at most a few years, so we will discuss procedures for extrapolating these datasets to long-term projections using longer term (up to 45 years) modeled DNI data from the NSRDB as well as how to relate the nearest NSRDB stations to site-specific data.
Temporal performance and system operating strategies	How important are seasonal and diurnal patterns for DNI?	Most CSP projects will produce electricity for the public utility grid. If time-of-day pricing has been implemented for the consumer, an understanding of the diurnal patterns and monthly mean values during those months when time-of-day pricing is in place may be more important than the estimate of the annual average. If the CSP project includes thermal storage, the need to analyze when the system will build up storage versus when the system provides power to the grid during daylight hours also emphasizes the importance of understanding the diurnal patterns. Thermal storage greatly mitigates the effect of system intermittency, but accurate or realistic daily, hourly, or subhourly solar radiation data may still be needed.
	Are data needed that most closely match actual concurrent utility load data to conduct grid-integration studies and system intermittency?	In this case, daily, hourly, or even subhourly data may be needed for a specific time period, which cannot be provided by TMY data.
	What are the temporal and spatial characteristics of the data sources available to the developer, and how do these characteristics influence the evaluation of system performance? Satellite data usually represent snapshots in time due to the scanning characteristics of the on-board radiometers and are typically considered to range from nearly instantaneous to about 5-minute averages. For SUNY satellite data used in the NSRDB, individual pixel size is 1 km, and the pixel is at the center of the 10-km grid cell. Newer satellite-based methodologies now average the 1-km pixel to 3- or 5-km grid cells.	Example: Measured solar data apply to a specific location, and are usually recorded at short time intervals (6 minutes or less), then averaged to the desired time interval (often hourly). Example: Surface modeled data (e.g., NSRDB/METSTAT) are somewhat smoothed, because they are based on cloud cover observations that can be seen from a point location, typically a circle 40 km in radius, averaged over roughly a 30-minute period.

Data Applications for Site Screening and Prefeasibility Assessment

Review of Data Sources for Direct Normal Irradiance Estimation

The following information is for locations in the United States, mostly in the Southwest. The selected data sources are those most likely to be used by a project developer for a CSP plant. These data sources are summarized in Table 6-2. Similar data sources may be available for other locations (see Chapter 3).

Table 6-2. Data Sources for DNI Estimation

Source	Period of Record	Origin	Comments
NSRDB/SUNY Gridded monthly and annual mean DNI values	1998–2005	SUNY model (see Chapter 4)	Monthly and annual mean values available for uniform grid (CONUS and HI) with 0.1-degree spacing. DNI values for about 2100 grid cells in the Southwest have been adjusted upward to correct for satellite model underestimates of DNI in areas of high surface albedo (snow, sand, salt flats).
NSRDB/SUNY Gridded hourly DNI Values	1998–2005	SUNY model (see Chapter 4)	Hourly time series data available from NREL's Solar Prospector and NCDC Web sites in different formats. The mean DNI values have NOT been corrected for the surface albedo issue.
TMY2	1961–1990	1961–1990 NSRDB (see Chapter 4)	The annual and monthly mean DNI for the selected "typical" months may NOT agree with the 30-year monthly means for the same station.
TMY3	1991–2005 1976–2005	1991–2005 NSRDB 1976–2005 NSRDB (see Chapter 4)	Based on 24 years of data for sites near the 1961–1990 NSRDB locations and 12 years of data for remaining sites. Years with large amounts of stratospheric aerosol loading caused by volcanic eruptions are excluded from selection. The mean DNI values may NOT agree with the long-term means for the same location.
DNI measurements	1977–present	Various (see Chapter 4)	Measurement networks in operation 1977–1980 (NOAA network) and 1993-present (SURFRAD)
Surface weather observations	1961–2005	NSRDB	Observations for 15- and 30-year datasets available from NSRDB (usually NWS stations located at airports). Most reliable source.
Modeled weather data	1998–2005	North American Regional Reanalysis	Data from model with 32-m spatial resolution and 3-hour time resolution. Advisable for user to calculate average temperature and dew point for times of interest for comparison with other (best available observations from nearest site).

### The Site Screening Process

In the early stages of project development, a prefeasibility assessment of possible sites is undertaken. A desired outcome at this stage is the estimated annual energy production that could be expected from CSP plants in various proposed locations. Historical solar resource datasets are generally used in this stage, often in the form of maps, such as the NSRDB/SUNY gridded maps (Table 6-2). These datasets use a fairly consistent methodology to reliably identify the regions of highest solar potential. The maps should be used to make a preliminary assessment of solar resource, assuming a fairly large potential for error (about 15%). Thus, if a desirable level of solar resource is 7.0 kWh/m²/day, sites with mapped resource values down to about 6.0 kWh/m²/day should be considered.

Examples of a "first order" prefeasibility assessment include the analysis of CSP potential in the southwestern United States conducted by NREL's Concentrating Solar Power Program (www.nrel.gov/csp/maps.html; Mehos and Perez 2005). Using GIS screening techniques, CSP resource maps were developed that highlighted regions potentially suitable for CSP development once various land use constraints, such as protected land areas, sloping terrain, and distance from transmission were taken into consideration (Figures 6-2 and 6-3). The results of these studies show that, even with these constraints, vast areas in the southwestern United States are potentially suitable for CSP development (Mehos and Perez 2005). Maps such as these have been valuable to project developers to highlight specific regions under which various levels of site prospecting and prefeasibility analysis can take place.
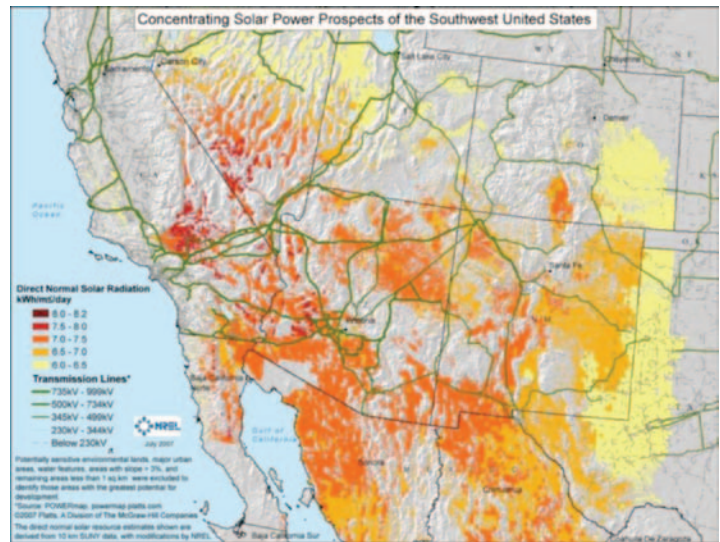
Figure 6-2. GIS analysis for available site selection using DNI resource, land use, and 3% terrain slope
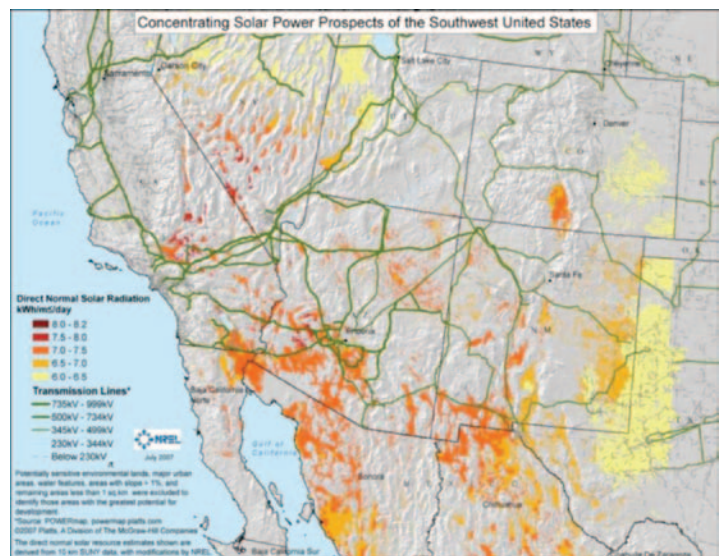
Figure 6-3. GIS analysis for available site selection using DNI resource, land use, and 1% terrain slope

With the introduction of powerful, easy to use tools such as the Solar Advisor Model (www.nrel.gov/analysis/analysis_tools_tech_sol.html) and the NREL Solar Power Prospector Web site (http://maps.nrel.gov/node/10/), many analysts now expect to use time-dependent modeling of their prospective CSP systems as part of the preliminary analysis. Considerable care must be taken to choose the correct hourly datasets for input to the CSP model. NREL recommends multiple years of hourly input data, rather than data from only one year, or even TMYs, to assess the effects of interannual variability of the solar resource on year-to-year system performance. Each hourly dataset should be evaluated, at least to determine whether the monthly mean values from hourly data match the best estimate of monthly mean DNI at the proposed site (Meyer et al. 2008). Example 1 on page 110 shows an evaluation of the monthly mean values from the 1998–2005 data, and from a TMY3 proposed as a surrogate.

Clean Air Prospecting

For CSP projects, a key step in site screening is to implement a concept we call *clean air prospecting*. In deserts and other areas with high DNI, most sites have low annual cloud cover. For these locations, the annual average DNI is strongly influenced by the aerosol optical depth (AOD). Figure 6-4 shows the dependence of the annual DNI on the average AOD for the Daggett, California, area. (Similar dependencies will be found for any location in the southwestern United States.) Knowing the AOD characteristics is vital for assessing the DNI resource and the performance of CSP installations.
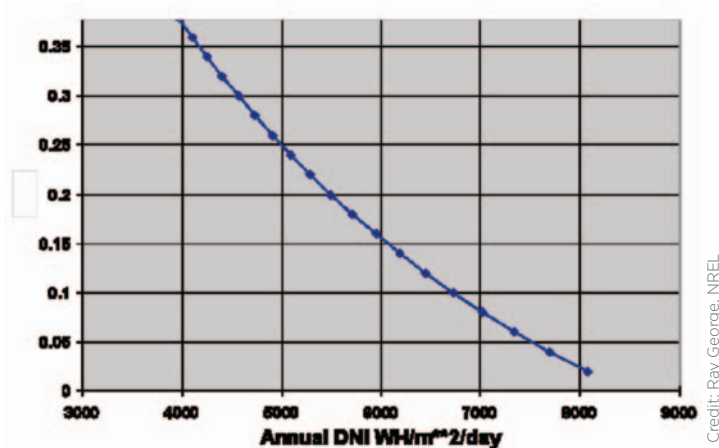

Credit: Ray George, NREL

Figure 6-4. Annual average DNI (in Wh/m²/day) as a function of annual average broadband AOD (y-axis). This is based on cloud conditions for the Daggett, California, area.

AOD is a measure of haze and smoke effects in DNI that are not caused by clouds. Sources of AOD include dust and particulates, air pollution, smoke from wildfires and agricultural burning, and sea salt (near coastlines). CSP facilities should, if possible, be sited at locations that are protected from sources of these aerosols. For the NSRDB/SUNY data and the 1991–2005 NSRDB update, NREL provided the average monthly AOD in the southwestern United States and northwest Mexico based on the map in Figure 6-5. For each location in the NSRDB, and the NSRDB/SUNY 10-km grid, the annual value for AOD from this map was adjusted downward based on the local elevation, using an exponential function that reduces AOD by 50% at an elevation of 2000 meters above sea level. This dependence of AOD on elevation is shown in Figure 6-6.
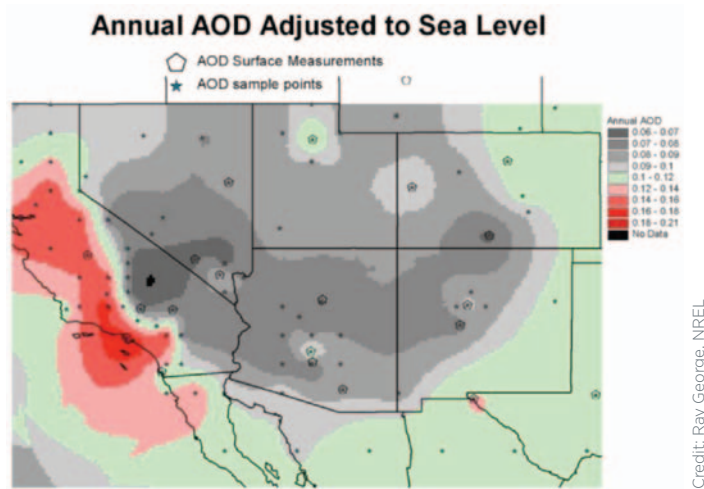
Figure 6-5. Annual AOD adjusted to sea level

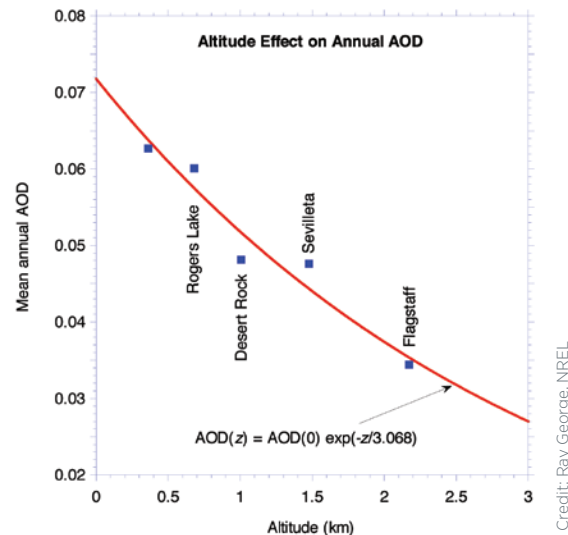
$$AOD(z) = AOD(0)\ exp(-z/3.068)$$

Figure 6-6. Dependence of annual average AOD on ground elevation. This relationship is used to create the AOD for all modeled solar data in the NSRDB 1991–2005 Update, for 15-year NSRDB and gridded 8-year NSRDB/SUNY data.

The map in Figure 6-5 assumes that, for most rural areas outside of urban areas or valleys, the AOD is very low; therefore, DNI should be higher than in the urban areas. Several major urban areas, including Salt Lake City, Las Vegas, Phoenix, and Albuquerque, have increased AOD because of air pollution and other factors, so additional artificial data points were added to define the boundaries of the region with enhanced AOD. We refer to these AOD data points as *artificial points.*

For rural areas with low AOD on the map, the DNI averages from the NSRDB/SUNY (gridded) data are more likely to be correct, if we can confirm that the area is indeed protected from sources of aerosols. The analyst should ask the following questions about the site:

- What are sources of potential aerosols?
  o Dust storms
  o Air pollution
  o Fires.

- How close is the site to urban areas?

- Is the site near power plants, mines, etc?

- Does this area have good visibility most of the time?

- Are distant hills or features visible without effects of haze?

    o No visible haze would indicate that the AOD is indeed low and, therefore, the DNI is similar to the NREL map values.

    o If the area is known to have some form of visible haze, there may (or may not) be a problem with the aerosols at the site. Further research or measurements may be necessary.

- How does the U.S. Environmental Protection Agency classify this area?

    o The U.S. Environmental Protection Agency or the utility companies should have projections of future growth, and of possible increases in air pollution or degradation in air quality.

    o If the area is covered by a State Implementation Plan, there should be detailed assessments of future air quality. If changes in the air quality are projected, more research may be needed to quantify the possible changes in solar resource.

If the candidate site is close to an urban area, the (estimated) AOD could also be too large. Figure 6-5 shows urban areas defined by the array of "artificial points" surrounding larger cities (Phoenix, Salt Lake City, Las Vegas, etc.). These are only approximate locations; thus, the areas near these points (on the fringes of the urban areas) are zones of higher uncertainty in AOD. For example, in the Salt Lake City and Albuquerque areas, a site just beyond the nearby mountains may actually be protected from sources of pollution, but appear on the map as areas of higher AOD. Areas on the fringes of these metropolitan areas may well be good candidates for CSP plants, for economic and infrastructure reasons. New measured DNI data may be necessary to resolve whether the site is sufficiently protected from urban sources of aerosols. Future releases of NREL data products such as the NSRDB will incorporate AOD estimates at higher spatial resolution, such as gridded AOD retrievals from space-borne instruments, as well as ground-truth data to correct these satellite observations wherever necessary.

Comparison of Satellite-Derived Direct Normal Irradiation Resource Data Using Geographic Information System Tools

A study conducted by the MESoR project in Europe (Hoyer-Klick et al. 2009) provides insights into the spatial distribution of uncertainty of the estimates of DNI by relative cross-comparison of five data sources: METEONORM, Satel-Light, NASA SSE, SOLEMI, and PVGIS (Šúri et al. 2009).

The map-based comparison is performed as a type of relative benchmarking of solar databases. It does not point to the "best" database, but it gives an indication of the user's uncertainty at any location in the region from comparing data from different sources. As the spatial products cover different periods of time, this comparison also introduces uncertainty resulting from the interannual variability of solar radiation. The maps of long-term average of DNI yearly sum are cross-compared. The map of standard deviation from the average indicates the combined effect of differences between the databases, and in this study it is used as an indicator of model uncertainty.

As shown on the maps of standard deviation (Figure 6-7), the solar industry in some regions in Europe might expect higher variability in the outputs from the analyzed databases. These variations are found mainly in complex climatic conditions such as mountainous regions and in some coastal zones, and in areas where solar radiation modeling cannot rely on sufficient

density and quality of input data. Significant differences are found in some regions with high DNI potential, such as the Balkan region, Greece, parts of the Iberian Peninsula, and Italy.
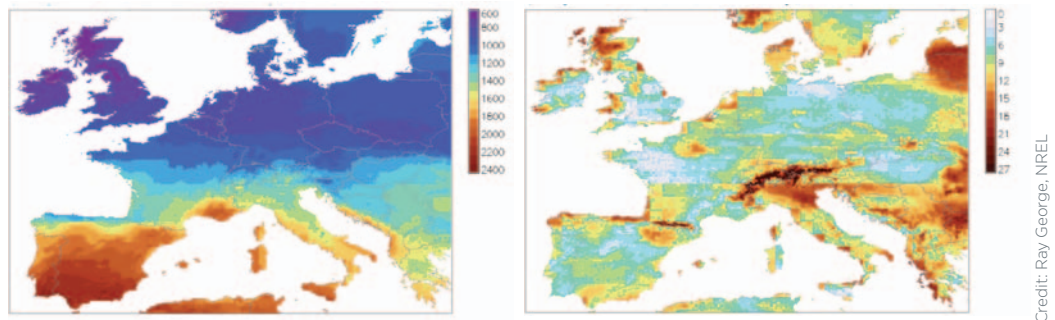

Figure 6-7. Yearly sum of DNI as calculated from five modeled datasets: METEONORM, PVGIS, NASA SSE, Satel-Light, and SOLEMI. Left – average of five databases (kWh/m²); right – relative standard deviation (%).

The MESoR map comparison studies have provided the following results:

- DNI is sensitive to the determination of cloud index that attenuates the solar irradiance reaching the surface. With the older generation satellites (METEOSAT First Generation), effects of snow, ice, and fog interfere with cloud detection. This often leads to underestimation of DNI, mostly in mountainous regions. The current satellite instrument MSG SEVIRI, in orbit since 2004, provides a high-quality calibrated signal with stable and known properties over continents, and with high information potential of 11 multispectral channels. This shows promising improvements in cloud detection.

- DNI is more sensitive than GHI to atmospheric parameters. The quality and spatial detail of satellite-derived databases are determined by input data used in the models, mainly parameters describing the optical state of the atmosphere, such as Linke atmospheric turbidity, or the analytical datasets (ozone, water vapor, and aerosols). The effect of aerosols represented by AOD is, after cloudiness, the most important variable affecting DNI (Gueymard and George 2005).

- Like cloudiness, AOD is highly variable over time and space. Its measurement requires sophisticated instrumentation and complex satellite models. The numerous AOD datasets available to the solar radiation modeling community come from various sources. However, except for the AERONET measurements, they represent only climate (averaged) values for a few years, which do not address high-frequency changes.

- There is an inherent difference between in-situ (ground) and satellite observations, and in the methods of processing these data. Databases relying on the interpolation of ground observations (PVGIS Europe, and partially METEONORM) are sensitive to the quality and completeness of ground measurements (especially those from earlier time periods) and density of the measurement network. PVGIS and METEONORM include long-term statistical averages, and some geographical regions may show higher uncertainty because of the lower concentration of measurement sites with varying data consistency. The satellite-derived databases (NASA SSE, SOLEMI, and Satel-Light) offer time series with high time resolution (3-hourly, hourly, and 30-min data, respectively) and provide spatially continuous coverage, but the results may be affected by higher uncertainty of the cloud cover assessment when the ground is covered by snow and ice and for low sun angles. However, these regions are typically not high-value sites for DNI applications.

- Terrain effects (e.g., differences in AM, shadowing by surrounding terrain) play a role in solar radiation modeling in hilly and mountainous regions. The spatial resolution of the input data and the selected DEM have direct impacts on the accuracy of the estimates. A coarse resolution DEM results in a smoother spatial pattern of solar irradiance, which also affects the regional mean of the irradiation. However, a high-resolution DEM is presently being used only in METEONORM and PVGIS. Databases with coarser spatial resolution (e.g., NASA SSE) provide global estimates; however, for studies at a local level they may show higher deviations as they smooth out local climate and terrain features.

The studies conducted under the MESoR program provide only a preliminary outline of the state of the art of current knowledge of DNI in Europe. Such a simple data comparison as provided above does not fully address the needs of the solar energy industry, so further work is needed to improve our knowledge and decrease the uncertainties.

Data Applications for Feasibility, Engineering, and Financial Assessments

Once one or more candidate sites have been selected for engineering feasibility assessment, a common problem facing CSP project developers is how to produce datasets that allow for the most reliable calculation of annual or interannual system performance when only short-term ground measurements, along with other estimated data sources, are available. In the wind energy industry, solutions to this problem are known as measure-correlate-predict (MCP) (Thøgersen et al. 2007). MCPs are based on various statistical procedures whereby short-term on-site measurements are related to nearby long-term measurements to obtain estimates of the site's long term wind energy potential and interannual variability. The correlation is then used to predict resources for the new site.

The problem tends to be more complex for the wind industry than for the CSP industry because:

- Wind resources are generally much more variable spatially than solar resources.

- Wind characteristics can vary significantly with height above the ground, which complicates the comparison of short-term with long-term measurements if the heights of the two measurement systems are different.

- Wind resources must take speed and direction into account, which complicates the MCP statistical procedures.

- Long-term data, such as those developed from a satellite methodology for solar radiation resources, are generally lacking for wind resources that overlie a proposed site.

For these reasons it is not necessary to employ some of the more complex MCP methods available in the literature for wind energy assessments to CSP analyses. We suggest a simpler approach that should be reasonably viable. Readers interested in learning more about wind-energy related MCP methods will find a good summary of various approaches in Thøgersen et al. (2007).

The degree of accuracy required for system performance and energy yield estimates depends on the stage of project development, as follows:

- **Prefeasibility stage.** Specific sites are evaluated to determine whether they may be suitable for development and thus require more comprehensive evaluation.

- **Feasibility stage.** Sites have been selected for actual project implementation, where system design and energy performance estimates become very important. At this stage, a more comprehensive knowledge of the annual resource, as well as seasonal and diurnal characteristics, with known accuracies, is required. After (or concurrent with) this detailed analysis, due diligence on the chosen project site is required, which involves accurate cash flow analysis over the life of the project. In this case, accurate long-term site performance estimates are required, and the variability of the system output from

year to year (caused by interannual variability of the resource, again within well-established confidence limits) is required.

Extrapolating Short-Term Measured Datasets

The basic methodology for obtaining an estimate of the annual solar resource suitable for prefeasibility analysis that can be used to make energy yield estimates is to acquire available long-term site estimates, such as satellite-derived estimates or nearby modeled station values (such as those available through the NSRDB or TMYs). These datasets and their uncertainties have already been described in previous chapters and sections. When short-term, on-site estimates from new solar radiation measurements are available, they can be used to reduce the uncertainty of the modeled estimates (Gueymard and Wilcox 2009). This process becomes critical in the project feasibility and due diligence stages of project development.

Two methods by which we can combine the short- and long-term data to obtain a more accurate estimate of the long-term solar resource (such as what may be needed for project feasibility studies) are discussed here.

The *ratio method* assumes that at least two independent datasets are available: an on-site measurement dataset (presumed to be relatively short term), and a long-term climatological dataset, such as a satellite-derived database (e.g., the 8-year Perez SUNY data supplied to the NSRDB) or a nearby long-term measurement station or modeled data. The latter is found for many U.S. locations in the NSRDB. Ideally, at least part of the two datasets should be concurrent. If there is no concurrency in the data, the ratio method can still be applied, but the uncertainty of the resulting long-term on-site data profile will likely be much higher than if concurrent data periods are available. This method is described in Gueymard and Wilcox (2009). Basically the method involves calculating the ratios of a selected averaging period of the concurrent datasets, such as hourly or monthly averages, then applying these ratios to the balance of the long-term dataset to produce a long-term estimate for the site.

There are several important considerations to applying this approach, especially if the long-term dataset involves the use of satellite-derived data for the same location as the site data. Although the ratio method removes biases between the short-term and long-term datasets, the biases may in fact vary from year to year, or from season to season. Variations in biases suggest the cross-correlation between the two concurrent measurement sources is less than 1.0, and lower cross-correlation values indicate more uncertainty associated with extrapolating short-term data to long-term means (Gueymard and Wilcox 2009). Consider these possible scenarios:

- In an ideal scenario, there is low month-to-month variability in biases between the reference data and on-site measurements. Under these circumstances, a simple correction factor based on the ratio method should be acceptable for extrapolating the short-term dataset.

- A second scenario is high random variability between the short-term on-site data and the long-term reference data source, indicating a strong random variability (and low cross-correlation) between the two data sources, meaning that an accurate extrapolation to a longer-term value at the site will have high uncertainty.

- A third scenario is a situation where there are strong seasonal trends in the data, which may require additional years of on-site data to better confirm or define the trend. This scenario would ultimately lead to long-term extrapolations with low uncertainty.

A second method is to combine two different datasets by weighting each. They could be weighted equally, or as suggested by Meyer et al. (2008), the weighting can be determined based on the inverse of the uncertainty of each dataset. By assuming that the deviations from truth follow a normal distribution and are statistically independent, the Gaussian law for error propagation can be applied. Meyer et al. (2008) then provides curves showing how the

additional datasets do not need to be of the same high quality as the base dataset to add value to the combined datasets (Figure 6-8).
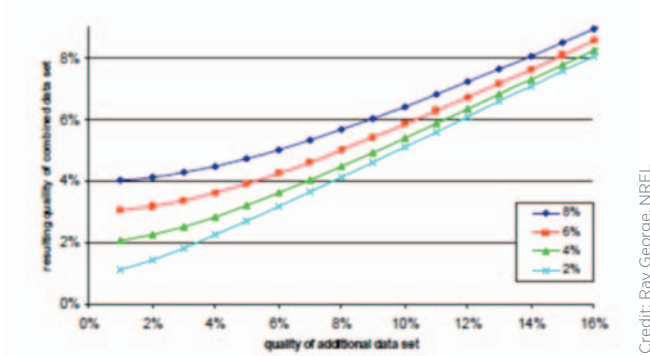
Figure 6-8. Resulting uncertainty when combining a base dataset of 2%, 4%, 6%, or 8% overall uncertainty with an additional dataset of varying quality
(from Meyer et al. 2008)

Meyer et al. (2008) shows that by using more than two datasets, the resulting quality of the combined dataset can be even further improved. For example, where the base dataset has an uncertainty of 4%, the resulting dataset can be improved by adding two datasets with a moderate 7% quality, rather than 10% (Figure 6-9). However, if the two additional datasets have an uncertainty of 10% or more, the base dataset cannot be improved. Therefore, datasets with such high uncertainties should not be used. If the analyst uses this method, he or she should be prepared to demonstrate that the incorporated datasets are truly independent and there are no correlations (similar instrumentation and measurement protocols, common estimates for model parameters such as aerosols or clouds). This methodology of combining the uncertainties of various input datasets to provide the resulting uncertainty of the "best guess" DNI estimate for a site is elaborated in a more recent paper by Meyer et al. (2009). In this paper, further elaboration on the optimal minimal time period for ground measurements, and exclusion of satellite data from years when abnormal AOD conditions might exist (such as years of major volcanic activity) are also discussed.

Figure 6-9. Resulting uncertainty for a case in which the base dataset has an uncertainty of 4% and is combined with two other datasets of varying uncertainties. Good combinations, which should improve the quality of the combined datasets, are highlighted in green, yellow for indifferent situations, and red for combinations that would decrease quality.

Studies have also been undertaken to determine how long surface measurements at a proposed site should be taken before the true long-term mean is captured. This is important when no concurrent datasets are available and yet project finance decisions must still be made. Another way to look at the problem is to ask, How representative is a short-term (say, 1-year)

measurement to the "true" climatological (nominally, 30 years) mean? In the wind industry, a rule of thumb is that it takes 10 years of on-site wind measurement to obtain a mean annual wind speed that is within ± 10% of the true long-term mean, which is generally required by financial institutions. What about the case with only 1 or 2 years of on-site measurements? These data may be all that are available to a financial institution conducting due diligence on a project.

Gueymard and Wilcox (2009) begin to address this problem through an analysis of the 8-year SUNY dataset used in the updated 1991–2005 NSRDB with coincident measured hourly data at 37 sites from various networks in the conterminous United States. However, only four stations have continuous measurements of 25 years or more, which are needed to determine the climatological average. These stations are Burns, Eugene, and Hermiston, Oregon, and NREL's SRRL station on top of South Table Mountain near Golden, Colorado.

Tomson et al. (2008) show that the mean annual global irradiation in any year is virtually independent of the previous year, which means that 11 years of on-site measurements does not represent the long-term mean. Thus, Gueymard and Wilcox (2008) examined the long-term data from the four stations mentioned to address the questions: How many years of measurements does it take to converge to the long-term mean? Does the variability in annual radiation change significantly from one site to another?

For these stations, Gueymard's and Wilcox's results show that, first, there is much lower interannual variability with GHI than with DNI. GHI is almost always within ± 5% of the true long-term mean after just one year of measurements, regardless of which year these measurements are taken. The situation is quite different for DNI, however. After only one year of measurements, the study shows that the estimate of the average DNI is no better than ± 10% to ± 20% of the true long-term mean. At two of the sites, upwards of 10 years of measurements are required to be within ± 5% of the true long-term mean, which is consistent with the findings of the wind energy industry. Financial institutions prefer to evaluate the risk of uncertainty with solar resource data in terms of exceedance probabilities (e.g., P50 or P90). P50 is the result of achieving an annual energy production based on the long-term median resource value. For this value, the probability of reaching a higher or lower energy value is 50:50. For an exceedance probability of P90, the risk that an annual energy value is not reached is 10% (90% of all values in a distribution exceed the P90 value). Another way of stating this finding is the COV for DNI is generally two to three times higher than the COV for GHI.

Figure 6-10 provides other interesting observations about multiple years of DNI measurements, particularly for Hermiston and Burns, which are in the arid eastern part of Oregon. Even in Golden, Colorado, a cloudier than average year will strongly influence negative anomalies, but these generally converge to zero more quickly than do the positive anomalies. Another factor, especially for clear sites, is that AOD becomes the primary influence on DNI variability; events such as volcanic eruptions or regional forest fires produce significant AOD anomalies that could be the main cause of the asymmetries in Figure 6-10.

These results indicate the importance of having a second, independent quality dataset, such as a satellite-derived dataset, available to reduce the uncertainty of the long-term average DNI estimates for a proposed CSP site to provide reasonable due diligence of a plants estimated performance over the life of the project.
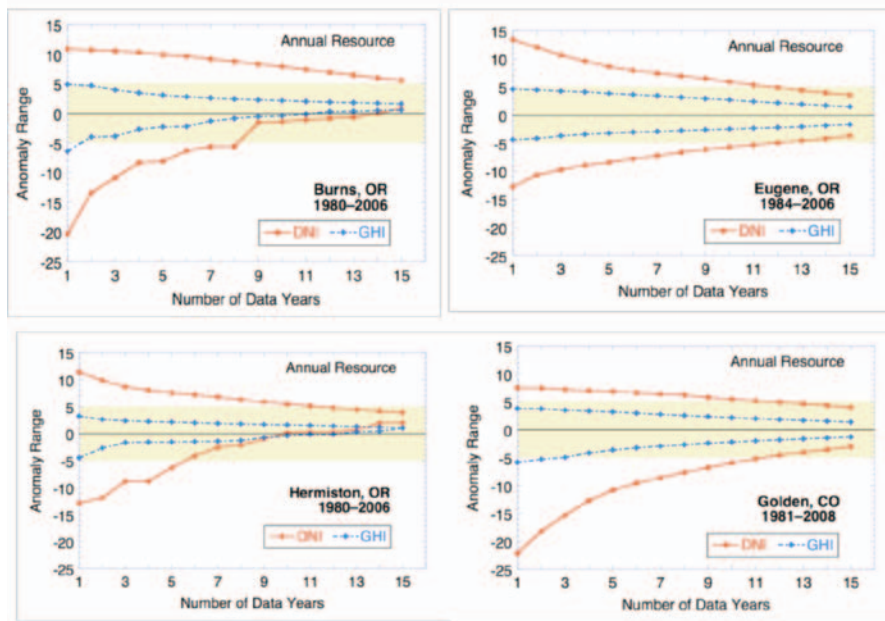
Figure 6-10. Number of years to stabilize DNI and GHI in Burns, Oregon; Eugene, Oregon; Hermiston, Oregon; and Golden, Colorado.

Examples of Mean DNI Estimation and Hourly Data Selection Using NSRDB/SUNY, TMY3, and Measured DNI Data

Example 1 is a proposed trough plant near Harper Lake, California. Harper Lake is actually a dry lake bed with very bright salt deposits on the surface. Our goals for exploring this example are to:

- Determine the best estimate for mean DNI by month and year for a chosen site.

- Procure one or more years of time series DNI (and weather) data for use in time-dependent modeling (CSP plant models or electrical grid models).

To quickly assess the annual and monthly mean DNI, we use the Solar Prospector (http://maps.nrel.gov/node/10/) with satellite ground surface imagery (from Google Maps) as background. Figure 6-11 shows nine NSRDB/SUNY grid cells in the area near Harper Lake in the Mojave Desert. The values of average DNI can be obtained from the Solar Prospector. The upper value is the mean DNI from the hourly data, which is not corrected for specular reflection. The lower is from the map, which has been corrected for this artifact. Next, we look at the mean DNI values, by month, for the 8 years of data from the 1998–2005 NSRDB. We do this for the desired location and a few nearby locations. If the map value and the hourly averaged values are different by more than 0.2 (kWh/m²/day), the grid cell map was corrected. In this example, Cells B1 and B2 were corrected. If the candidate site for a CSP plant is located in cell B2, the analyst could select hourly data from another cell that has not been corrected, such as A2 or C2. This procedure will ensure that the hourly simulations (e.g., Solar Advisor Model for CSP www.nrel.gov/analysis/sam/) produce results that are more consistent with the mean value at the proposed site.
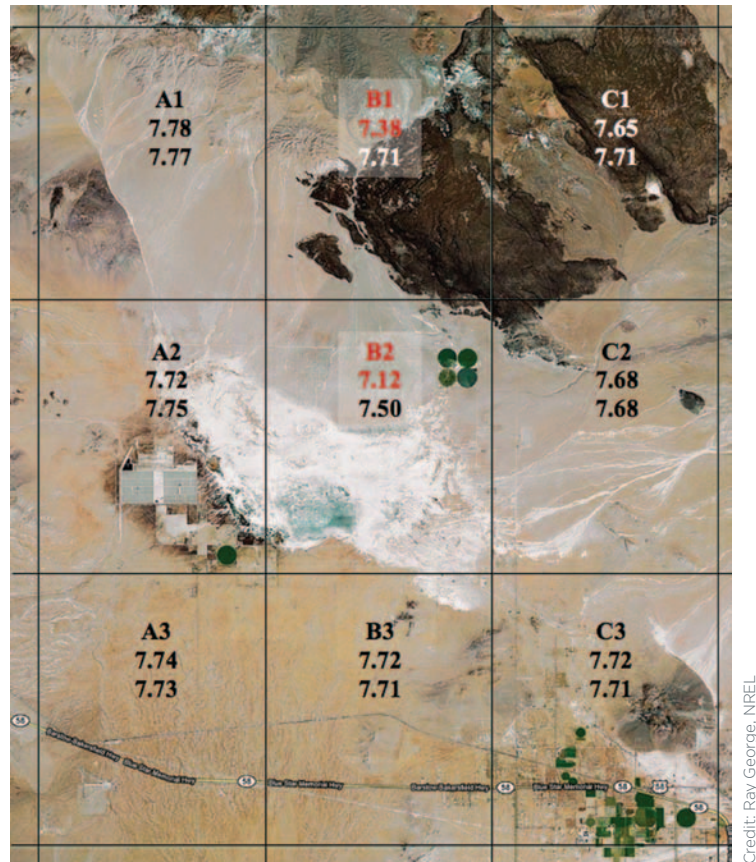
Figure 6-11. NSRDB/SUNY 10-km grid cells near Harper Lake, California. Upper value in text box is average from (uncorrected) hourly files. Lower value is average DNI from corrected maps. Values in red show uncorrected time series mean values, substantially lower than the corrected map values.

In general, cells in need of correction have bright or uneven areas, especially near the center. Adjacent cells with a darker, more uniform background will have more reliable hourly DNI data. The goal is to select the correct time-series to match the estimate of the mean values. The Google map shows that the time series data from the selected cell should not be used, because the time-series produces different (lower) means. The SUNY team developed corrections to this artifact; in the near future, corrected maps will be available that avoid this problem.

Although not recommended, the user could choose one of the TMY2 or TMY3 datasets to act as a surrogate for the 8 years of data. If a TMY2 or TMY3 dataset is proposed as a surrogate for this site, the dataset should be carefully evaluated for applicability of the mean values in space and time. Figure 6-12 shows the monthly DNI values for the C2 site and the nearby Daggett, California, TMY3, which is a higher quality, Class I, NSRDB site. In this case, the TMY3 may be a suitable surrogate for the site-specific SUNY data.
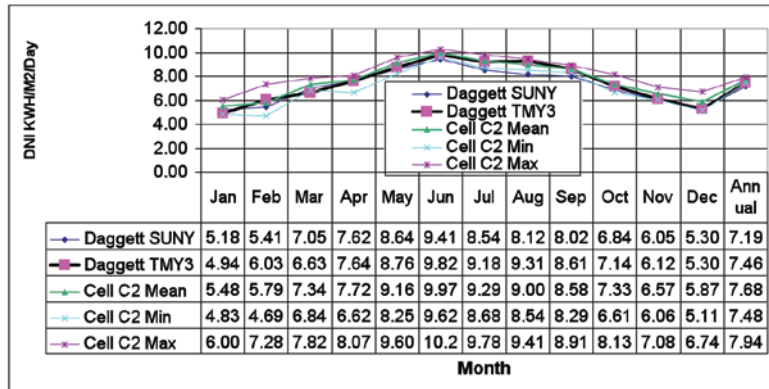
Figure 6-12. Monthly mean DNI for Harper Lake (Cell C2) and Daggett TMY3. Minimum and maximum values for cell C2 are also shown for each month.

Example 2 is a proposed CSP site near Desert Rock, Nevada. We assume for this example that we have chosen the NSRDB/SUNY data for preliminary analysis, and have now obtained new measured data for the desired site. We show the effects on the annual DNI estimate of including measured and modeled data. Table 6-3 shows the results of using 8 years of modeled NSRDB data with:

- Two years of measured data (2004–2005)

- Year 2004 measured data only

- Year 2005 measured data only.

Table 6-3. Annual Mean Values of Global and Direct Radiation for Measured and Modeled Data at Desert Rock, Nevada

Measured Time Period	2004–2005 (kWh/m²/day)	2004 only (kWh/m²/day)	2005 only (kWh/m²/day)	1998–2005 (kWh/m²/day)
Model global	5.615	5.656	5.574	5.622
Model direct	7.642	7.720	7.564	7.658
Measured global	5.703	5.799	5.607	
Measured direct	7.564	7.901	7.227	
MBE global	−1.54%	−2.46%	−0.58%	
MBE direct	1.04%	−2.28%	4.67%	
Adjusted direct 8-year mean	7.579	7.833	7.300	
Meyer corrected mean DNI	7.582	7.859	7.305	
Meyer MBE direct	0.8%	−1.8%	3.6%	
Meyer adjusted 8-year mean	7.597	7.793	7.386	

We adjust the average DNI from the 8-year period using the bias error from our observed data, with the simple "ratio method" described above. The bias error using both years is a relatively low value of 1.04%. The bias errors from individual years are higher, and do not show a consistent pattern. The adjusted direct is the new estimate of the long-term mean DNI, and is simply the 8-year mean DNI (7.658) times (1.0 − MBE). The method of Meyer et al. (2008) described on page 107 can also be used advantageously here. If we assume the uncertainty is 3% for measured data and 10% for SUNY data, we can calculate the corrected means for all the

months we have both measured and modeled data. If we adopt this value as our best guess for the actual DNI for the years 2004 and 2005, then our new bias error is (SUNY-Meyer)/Meyer, and our bias errors are smaller. The Meyer estimate is calculated using the following equation:

$$I_{est} = (I_{me}/U_{me} + I_{mo}/U_{mo})/(1/U_{me} + 1/U_{mo})$$

where

the Meyer estimate $= I_{est}$

$I_{me} =$ measured value

$I_{mo} =$ modeled value

$U_{me} =$ measurement uncertainty (0.03)

$U_{mo} =$ modeled uncertainty (0.10)

Monthly mean values of GHI and DNI are shown for the Desert Rock site (see Figure 6-13). For many months, especially during 2005, the bias errors are very small for GHI and large for DNI. GHI and DNI bias errors are well correlated in 2004, but not in 2005. One interpretation is that the principal source of error during 2004 is the cloud estimation, and the principal source of error in 2005 is in the AOD. A small error in global radiation along with a large overestimate of the DNI indicates that AOD at the site may have been much higher than the estimated AOD used in the satellite model. A diligent analyst might pursue an explanation for the higher than normal AOD and ask, Could higher levels of AOD be caused by dust storms or forest fires? The average monthly values shown in Figure 6-12 would be helpful in pinpointing the cause of the problem.
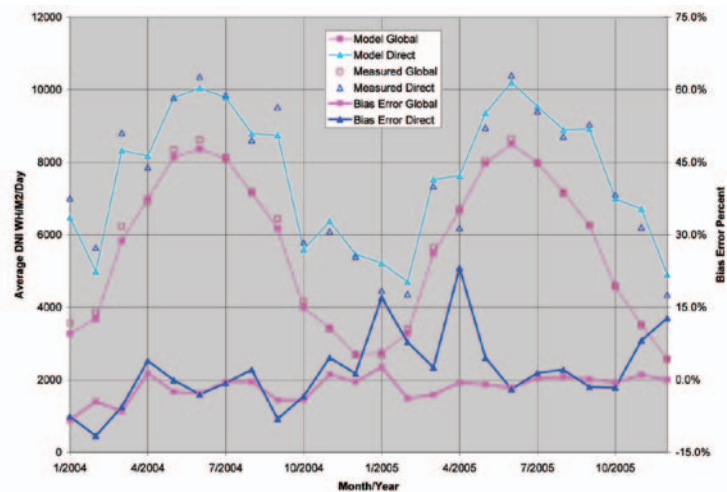
Figure 6-13. Desert Rock annual average, GHI and DNI, from satellite and measurements. Mean bias error is defined as (satellite – measured)/measured × 100%.

These show large shortfalls in the measured DNI in January and April 2005, indicating higher than normal AOD. Once the likely cause has been determined, the analyst should then assess whether that phenomenon might be more prevalent in the future, or is possibly a rare event.

The broadband AOD may be estimated from the new DNI measurements using a clear sky model such as the Bird model, with supplemental data to estimate total column water vapor. These values can then be used to adjust the modeled DNI estimates. However, AOD is also highly variable from month to month and from year to year, so it would take several years of data to show conclusively that the mean AOD used in the satellite model needs to be adjusted at this site.

In this example (see Table 6-3), the new estimate for the 2-year dataset DNI, 7.597 kWh/m²/day, is less than 1% different from the 8-year model estimate of 7.658. With only 1 year of measurements, the errors are larger, up to 3.6%.

Adjusting Direct Normal Irradiance Data for Concentrating Solar Power System Performance Estimates

The DNI is most often used to characterize the solar resource data for CSP plants. This solar component is the resource available to a two-axis tracking concentrator. If the CSP technology being considered is for trough plants (usually one-axis trackers), the collector-specific average radiation will be less than the average DNI. In this case a correction factor needs to be applied to the average DNI. Figure 6-14 shows such correction factors for three locations at different latitudes. *The Solar Radiation Data Manual for Flat-Plate and Concentrating Collectors* (Marion and Wilcox 1994) is based on data from the 1961–1990 NSRDB and provides statistical tables that include both DNI and single-axis N-S tracker resource data, so monthly correction factors are easily developed from these tables.
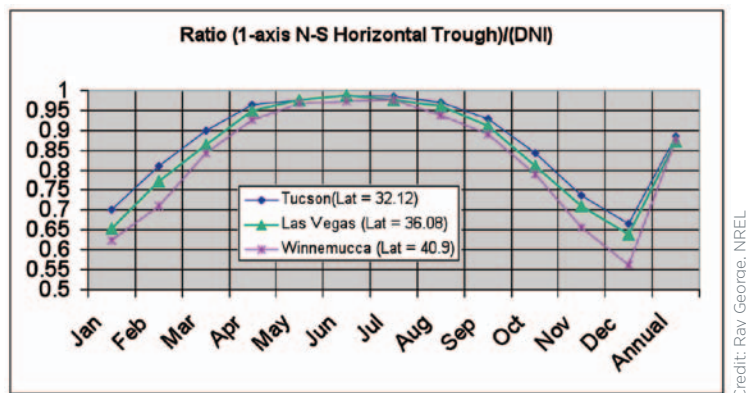
Figure 6-14. Ratio of monthly average solar resource available to a trough plant, divided by monthly average DNI. The ratio decreases for locations farther from the equator, especially in winter. These ratios represent correction factors that need to be applied to the DNI solar resource when considering trough plants with an N-S orientation.

Variability of the Solar Resource

The variability of the solar resource is an important consideration in the need to adequately characterize the variability with measurements and for predicting future plant performance. This analysis disregards predictable variability, such as that caused by site latitude and time of day, and concentrates on less predictable behavior caused by climate. The solar variability is closely related to the variability of climate in time and space, because atmospheric forces and constituents have a strong impact on the amount of solar radiation absorbed, reflected, or otherwise prevented from reaching the Earth's surface.

With knowledge of the likelihood of variability from year to year, users are provided some justification for selecting a particular period of time for measurements adequate to characterize the solar resource. Likewise, with knowledge of variability across distance, users can make some statement of the applicability of a measurement to a location some distance away. Knowledge of variability then becomes valuable when deciding how long to make measurements at a particular location and whether the character of the solar resource at that location can be extended to other nearby locations.

NREL has analyzed 8 years of data (1998–2005) from the NSRDB in the realms of temporal and spatial variability. The analysis summarized the values in each 10-km × 10-km cell in the SUNY satellite-derived data in the NSRDB and calculated monthly mean daily totals, annual mean daily totals, and mean daily total for the entire 8-year period.

The values were analyzed by temporal and spatial variability.

Temporal variability. For each cell, the 8 annual values were used to calculate a COV. The 8-year mean irradiance $<E_p>$ and each annual value E_i were used to derive the standard deviation of the dataset. Because there are no missing values, the standard deviation simplifies to

$$\sigma_t = [\, (<E_p> - E_i)^2 / 8 \,]^{1/2}.$$

The temporal COV is

$$C_t = \sigma_t / <E_p>.$$

To understand the variability in a seasonal scope, the process was repeated on a monthly level, e.g. the 8 Januarys, Februarys, etc. The results, expressed in percent, represent the variability in the solar resource year by year at the cell's geographic location. The resulting COV for DNI for all cells plotted as a contour map of the United States is shown in Figure 6-15, providing a quick visual measure of differences in interannual variability. The temporal COV for 48 U.S. states ranges from a low of 0.49% in south central Washington to a high of 15.8% in northwest Washington (an interesting contrast of climate within a single state).
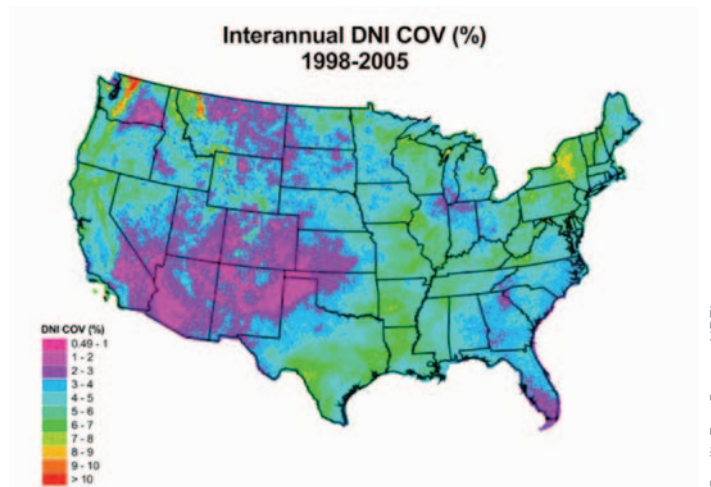
Figure 6-15. Interannual DNI variability (COV as percent) for 1998–2005

Spatial variability. The 8-year daily total irradiation means for each 10-km × 10-km cell were compared with a matrix of surrounding cells to determine the variability of the solar resource within the matrix (see Figure 6-16).
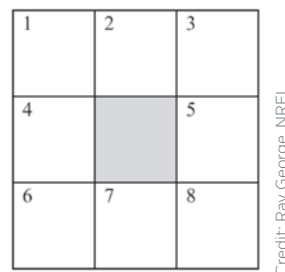
Figure 6-16. A 3 × 3 grid layout with anchor cell in the center and eight surrounding neighbor cells

Here the standard deviations of the surrounding cells were calculated as

$$\sigma_s = [\, \Sigma^{i=n} \, (E_p - E_i)^2 / n \,]^{1/2}.$$

The spatial COV is

$$c_s = \sigma_s / E_p.$$

The same process was applied to the 8-year means on a monthly level, all Januarys, Februarys, etc.

Two matrix sizes were analyzed: a 3×3 (see Figure 6-16) and a 5×5. These represent areas of approximately 30 km $\times$ 30 km and 50 km $\times$ 50 km, respectively, and likewise roughly represent an area within 15 km and 25 km of a measurement site. The results for DNI, expressed in percents, are mapped in Figure 6-17, which provides a quick visual representation of how the solar resource varies over space. For DNI, the values range from 0.12% in central Missouri to about 11.5% along a corridor between Los Angeles and San Bernardino, California. Variability tends to be higher in coastal areas (particularly the California coast) and in mountainous areas. Greater variability is seen in the 5×5 matrix, which is to be expected because of the effects of terrain. Further, the general pattern of high and low variability remains the same between the two maps, indicating that in locations of significant variability, the magnitude is much a function of distance.
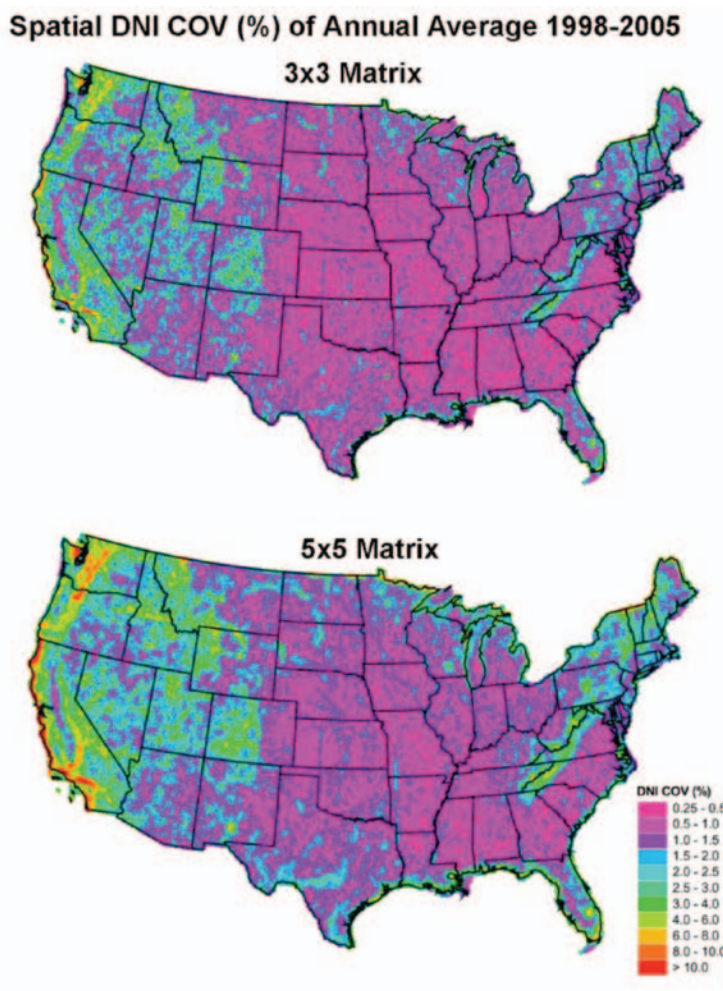
Figure 6-17. DNI spatial coefficient of variability for 3x3 cell matrix (upper) and 5 × 5 cell matrix (lower) for the average DNI from 1998–2005

The underlying data for these maps will be available from NREL to provide users with the actual values for each 10-km $\times$ 10-km cell both in units of % COV and Wh/m². Users should be cautioned that the 8-year period may not be long enough to produce definitive variability values, and the uncertainty of this analysis has not been defined. NREL plans to update this

dataset by drawing from a longer period of record; however, the results here are very likely accurate enough to reveal the relative variability of the solar resource throughout the United States.

Using these variability statistics, users can better understand the extent of measurements required to best characterize the solar resource for a particular application. In areas with low interannual variability, a shorter measurement period may suffice. In areas with low spatial variability, a measurement station could possibly represent the solar resource at nearby locations, negating the need for additional measurements. An analyst can use this information to better build confidence in a dataset as being sufficient for an analysis and can use these data to understand the consistency of future plant performance and how that relates to the economic viability of a particular location.

Summary of CSP Best Practices for Resource Characterization

Before making site-specific measurements (prefeasibility, feasibility stages)

1. Use NSRDB screening maps and other criteria o choose candidate sites.

2. Assess monthly/yearly mean DNI values from the NSRDB 8-year dataset. Compare with nearby NSRDB sites that have more years of data. Create a set of best guess target values for the monthly mean DNI.

3. Assess the uncertainty of DNI means in your target values. The uncertainty is higher if the site:

   - Is close to strong gradients in average DNI.

   - Is close to strong gradients in AOD.

   - Is subject to possible enhanced aerosols (close to urban areas, mines, power plants, etc.)

   - Has bright surface albedo, or highly variable albedo.

4. Adjust your expected monthly mean DNI values upward or downward, based on these parameters.

5. Choose hourly datasets to match expected mean value; at the same time have diurnal and seasonal patterns close to those of the candidate site.

6. If using TMY data, assess the data to see how closely the mean values match your expected patterns.

After new measurements are available (later stages in project development; project qualification phase)

1. Realistically assess the quality of the new measured DNI data.

2. Use ration method or Meyer method to compare measured and modeled data and create updated estimates of monthly mean DNI.

3. Use a comparison of measured and modeled DNI to assess the variability of aerosols.

4. Prepare best possible datasets, multiple year or TMY, based on all available data, for final simulation runs.

Chapter 7. Future Work

Advancing renewable energy technologies will require improvements to our understanding of solar radiation resources. This chapter briefly describes the areas of R&D identified by NREL as emerging technology needs.

Forecasting Solar Radiation

Industry representatives and private sector consultants have indicated there will be an increasing need for reliable short-term and day-ahead forecasting as more CSP installations are tied to the nation's electricity grid. Day-ahead forecasting for wind energy applications is already important, because knowledge of the availability of the wind resource influences decisions on implementing power purchase contracts with outside providers to maintain system performance and meet loads. For example, independent system operators need to make system availability forecasts at 15-min increments for traditional power generating equipment; for wind system operations, day-ahead wind energy forecasts are currently viewed as the most practical at this stage of wind farm development.

Industry has also expressed the need to better understand the capability of longer term forecasts (seasonal, annual, and interannual) to assist with system planning. In particular, a better understanding of long-term solar resource trends at a site or in a region would be useful for infrastructure planning and cash flow analyses.

Currently, no operational solar resource forecasts are being implemented in the United States, although several approaches for implementing forecasting procedures have been explored based on cloud observations from satellite (Perez et al. 2007) and using all-sky cameras at the site of interest. However, in Europe several institutions are developing reliable 1 to 3 day-ahead forecasts and some operational forecasts are being used on a limited basis. Solar resource forecasting methodologies is a major activity under the International Energy Agency Solar Heating and Cooling Programme's Task 36: Solar Resource Knowledge Management; NREL is the operating agent for the task (see http://re.jrc.cec.ue.int/iea-shc-task36/). This task provides an excellent opportunity to bring researchers together from around the world to share their approaches and experiences with implementing solar resource forecasts.

High-Resolution Temporal Data

Electrical generation by solar thermal electric power systems is directly proportional to the available DNI. Historical solar resource data are available for hourly time intervals. Subhourly time-series data (15-min or less) with dense spatial coverage (e.g., 5 km or less) are needed to address load-following simulations and related economic considerations.

Currently available instrumentation and measurement equipment can acquire solar irradiance data as often as 1-s intervals (Wilcox and Myers 2008). Research is underway at NREL to deploy solar resource measurement stations that will provide high-resolution data at single locations and within the collector fields.

Site-Specific Resource Data

Characterizing the spatial variability of solar irradiance over distances of 1 km or less is important for improving the siting, design, and performance monitoring of a solar energy conversion system. The latest NSRDB, along with the 1991–2005 update, provides historical solar irradiance data for specific locations from 1961 through 2005, with a resulting spatial scale of about 100 km. Additionally, based on satellite remote sensing model estimates, the NSRDB provides solar irradiance data for 10-km grid cells from 1998 through 2005. Methods for increasing the spatial resolution of satellite-based models for estimating solar irradiance at the surface are under development. Data from large CSP systems that may have high-quality radiometric instrumentation need to be systematically investigated.

Effects of Climate Change on Solar Resource Assessments

How representative will the more recent solar resource data be for estimating the performance of a CSP plant over the system design life (e.g., 25 years) due to changes in atmospheric aerosol loading from natural causes or industrial pollution, changing patterns of precipitation and cloudiness, temperature extremes, and other climatic variables? Research is needed to advance the climate modeling capabilities and merge the output with advanced system performance models.

Need for Cross-Disciplinary Analysis Projects

The use of solar resource and meteorological data to address complex problems such as time-dependent utility load estimations, cloud transient effects on grid stability, and solar generation dispatching, requires close collaboration between analysts, utility planners, and the resource and meteorology communities. Shared knowledge will advance the identification of resource data needs and the development of methods for improved resource data and information to meet those needs.

References, Resources, and Annotated Bibliography

Chapter 2: Overview of Solar Radiation Resource Concepts

Badescu V. (ed.) (2008). *Modeling Solar Radiation at the Earth's Surface*. Springer, Berlin.

Barnett, T.P.; Ritchie, J.; Foat, J.; Stokes, G. (1998). "On the Space–Time Scales of the Surface Solar Radiation Field." *Journal of Climate* 11:88–96.

BIPM. (1995). Guide to the Expression of Uncertainty in Measurement. Comité International des Poids et Mesures. www.bipm.org/utils/common/documents/jcgm/JCGM_100_2008_E.pdf.

De Toma, G.; White, O.R.; Chapman, G.A.; Walton, S.R. (2004). "Solar Irradiance Variability: Progress in Measurement and Empirical Analysis." *Advances in Space Research* Vol. 34, pp. 237–242.

Erbs, D.G.; Klein, S.A.; Duffie, J.A. (1982). "Estimation of the Diffuse Radiation Fraction for Hourly, Daily, and Monthly Average Solar Radiation." *Solar Energy* 28(4):293–304.

Grether, D.; Nelson, J.; Wahlig, M. (1975). "Measurement of Circumsolar Radiation." *Proceedings of the Society of Photo-Optical Instrumentation Engineers Vol. 68, Solar Energy Utilization*. SPIE, Bellingham, WA.

Gueymard, C. (2009). "Direct and Indirect Uncertainties in the Prediction of Tilted Irradiance for Solar Engineering Applications." *Solar Energy*, 83:432–444.

Iqbal, M. (1983). *An Introduction to Solar Radiation*. Academic Press, New York.

Liu, B.Y.H.; Jordan, R.C. (1960). "The Interrelationship and Characteristic Distribution of Direct Diffuse and Total Solar Radiation." *Solar Energy*, 3:1–19.

Major, G. (1994). "Circumsolar Correction for Pyrheliometers and Diffusometers." WMO-TD 635, World Meteorological Organization, Geneva.

Marion, W.; Riordan, C.; Renné, D. (1992). *Shining On: A Primer on Solar Radiation Data*. NREL/TP-463-4856. Golden, CO: National Renewable Energy Laboratory.

Maxwell, E. (1987). A Quasi-Physical Model for Converting Hourly Global Horizontal to Direct Normal Insolation. Golden, CO: Solar Energy Research Institute. www.nrel.gov/rredc.pdfs/3087.pdf.

Mie, G. (1908). "Beitrage zur Optiktrüber Medien Speziell Kolloidaler Metalosungen." *Annalen der Physik*, Vierte Folge 25(3):377–445.

Orgill, J.F.; Hollands, K.G. (1977). "Correlation Equation for Hourly Diffuse Radiation on a Horizontal Surface." *Solar Energy* 19(4):357–359.

Perez, R.; Seals, R.; Ineichen, P.; Stewart, R.; Menicucci, D. (1987). "A New Simplified Version of the Perez Diffuse Irradiance Model for Tilted Surfaces." *Solar Energy* 39(3):221–231.

Perez, R.; Seals, R.; Zelenka, A.; Ineichen, P. (1990). "Climatic Evaluation of Models That Predict Hourly Direct Irradiance From Hourly Global Irradiance: Prospects for Performance Improvements." *Solar Energy* 44(2):99–108.

Rayleigh, L. (1871). "On the Light From the Sky, Its Polarization and Colour." *Philosophical Magazine* pp. 107–120, 274–279.

Reda, I.; Stoffel T.; Myers, D. (2003). "A Method To Calibrate a Solar Pyranometer fr Measuring Reference Diffuse Irradiance." *Solar Energy* 74:103–112.

Spencer, J.W. (1982). "A Comparison of Methods for Estimating Hourly Diffuse Solar Radiation From Global Solar Radiation." *Solar Energy* 29(1):19–32

Wilcox, S.; Gueymard, C.A. (2010). "Spatial and Temporal Variability of the Solar Resource in the United States." *Proceedings of Solar 2010*, Phoenix, AZ, May 2010.

Chapter 3 – Measuring Solar Radiation

ASTM, (1997). Standard Test Method for Calibration of Pyrheliometers by Comparison to Reference Pyrheliometers. ASTM E816 – 05. 1997 *Annual Book of ASTM Standards*, Vol. 14. American Society for Testing and Materials, Conshohocken, MA.

Bahm, R.J.; Nakos, J.C. (1979). *The Calibration of Solar Radiation Measuring Instruments, Final Report*. BER-1(79)DOE-684-1. Albuquerque, NM: University of New Mexico College of Engineering.

BIPM; IEC; IFCC; ISO; IUPAC; IUPAP; OIML. (1995). Guide to the Expression of Uncertainty in Measurement. ISO TAG 4, Geneva.

Fröhlich, C. (1991). "History of Solar Radiometry and the World Radiation Reference." *Metrologia* 28:111–115.

ISO. (1990). Specification and Classification of Instruments for Measuring Hemispherical Solar and Direct Solar Radiation. ISO 9060. Geneva. www.iso.org.

Maxwell, E.L; Wilcox, S.M.; Cornwall, C.; Marion, B.; Alawaji, S.H.; Mahfoodh, M.; AL-Amoudi, A. (1999). Progress Report for Annex II – *Assessment of Solar Radiation Resources in Saudi Arabia 1993-1997*. NREL/TP-560-25374. Golden, CO: National Renewable Energy Laboratory.

Micek, L.V. (1981). *Direct Beam Insolation Measurement Errors Caused by Pyrheliometer Misalignment*. M.S. Thesis, Trinity University, San Antonio, TX.

Morrison, R. (1998). *Grounding and Shielding Techniques, Fourth Edition*. John Wiley & Sons. New York.

Myers, D.; Wilcox, S. (2009). *Relative Accuracy of 1-Minute and Daily Total Solar Radiation Data for 12 Global and 4 Direct Beam Solar Radiometers*. NREL/CP-550-45734. Golden, CO: National Renewable Energy Laboratory.

Myers, D.; Wilcox, S.; Marion, W.; Al-Abbadi, N.; Mahfoodh, M.; Al-Otaibi, Z. (2002). *Final Report for Annex II--Assessment of Solar Radiation Resources in Saudi Arabia,* 1998-2000. NREL/TP-50-31546. Golden, CO: National Renewable Energy Laboratory.

Reda, I. (1996). *Calibration of a Solar Absolute Cavity Radiometer with Traceability to the World Radiometric Reference*. NREL/TP-463-20619. Golden, CO: National Renewable Energy Laboratory.

Stoffel, T.L.; Reda, I.; Myers, D.R.; Renné, D.; Wilcox, S.; Treadwell, J. (2000). "Current Issues in Terrestrial Solar Radiation Instrumentation for Energy, Climate, and Space Applications." *Metrologia, Journal of the International Bureau of Weights and Measures* (BIPM) 54.

Taylor, B.N.; Kuyatt, C.E. (1987). Guidelines for Evaluation and Expressing the Uncertainty of NIST Measurement Results. NIST Technical Note 1297, National Institute of Standards and Technology, Gaithersburg, MD.

Vignola, F.; Long, C.N.; Reda, I. (2009). Testing a Model of IR Radiative Losses. NREL/CP-3B0-46411. Presented at the Society of Photo-Optical Instrumentation Engineers (SPIE) 2009 Conference, San Diego, CA.

Wilcox, S.; Myers, D. (2008). *Evaluation of Radiometers in Full-Time Use at the National Renewable Energy Laboratory Solar Radiation Research Laboratory*. NREL/TP-550-44627. Golden, CO: National Renewable Energy Laboratory.

WMO. (2008). *WMO Guide to Meteorological Instruments and Methods of Observation, WMO-No. 8* (Seventh Edition), Geneva. www.wmo.int/pages/prog/www/IMOP/publications/CIMO-Guide/CIMO_Guide-7th_Edition-2008.html.

Chapter 4 – Modeling Solar Radiation—Current Practices

Augustine, J.A.; Deluisi, J.; Long, C.N. (2000). "SURFRAD-A National Surface Radiation Budget Network for Atmospheric Research." *Bulletin of the American Meteorological Society* 81:2341–2357.

Ben Djemaa, A.; Delorme, C. (1992). "A Comparison Between One Year of Daily Global Irradiation From Ground-Based Measurements Versus METEOSAT Images From Seven Locations in Tunisia." *Solar Energy* 48(5):325–333.

Beyer, H.; Costanzo, C.; Heinemann, D. (1996). "Modifications of the HELIOSAT Procedure for Irradiance Estimates From Satellite Images." *Solar Energy* 56:207–221.

Bird, R.E.; Hulstrom, R.L. (1981). *A Simplified Clear-Sky Model for Direct and Diffuse Insolation On Horizontal Surfaces*. SERI/TR-642-761, Golden, CO: Solar Energy Research Institute.

Cano, D.; Monget, J.M.; Albuisson, M.; Guillard, H.; Regas, N.; Wald, L. (1986). "A Method for the Determination of the Global Solar Radiation From Meteorological Satellite Data." *Solar Energy* 37:31–39.

Cebecauer T.; Suri, M.; Perez, R. (2010). "High Performance MSG Satellite Model for Operational Solar Energy Applications." *Proceedings of the ASES Annual Conference*, Phoenix, AZ.

Czeplak, G.; Noia, M.; Ratto, D.F. (1991). "An Assessment of a Statistical Method To Estimate Solar Irradiance at the Earth's Surface From Geostationary Satellite Data." *Renewable Energy* 1:737–743.

Darnell, W.L.; Staylor (1992). "Seasonal Variation of Surface Radiation Budget Derived From International Satellite Cloud Climatology Project C1 Data." *Journal of Geophysical Research* 97(15):741–760.

Darnell, W.L.; Staylor, W.F.; Gupta, S.K.; Denn, M. (1988). "Estimation of Surface Insolation Using Sun-Synchronous Satellite Data." *Journal of Climate* 1:820–835.

Dedieu, G.; Deschamps, P.Y.; Kerr, Y.H. (1987). "Satellite Estimation of Solar Irradiance at the Surface of the Earth and of Surface Albedo Using a Physical Model Applied to Meteosat Data." *Journal of Climate and Applied Meteorology* 26:79–87.

Delorme, C.; Gallo, A.; Oliveiri, J. (1992). "Quick Use of WEFAX Images From METEOSAT To Determine Daily Solar Radiation in France." *Solar Energy* 49(3):191–197.

Diabate, L.; Demarcq, H.; Michaud-Regas, N.; Wald, L. (1988). "Estimating Incident Solar Radiation at the Surface From Images of the Earth Transmitted by Geostationary Satellites: The Heliosat Project." *International Journal of Solar Energy* 5:261–278.

Diak G.R.; Gautier, C. (1983). "Improvements to a Simple Physical Model for Estimating Insolation From GOES Data." *Journal of Climate and Applied Meteorology* 22:505–508.

Dürr, B.; Zelenka, A. (2009). "Deriving Surface Global Irradiance Over the Alpine Region From METEOSAT Second Generation Data by Supplementing the HELIOSAT Method." *International Journal of Remote Sensing* 30:5821–5841.

Frouin, R.; Gautier, C.; Katsaros, K.B.; Lind, R.J. (1988). "A Comparison of Satellite and Empirical Formula Techniques for Estimating Insolation Over the Oceans." *Journal of Applied Meteorology* 27:1016–1023.

Frulla, L.A.; Gagliardini, D.A.; Grossi Gallegos, H.; Lopardo, R. (1988). "Incident Solar Radiation on Argentina From the Geostationary Satellite GOES: Comparison With Ground Measurements." *Solar Energy* 41(1):61–69.

Gautier, C. (1988). "Surface Solar Irradiance in the Central Pacific During Tropic Heat: Comparisons Between in situ Measurements and Satellite Estimates." *Journal of Climate* 1:600–608.

Gautier, C.; Diak, G.; Masse, S. (1980). "A Simple Physical Model To Estimate Incident Solar Radiation at the Surface From GOES Satellite Data." *Journal of Applied Meteorology* 19:1005–1012.

Gautier, C.; Frouin, R. (1984). "Satellite-Derived Ocean Surface Radiation Fluxes." *Proceeding of the Workshop on Advances in Remote Sensing Retrieval Methods*, Williamsburg, VA.

George, R.; Wilcox, S.; Anderberg, M.; Perez, R. (2007). "National Solar Radiation Database (NSRDB) -- 10 Km Gridded Hourly Solar Database." *Proceedings of the Solar 2007 Conference*, Cleveland, OH (CD-ROM). Boulder, CO: ASES. NREL/CP-581-41599. Golden, CO: National Renewable Energy Laboratory.

Gueymard C.A. (2003a). "Direct Solar Transmittance and Irradiance Predictions With Broadband Models. Part I: Detailed Theoretical Performance Assessment." *Solar Energy* 74:355–379; *Corrigendum* 76:513 (2004).

Gueymard C.A. (2003b). "Direct Solar Transmittance and Irradiance Predictions With Broadband Models. Part II: Validation With High-Quality Measurements." *Solar Energy*74:381–395; *Corrigendum* 76:515 (2004).

Gueymard C.A. (1993). "Critical Analysis and Performance Assessment of Clear Sky Irradiance Models Using Theoretical and Measured Data." *Solar Energy* 51:121–138.

Gueymard C.A.; Myers D. (2008). "Validation and Ranking Methodologies for Solar Radiation Models" In *Modeling Solar Radiation at the Earth's Surface.* V. Badescu (ed.) and Springer.

Hammer, A.; Heinemann, D.; Hoyer, C.; Kuhlemann, R.; Lorenz, E.; Muller, R.; Beyer, H.G. (2003). "Solar Energy Assessment Using Remote Sensing Technologies," *Remote Sensing of Environment* 8:423–432.

Hay, J.E.; Hanson, K.; Hanson, J. (1978). "A Satellite-Based Methodology for Determining Solar Irradiance at the Ocean Surface During GATE." *Bulletin of the American Meteorological Society* 59:1549.

Heidinger, A.K. (2003). "Rapid Daytime Estimation of Cloud Properties Over a Large Area From Radiance Distributions." *Journal of Atmospheric and Oceanic Technology* 20:1237–1250.

Hu, Y.X.; Stamnes, K. (1993). "An Accurate Parameterization of the Radiative Properties of Water Clouds Suitable for Use in Climate Models." *Journal of Climate* 6:728–742.

Ineichen, P. (2008). "A Broadband Simplified Version of the Solis Clear Sky Model." *Solar Energy* 82:758–762.

Iqbal, M. (1983). *An Introduction to Solar Radiation*. Academic Press, New York.

Joseph, J.H.; Wiscombe, W.J.; Weinman, J.A. (1976). "The Delta-Eddington Approximation for Radiative Transfer." *Journal of Atmospheric Science* 33:2452–2459.

Justus, C.; Paris, M.V.; Tarpley, J.D. (1986). "Satellite-Measured Insolation in the United States, Mexico and South America." *Remote Sensing of Environment* 20:57–83.

Kato, S.; Ackerman, T.P.; Mather, J.H.; Clothiaux, E.E. (1999). "The k-Distribution Method and Correlated-k Approximation for a Shortwave Radiative Transfer Model." *Journal of Quantitative Spectroscopy & Radiative Transfer* 62:109–121.

Kerschegens, M.; Pilz, U.; Raschke, E. (1978). "A Modified Two-Stream Approximation for Computations of the Solar Radiation in a Cloudy Atmosphere." *Tellus* 30:429–435.

Klink, J.C.; Dollhopf, K.J. (1986). An Evaluation of Satellite-Based Insolation Estimates for Ohio. *Journal of Climate and Applied Meteorology* 25:1741–1751.

Kylling, A.; Stamnes, K; Tsay, S.C. (1995). "A Reliable and Efficient Two-Stream Algorithm for Radiative Transfer; Documentation of Accuracy in Realistic Layered Media." *Journal of Atmospheric Chemistry* 21:115–150.

Laszlo, I.; Ciren, P.; Liu, H.; Kondragunta, S.; Tarpley, J.D.; Goldberg. M.D. (2008). "Remote Sensing of Aerosol and Radiation From Geostationary Satellites." *Advances in Space Research* 41:1882–1893.

Lefe've, M., Wald, L.; Diabate, L. (2007). "Using Reduced Datasets ISCCP-B2 From the Meteosat Satellites To Assess Surface Solar Irradiance." *Solar Energy* 81:240–253.

Lohmann, S.; Schillings, C.; Mayer, B.; Meyer, R. (2006). "Long-Term Variability of Solar Direct and Global Irradiance Derived From ISCCP Data and comparison With Re-Analysis Data." *Solar Energy* 80:1390–1401.

Marion, W.; Wilcox, S. (1994). *Solar Radiation Data Manual for Flat-Plate and Concentrating Collectors.* NREL/TP-463-5607. Golden, CO: National Renewable Energy Laboratory.

Massey Jr., F.J. (1951). "The Kolmogorov–Smirnov Test for Goodness of Fit." *Journal of the American Statistical Association* 56:68–78.

Maxwell, E.L. (1998). "METSTAT-the Solar Radiation Model Used in the Production of the National Solar Radiation Database (NSRDB)." *Solar Energy* 62:263–279.

Maxwell, E.L.; George, R.L.; Wilcox, S.M. (1998). "A Climatological Radiation Model." Proceedings of the Annual Conference of the American Solar Energy Society, June 14–17, Albuquerque, NM.

Mayer, B.; Kylling, A. (2005). "The libRadtran Software Package for Radiative Transfer Calculations: Description and Examples of Use." *Atmospheric Chemistry and Physics Discussions* 5:1855–1877.

Möser, W.; Raschke, E. (1983). "Mapping of Global Radiation and Cloudiness From METEOSAT Image Data." *Meteorologische Rundschau* 36:33–41.

Möser, W.; Raschke, E. (1984). "Incident Solar Radiation Over Europe Estimated From METEOSAT Data." *Journal of Climate and Applied Meteorology* 23:166–170.

Moussu, G.; Diabaté, L.; Obrecht, D.; Wald, L. (1989). "A Method for the Mapping of the Apparent Ground Brightness Using Visible Images From Geostationary Satellites." *International Journal of Remote Sensing* 10(7):1207–1225.

Mueller, R.W.; Dagestad, K.F.; Ineichen, P.; Schroedter, M.; Cros, S.; Dumortier, D.; Kuhlemann, R.; Olseth, J.A.; Piernavieja, G.; Reise, C.; Wald, L.; Heinnemann, D. (2004). "Rethinking Satellite Based Solar Irradiance Modelling: The SOLIS Clear Sky Module." *Remote Sensing of Environment* 90(2):160–174.

NREL. (1993). *Users Manual for SERI QC Software: Assessing the Quality of Solar Radiation Data.* NREL/TP-463-5608. Golden, CO: National Renewable Energy Laboratory.

Nullett, D. (1987). "A Comparison of Two Methods of Estimating Insolation Over the Tropical Pacific Ocean Using Cloudiness From Satellite Observations." *Solar Energy* 39(3):197–201.

Nunez. M. (1990). Solar Energy Statistics for Australian Capital Regions. *Solar Energy* 44:343–354.

Pavolonis, M.; Heidinger, A.K.; Uttal, T. (2005). "Daytime Global Cloud Typing From AVHRR and VIIRS: Algorithm Description, Validation, and Comparisons." *Journal of Applied Meteorology* 44:804–826.

Pereira, E.B.; Abreu, S.L.; Stuhlmann, R.; Rieland, M.; Colle, S. (1996). "Survey of the Incident Solar Radiation Data in Brazil by Use of METEOSAT Satellite Data." *Solar Energy* 57(2):125–132.

Perez, R.; Ineichen, P. (2002). "A New Operational Model for Satellite-Derived Irradiances: Description and Validation." *Solar Energy* 73:307–317.

Perez, R.; Ineichen, P.; Moore, K.; Kmiecik, M.; Chain, C.; George, R.; Vignola, F. (2002). "A New Operational Satellite-to-Irradiance Model." *Solar Energy* 73(5):307–317.

Perez, R.; Ineichen, P.; Maxwell, E.; Seals, R.; Zelenka, A. (1992). "Dynamic Global-to-Direct Irradiance Conversion Models." *ASHRAE Transactions-Research Series* 354–369.

Perez, R.; Seals, R.; Ineichen, P.; Stewart, P.; Menicucci, D. (1987). "A New Simplified Version of the Perez Diffuse Irradiance Model for Tilted Surfaces. Description Performance Validation." *Solar Energy* 39:221–232.

Pinker, R.T.; Ewing, J.A. (1985). "Modeling Surface Solar Radiation: Model Formulation and Validation." *Journal of Climate and Applied Meteorology* 24:389–401.

Pinker, R.T.; Frouin, R.; Li, Z. (1995). "A Review of Satellite Methods To Derive Surface Shortwave Irradiance." *Remote Sensing of Environment* 51:108–124.

Pinker, R.T.; Laszlo, I. (1992). "Modeling Surface Solar Irradiance for Satellite Applications on a Global Scale." *Journal of Applied Meteorology* 31:194–211.

Pinker, R.T.; Ewing, J.A. (1985). "Modeling Surface Solar Radiation: Model Formulation and Validation." *Journal of Climate and Applied Meteorology* 24:389–401.

Raschke, E.; Stuhlmann, R.; Palz, W.; Steemers, T.C. (1991). *Solar Radiation Atlas of Africa.* A.A. Balakema Publishers, Rotterdam for the Commission of European Communities, p. 155.

Renné, D.S.; Perez, R.; Zelenka, A.; Whitlock, C.; DiPasquale, R. (1999). *Advances in Solar Energy: An Annual Review of Research and Development,* Vol. 13. Goswami, D. Y. and Boer, K.W., eds., American Solar Energy Society, Boulder, CO.

Rigollier, C.; Lefèvre, M.; Wald L. (2004). "The Method Heliosat-2 for Deriving Shortwave Solar Radiation Data From Satellite Images." *Solar Energy* 77:159–169.

Ruiz-Arias, J.A.; Cebecauer, T.; Tovar-Pescador; Šúri , M. (2010). "Spatial Disaggregation of Satellite-Derived Irradiance Using a High-Resolution Digital Elevation Model." *Solar Energy* 84(9):1644–1657.

Sadler, J.C.; Oda, L.; Kilonsky, B.J. (1976). *Pacific Ocean Cloudiness From Satellite Observations.* University of Hawaii Department of Meteorology.

Schiffer, R.A.; Rossow, W.B. (1983). The International Satellite Cloud Climatology Project (ISCCP): The First Project of the World Climate Research Programme. *Bulletin of the American Meteorological Society* 64:779–784.

Schmetz, J. (1989). "Towards a Surface Radiation Climatology: Retrieval of Downward Irradiances From Satellites." *Atmospheric Research* 23:287–321.

Schmetz, J.; Pili, P.; Tjemkes, S.; Just, D.; Kerkmann, J.; Rota, S.; Ratier, A. (2002). "An Introduction to Meteosat Second Generation (MSG)." *Bulletin of the American Meteorological Society* 83:977–992.

Shaltout, M.A.M.; Hassen, A.H. (1990). "Solar Energy Distribution Over Egypt Using METEOSAT Photos." *Solar Energy* 45(6):345–351.

Stowe, L.L.; Davis, P.A.; McClain, E.P. (1999). "Scientific Basis and Initial Evaluation of the CLAVR-1 Global Clear Cloud Classification Algorithm for the Advanced Very High Resolution Radiometer." *Journal of Atmospheric and Oceanic Technology* 16:656–681.

Stuhlmann, R.; Rieland, M.; Raschke, E. (1990). "An Improvement of the IGMK Model To Derive Total and Diffuse Solar Radiation at the Surface From Satellite Data." *Journal of Applied Meteorology* 29:586–603.

Tarpley, J.D. (1979). "Estimating Incident Solar Radiation at the Surface From Geostationary Satellite Data." *Journal of Applied Meteorology* 18:1172–1181.

Thøgersen, M.L.; Motta, M.; Sørensen, T.; Nielsen, P. (2007). "Measure-Correlate-Predict Methods: Case Studies and Software Implementation." European Wind Energy Conference 2007.

White Paper. (2009a). 3-TIER Western Hemisphere Solar Dataset: Methodology and Validation, available at http://c0402442.cdn.cloudfiles.rackspacecloud.com/static/ttcms/1.0.0.16/us/documents/publications/validations/solar_wh_validation.pdf.

White Paper. (2009b). 3-TIER Solar Dataset: India Validation, available at http://c0402442.cdn. cloudfiles.rackspacecloud.com/static/ttcms/1.0.0.16/us/documents/publications/validations/ solar_india_validation.pdf.

White Paper. (2009c). 3-TIER Solar Dataset: Australia Validation, available at http://c0402442.cdn. cloudfiles.rackspacecloud.com/static/ttcms/1.0.0.16/us/documents/publications/validations/ solar_australia_validation-final.pdf.

Whitlock, C.H.; Charlock, T.P.; Staylor, W.F.; Pinker, R.T.; Laszlo, I.; Ohmura, A.; Gilgen, H.; Konzelman, T.; DiPasquale, R.C.; Moats, C.D.; LeCroy, S.R.; Ritchey, N.A. (1995). "First Global WRCP Shortwave Surface Radiation Budget Dataset." *Bulletin of the American Meteorological Society* 76:905–922.

Wilcox, S.; Anderberg, M.; Beckman, W.; DeGaetano, A.; George, R.; Gueymard, C.; Lott, N.; Marion, W.; Myers, D.; Perez, R.; Renné, D.; Stackhouse, P.; Vignola, F.; Whitehurst, T. (2007). *National Solar Radiation Database 1991–2005 Update: User's Manual.* NREL/TP-581-41364, Golden, CO: National Renewable Energy Laboratory.

Yang, P.; Liou, K.N.; Wyser, K.; Mitchell, D. (2000). "Parameterization of the Scattering and Absorption Properties of Individual Ice Crystals." *Journal of Geophysical Research* 105:4699–4718.

Zelenka, A.; Perez, R.; Seals R.; Renné, D. (1999). "Effective Accuracy of Satellite-Derived Irradiance." *Theoretical and Applied Climatology* 62:199–207.

Zhang, Y.C.; Rossow, W.B.; Lacis, A.A.; Oinas, V.; Mishchenko, M.I. (2004). "Calculation of Radiative Fluxes From the Surface to Top of Atmosphere Based on ISCCP and Other Global Datasets: Refinements of the Radiative Transfer Model and the Input Data." *Journal of Geophysical Research* 109.

Chapter 5 – Historical Solar Resource Data

Dumortier, D. (1998). Ecole Nationale des Travaux Publics de l'Etat, Vaulx-en-Velin, France. (1998). "Daylight Availability in Freiburg and Nantes, Two Sites Close in Latitude." *Report for the Sixth SATELLIGHT* Meeting in Freiburg, Germany, September 1998.

Hall, I.; Prairie, R.; Anderson, H.; Boes, E. (1978). *Generation of Typical Meteorological Years for 26 SOLMET Stations.* SAND78-1601. Albuquerque, NM: Sandia National Laboratories.

Hegner, H.; Müller, G.; Nespor, V.; Ohmura, A.; Steigrad, R.; Gilgen, H. (1998). *Technical Plan for BSRN Data Management* (WRMC technical report no. 2), WMO/TD-No. 882, WCRP/WMO. Geneva.

Hulstrom, R.L., ed. (1989). *Solar Resources.* The MIT Press, Cambridge, MA.

Kalnay, E.; Kanamitsu, M.; Kistler, R.; Collins, W.; Deaven, D.; Gandin, L.; Iredell, M.; Saha, S.; White, G.; Woollen, J.; Zhu, Y.; Chelliah, M.; Ebisuzaki, W.; Higgins, W.; Janowiak, J.; Mo, K.C.; Ropelewski, C.; Wang, J.; Leetmaa, A.; Reynolds, R.; Jenne, R.; Joseph, D. (1996). "The NCEP/NCAR 40-Year Reanalysis Project." *Bulletin of the American Meteorological Society* 77:437–471.

Kistler, R.; Kalnay, E.; Collins, W.; Saha, S.; White, G.; Woollen, J.; Chelliah, M.; Ebisuzaki, W.; Kanamitsu, M.; Kousky, V.; van den Dool, H.; Jenne, R.; Fiorino, M. (2001). "The NCEP-NCAR 50-Year Reanalysis: Monthly Means CD-ROM and Documentation." *Bulletin of the American Meteorological Society* 82:247–267.

Lohmann, S.; Schillings, C.; Mayer, B.; Meyer, R. (2006). "Long-Term Variability of Solar Direct and Global Irradiance Derived From ISCCP Data and Comparison With Re-Analysis Data." *Solar Energy* 80:1390–1401.

Marion, W. (1994). *Summary Information and Data Sets for the HBCU Solar Measurements Network.* NREL/TP-463-7090. Golden, CO: National Renewable Energy Laboratory.

Marion, W.; Myers, D. (1992). *A Comparison of Data from SOLMET/ERSATZ and the National Solar Radiation Database.* NREL/TP-463-5118. Golden, CO: National Renewable Energy Laboratory.

Marion, W.; Urban, K. (1995). *Users Manual for TMY2s-Typical Meteorological Years Derived From the 1961–1990 National Solar Radiation Database*. NREL/TP-463-7668. Golden, CO: National Renewable Energy Laboratory.

Maxwell, E.L. (1998). "METSTAT – The Solar Radiation Model Used in the Production of the National Solar Radiation Database (NSRDB)." *Solar Energy* 62:263–279.

Mehos, M.; Perez, R. (2005). Mining for Solar Resources: U.S. Southwest Provides Vast Potential. *Imaging Notes* 20(2):12–15; NREL/JA-550-37799. Golden, CO: National Renewable Energy Laboratory.

Meyer, R; Butron, J.T. Marquardt, G.; Schwandt, M.; Geuder, N.; Hoyer-Klick, C.; Lorenz, E.; Hammer, A.; Beyer, H.G. (2008). "Combining Solar Irradiance Measurements and Various Satellite-Derived Products to a Site-Specific Best Estimate." Solar PACES Symposium, Las Vegas, NV, 2008.

Mueller, R.W.; Dagestad, K.F.; Ineichen, P.; Schroedter, M.; Cros, S.; Dumortier, D.; Kuhlemann, R.; Olseth, J.A.; Piernavieja, G.; Reise, C.; Wald, L.; Heinnemann, D. (2004). "Rethinking Satellite Based Solar Irradiance Modelling: The SOLIS Clear Sky Module." *Remote Sensing of Environment 90* (2):160–174.

Myers, D.R.; Stoffel, T.L.; Reda, I.; Wilcox, S.M.; Andreas. A. (2002). "Recent Progress in Reducing the Uncertainty in and Improving Pyranometer Calibrations." *Transactions of the ASME* 124:44–50.

NASA (2008). http://eosweb.larc.nasa.gov/cgi-bin/sse/print.cgi?accuracy.txt.

NCDC. (1979 a). *Final Report – Hourly Solar Radiation-Surface Meteorological Observations.* TD-9724. Asheville, NC: National Climatic Data Center.

NCDC. (1979 b). *SOLDAY User's Manual (TD9739) Daily Solar Radiation – Surface Meteorological Data.* Asheville, NC: Environmental Data and Information Service.

NCDC (1978). *User's Manual – Hourly Solar Radiation-Surface Meteorological Observations. T*D-9724. Asheville, NC: National Climatic Data Center.

NREL. (1993). *User's Manual for SERI_QC Software – Assessing the Quality of Solar Radiation Data.* NREL/TP-463-5608. Golden, CO: National Renewable Energy Laboratory.

NSRDB. (1992). *User's Manual – National Solar Radiation Database (1961-1990). Version 1.0.* Golden, CO: National Renewable Energy Laboratory and Asheville, NC: National Climatic Data Center.

NSRDB (1995). *Final Technical Report: National Solar Radiation Database* (1961-1990). NREL/TP-463-5784. Golden, CO: National Renewable Energy Laboratory.

Olseth J.A.; Skartveit A. (1998). "High Latitude Global and Diffuse Radiation Estimated From METEOSAT Data." *European Conference on Applied Climatology*, ECAC 98, Vienna, Austria, October 19–23, 1998.

Perez, R.; Ineichen, P.; Moore, K.; Kmiecik, M.; Chain, C.; George, R.; Vignola, F. (2002). "A New Operational Satellite-to-Irradiance Model." *Solar Energy* 73(5):307–317.

Pinker, R.T.; I. Laszlo (1992). "Modeling Surface Solar Irradiance for Satellite Applications on a Global Scale." *Journal of Applied Meteorology* 31:194–211.

Remund, J.; Lefèvre, W.L.; Ranchin, M.; Page, T. (2003). "Worldwide Linke Turbidity Information, ISES Solar World Congress." Solar Energy for a Sustainable Future, Göteborg, Sweden.

Rigollier, C.; Bauer, O.; Wald, L. (2000). "On the Clear Sky Model of the 4th European Solar Radiation Atlas With Respect to the Heliosat Method." *Solar Energy* 68(1):33–48. See also Geiger, M.; Diabaté ,L.; Ménard L.; Wald, L. (2002). "A Web Service for Controlling the Quality of Global Solar Irradiation." *Solar Energy* 73(6):475–480.

Thornton, P.E.; Running, S.W. (1999). "An Improved Algorithm for Estimating Incident Daily Solar Radiation From Measurements of Temperature, Humidity, and Precipitation." *Agriculture and Forest Meteorology* 93:211–228.

Thornton, P.E.; Hasenauer, H.; White. M.A. (2000). "Simultaneous Estimation of Daily Solar Radiation and Humidity From Observed Temperature and Precipitation: An Application Over Complex Terrain in Austria." *Agricultural and Forest Meteorology* 104:255–271.

Tomson, T.; Russak, V.; Kallis, A. (2008). "Dynamic Behavior of Solar Radiation." In *Modeling Solar Radiation at the Earth's Surface.* V. Badescu, ed., Heidelberg, Berlin: Springer, pp. 257–281.

Wilcox, S. (2007). *National Solar Radiation Database 1991–2005 Update: User's Manual.* NREL/TP-581-41364. Golden, CO: National Renewable Energy Laboratory.

Wilcox, S.; Marion, W. (2008). "Development of an Updated Typical Meteorological Year Data Set for the United States." Proceedings of the Solar 2008 Conference.

Wilcox, S.; Marion, W. (2008). *Users Manual for TMY3 Data Sets.* NREL/TP-581-43156, Revised May 2008. Golden, CO: National Renewable Energy Laboratory.

Wilcox, S.; Myers. D. (2008). *Evaluation of Radiometers in Full-Time Use as the National Renewable Energy Laboratory Solar Radiation Research Laboratory*. NREL/TP-550-44627. Golden, CO: National Renewable Energy Laboratory. www.nrel.gov/docs/fy09osti/44627.pdf.

Wilcox, S.; Marion, W. (2008). *Users Manual for TMY3 Data Sets.* NREL/TP-581-43156, revised May 2008. Golden, CO: National Renewable Energy Laboratory.

Zelenka, A.; Perez, R.; Seals, R.; Renné, D. (1999). "Effective Accuracy of Satellite-Derived Irradiance." *Theoretical and Applied Climatology*, 62:199–207.

Chapter 6 – Applying Solar Resource Data to Concentrating Solar Power Projects

George, R.; Wilcox, S.; Anderberg, M.; Perez, R. (2007). National Solar Radiation Database (NSRDB) -- 10 Km Gridded Hourly Solar Database. Campbell-Howe, R., ed. Proceedings of the Solar 2007 Conference, 8-12 July 2007, Cleveland, Ohio (CD-ROM). Boulder, CO: ASES 8 pp.; NREL/ CP-581-41599. Golden, CO: National Renewable Energy Laboratory.

Gueymard, Christian A. and Stephen M. Wilcox. (2009). Spatial and Temporal Variability in the Solar Resource: Assessing the Value of Short-Term Measurements at Potential Solar Power Plant Sites. Boulder, CO: ASES. Solar 2009 Conference, Buffalo, NY, May 2009.

Marion, W.; Wilcox, S. (1994). *Solar Radiation Data Manual for Flat-Plate and Concentrating Collectors*. NREL/TP-463-5607. Golden, CO: National Renewable Energy Laboratory.

Mehos, M.; Perez, R. (2005). "Mining for Solar Resources: U.S. Southwest Provides Vast Potential." *Imaging Notes* 20(2):12–15; NREL/JA-550-37799. Golden, CO: National Renewable Energy Laboratory.

Meyer, R.; Torres Butron, J.; Marquardt, G; Schwandt, M.; Geuder, N.; Hoyer-Klick, C.; Lorenz, E.; Hammer, A.; Beyer, H.G. (2008). "Combining Solar Irradiance Measurements and Various Satellite-Derived Products to a Site-Specific Best Estimate." Solar PACES Symposium, Las Vegas, NV, 2008.

Thøgersen, M.LL.; Motta, M.; Sørensen, T.; Nielsen, P. (2007). "Measure-Correlate-Predict Methods: Case Studies and Software Implementation." European Wind Energy Conference, 2007.

Tomson, T.; Russak, T.V.; Kallis, V.A. (2008). "Dynamic Behavior of Solar Radiation." *In Modeling Solar Radiation at the Earth's Surface.* Badescu, V., ed., Springer, New York.

Chapter 7 – Future Work

Perez, R., Wilcox, S.; Renné, D.; Moore, K.; Zelenka, A. (2007). "Forecasting Solar Radiation - Preliminary Evaluation of an Approach Based Upon the National Forecast Database." *Solar Energy* 81(6):809–812.

Wilcox, S.M.; Myers, D.R. (2008). *Evaluation of Radiometers in Full-Time Use at the National Renewable Energy Laboratory Solar Radiation Research Laboratory*. NREL/TP-550-44627. Golden, CO: National Renewable Energy Laboratory.

Appendix. Radiometer Manufacturers and Distributors

This list is provided for information only.

Neither the United States government nor any agency thereof, nor any of their employees, makes any warranty, express or implied, or assumes any legal liability or responsibility for the accuracy, completeness, or usefulness of any information, apparatus, product, or process disclosed, or represents that its use would not infringe privately owned rights. Reference herein to any specific commercial product, process, or service by trade name, trademark, manufacturer, or otherwise does not necessarily constitute or imply its endorsement, recommendation, or favoring by the United States government or any agency thereof.

Analytical Spectral Devices, Inc.
5335 Sterling Drive, Suite A
Boulder, CO 80301 USA
Telephone: (303) 444-6522
Fax: (303) 444-6852
www.asdi.com
Spectral irradiance measurements

Brusag
Chapfwiesenstrasse 14
CH-8712 Stäfa
Switzerland
Telephone: +41 1 926 74 74
Fax: +41 1 926 73 34
Automatic solar trackers

Campbell Scientific, Inc.
815 West 1800 North
Logan, UT 84321 USA
Telephone: (435) 753.2342 (Info)
Telephone: (435) 750.9681 (Orders)
Fax: (435)750.9540
E-mail: info@campbellsci.com
www.campbellsci.com
Data logger systems, weather stations

Casella London Limited
Regent House
Britannia Walk
London N1 7ND
Telephone: 01-253-8581
Telex: 26 16 41
Radiometers

Davis Instruments Corporation
3465 Diablo Avenue
Hayward, CA 94545 USA
Telephone: (510) 732 9229
Fax: (510) 670 0589
www.davisnet.com
Weather stations

DAYSTAR
3250 Majestic Ridge
Las Cruces, NM 88011 USA
Telephone: (505) 522-4943
www.raydec.com/daystar
Radiometers

Delta-T Devices Ltd
130 Low Road, Burwell
Cambridge, CB25 0EJ
UK

U.S. Distributor:
Gary L. Woods, Sales Manager
garywood s@dynamax.com
www.dynamax.com
Telephone: (800) 896-7108 (toll free)
Telephone: (281) 564-5100
Fax: (281) 564-5200
Radiometers, weather stations, data loggers

EKO Instruments Trading Co., LTD.
21-8
Hatagaya 1-chome
Shibuyaku, Tokyo 151
Japan
Telephone: 81-3-3469-4511
Fax: 81-3-3469-4593
Telex: J25364 EKOTRA
www.eko.co.jp/eko/english/03/a.html

U.S. Distributor:
SC-International, Inc.
346 W. Pine Valley Drive
Phoenix, AZ 85023 USA
Telephone: (602) 993-7877
Fax: (602) 789-6616
Radiometers, trackers, data loggers

The Eppley Laboratory, Inc.
12 Sheffield Avenue
Newport, RI 02840 USA
Telephone: (401) 847-1020
Fax: (401) 847-1031
www.eppleylab.com/
Radiometers, trackers, data loggers

Hukseflux Thermal Sensors B.V.
Elektronicaweg 25
2628 XG Delft
The Netherlands
Telephone: +31-15-2142669
Fax: +31-152574949
Radiometers

Hukseflux U.S. Sales Representative
Robert Dolce
HuksefluxUSA
P.O. Box 850
Manorville, NY 11949 USA
Telephone: (631) 251-6963
E-mail: rdolce@HuksefluxUSA.com

Irradiance. Inc.
41 Laurel Drive
Lincoln, MA 01773 USA
Phone/Fax: (781) 259-1134
www.irradiance.com/rsr.html
Rotating Shadowband Radiometer (RSR)

Kipp & Zonen, Delft BV
P.O. Box 507
2600 AM Delft Holland
Mercuriusweg 1
2624 BC Delft Holland
Telephone: 015-561 000
Fax: 015-620351
Telex: 38137
www.kippzonen.com

U.S. Sales Representative
Victor Cassella
Kipp & Zonen
125 Wilbur Place
Bohemia, NY 11716 USA
Telephone: (631) 589-2065 ext 22
Fax: (631) 589-2068
Radiometers, trackers, data loggers

LI-COR, Inc.
4421 Superior Street
Lincoln, NE 68504 USA
Telephone: (800) 447-3576 (toll free)
Telephone: (402) 467-3576
Fax: (402) 467-2819
http://licor.com/
Radiometers, data loggers, weather stations

Matrix, Inc.
537 S. 31st Street
Mesa, AZ 85204 USA
Telephone: (480) 832-1380
Radiometers

Medtherm Corporation
P.O. Box 412
Huntsville, AL 35804 USA
Telephone: (256) 837-2000
Fax: (256) 837-2001
www.medtherm.com
Cavity radiometers

MicroStrain, Inc.
459 Hurricane Lane, Suite 102
Williston, VT 05495
(800) 449-3878
www.microstrain.com/
Wireless sensors, data loggers

Middleton Solar
Factory 20, 155 Hyde Street
Yarraville, Victoria 3013 Australia
Telephone: +61-3-9396 1890
Fax: +61-3-9689 2384 (Fax)
Radiometers

Ocean Optics, Inc.
830 Douglas Ave.
Dunedin, FL 34698 USA
Telephone: (727) 733.2447
Fax: (727) 733.3962
www.oceanoptics.com

European Sales Office:
Geograaf 24
 6921 EW DUIVEN
 The Netherlands
Telephone: +31 (0) 26 319 0500
Fax: +31 (0) 26 319 05 05

Onset
470 MacArthur Boulevard
Bourne, MA 02532 USA
Telephone: (508) 743-3210
www.onsetcomp.com
HOBO loggers, radiometers, met sensors

PH. Schenk GmbH & Co KG
Jedleseer Strasse 59
A-1210 Wien, Austria
Telephone: +43/1 271 51 31-0
E-mail: office@schenk.co.at
www.schenk.co.at/schenk
Radiometers

Solar Light Company
721 Oak Lane
Philadelphia, PA 19126 USA
Telephone: (215) 927-4206
www.solarlight.com/
Radiometers

Yankee Environmental Systems, Inc.
Montaque Industrial Park
101 Industrial Road
P.O. Box 746
Turners Falls, MA 01376 USA
Telephone: (413) 863-0200
www.yesinc.com/
Radiometers, data systems, sky imagers

REPORT DOCUMENTATION PAGE

1. REPORT DATE *(DD-MM-YYYY)* 16-09-2010	**2. REPORT TYPE** Technical Report	**3. DATES COVERED** *(From - To)*

4. TITLE AND SUBTITLE

Concentrating Solar Power: Best Practices Handbook for the Collection and Use of Solar Resource Data

5a. CONTRACT NUMBER
DE-AC36-08GO28308

5b. GRANT NUMBER

5c. PROGRAM ELEMENT NUMBER

6. AUTHOR(S)

Tom Stoffel, Dave Renné, Daryl Myers, Steve Wilcox, Manajit Sengupta, Ray George, Craig Turchi

5d. PROJECT NUMBER
NREL/TP-550-47465

5e. TASK NUMBER
SS10.1720

5f. WORK UNIT NUMBER

7. PERFORMING ORGANIZATION NAME(S) AND ADDRESS(ES)
National Renewable Energy Laboratory
1617 Cole Blvd.
Golden, CO 80401

8. PERFORMING ORGANIZATION REPORT NUMBER
NREL/TP-550-47465

9. SPONSORING/MONITORING AGENCY NAME(S) AND ADDRESS(ES)

10. SPONSOR/MONITOR'S ACRONYM(S)
NREL

11. SPONSORING/MONITORING AGENCY REPORT NUMBER

12. DISTRIBUTION AVAILABILITY STATEMENT
National Technical Information Service
U.S. Department of Commerce
5285 Port Royal Road
Springfield, VA 22161

13. SUPPLEMENTARY NOTES

14. ABSTRACT *(Maximum 200 Words)*

As the world looks for low-carbon sources of energy, solar power stands out as the most abundant energy resource. Harnessing this energy is the challenge for this century. Photovoltaics and concentrating solar power (CSP) are two primary forms of electricity generation using sunlight. These use different technologies, collect different fractions of the solar resource, and have different siting and production capabilities. Although PV systems are most often deployed as distributed generation sources, CSP systems favor large, centrally located systems. Accordingly, large CSP systems require a substantial investment, sometimes exceeding $1 billion in construction costs. Before such a project is undertaken, the best possible information about the quality and reliability of the fuel source must be made available. That is, project developers need to have reliable data about the solar resource available at specific locations to predict the daily and annual performance of a proposed CSP plant. Without these data, no financial analysis is possible. This handbook presents detailed information about solar resource data and the resulting data products needed for each stage of the project.

15. SUBJECT TERMS
concentrating solar power; csp; pv; photovoltaic; sunlight; electricity generation; solar resource

16. SECURITY CLASSIFICATION OF:			**17. LIMITATION OF ABSTRACT**	**18. NUMBER OF PAGES**	**19a. NAME OF RESPONSIBLE PERSON**
a. REPORT Unclassified	**b. ABSTRACT** Unclassified	**c. THIS PAGE** Unclassified	UL		**19b. TELEPHONE NUMBER** *(Include area code)*